

**Functional properties of microglia in mouse models of
Alzheimer's disease**

Dissertation

for the award of the degree

“Doctor rerum naturalium” (Dr. rer. nat.)

In the GGNB program “Molecular Physiology of the Brain”

at the Georg-August University Göttingen

Faculty of Biology

submitted by

Nasrin Saiepour

Born in Semnan, Iran

Göttingen, 2015

Supervisors

Prof. Dr. Uwe. K. Hanisch[†]

Department of Neuropathology, University Medical Center Göttingen

Prof. Dr. Wolfgang Brück (Reviewer)

Department of Neuropathology, University Medical Center Göttingen

Prof. Dr. Hendrikus W.G.M. Boddeke

Department of Neuroscience, University Medical Center Groningen, the Netherlands

Thesis Committee Members

Prof. Dr. Thomas A. Bayer (Reviewer)

Department of Molecular Psychiatry, University Medical Center Göttingen

Prof. Dr. Mikael Simons

Department of Cellular Neuroscience, Max Planck Institute for Experimental Medicine, Göttingen

Further members of Examination Board

Prof. Dr. Tiago Fleming Outeiro

Department of Neurodegeneration and Restorative Research, University Medical Center Göttingen

Prof. Dr. Eberhard Fuchs

Clinical Neurobiology Laboratory, German Primate Center, Göttingen

Prof. Dr. Dr. Hannelore Ehrenreich

Department of Clinical Neurosciences, Max Planck Institute of Experimental Medicine, Göttingen

Date of oral examination: 24th February, 2016

Affidavit

I hereby declare that my doctoral thesis entitled "Functional properties of microglia in mouse models of Alzheimer's disease" has been written independently with no other sources and aids than quoted.

Nasrin Saiepour

Göttingen, 31st December 2015

Table of contents

Abstract	1
1 Introduction	3
1.1 Microglia	3
1.1.1 Origin	3
1.1.2 Homeostasis and defense function	3
1.1.3 Pattern-recognition receptors in microglia	4
1.1.3.1 Toll-like receptors in microglia	5
1.1.3.2 Nod-like receptors in microglia	6
1.1.4 Microglial role in pathology	7
1.2 Alzheimer's disease	8
1.2.1 Pathology	8
1.2.2 Onset and risk factors	9
1.2.3 Neuropathological hallmarks	9
1.2.3.1 A β production and contribution to AD pathology	10
1.2.3.2 Tau phosphorylation and contribution to AD pathology	12
1.2.4 Alzheimer's disease transgenic mouse models	12
1.2.4.1 5XFAD mouse model	12
1.2.4.2 APP/PS1 (APP ^{swe} PS1 ^{dE9}) mouse model	13
1.2.4.3 APP 23 mouse model	13
1.3 Adrenergic system	14
1.3.1 Effect of noradrenergic signalling on microglia	14
1.3.2 Effect of noradrenergic system on cognition and AD symptoms	14
1.4 Adrenergic receptors	15
1.5 Aims of the thesis	17

2	Materials and methods	19
2.1	Animals.....	19
2.1.1	5XFAD.....	19
2.1.2	APP23.....	19
2.1.3	APP/PS1 (APP ^{swe} PS1 ^{dE9}).....	20
2.2	Genotyping of 5XFAD mice	20
2.2.1	Isolation of mouse tail DNA	20
2.2.2	Polymerase chain reaction (PCR)	20
2.3	Microglial primary culture and harvests.....	21
2.3.1	Neonatal microglial culture.....	21
2.3.2	Adult microglial culture	22
2.4	Astrocyte culture.....	22
2.5	L929 mouse fibroblast culture.....	23
2.6	Bone marrow derived macrophages (BMDMs) preparation	23
2.7	<i>Ex vivo</i> microglia and BMDMs stimulation	23
2.8	Cyto- and chemokine measurement in the supernatants of cells.....	25
2.9	Cell harvest and preparation for flow cytometric analysis	25
2.9.1	<i>E. coli</i> phagocytosis.....	26
2.9.2	Myelin phagocytosis	26
2.9.3	Amyloid beta phagocytosis	26
2.9.4	MHC I expression	27
2.9.5	Intracellular cyto- and chemokine staining for flow cytometry analysis	27
2.10	Cells proliferation assessment	28
2.11	Cell viability assessment	28
2.12	PKA activity assay.....	28
2.13	Immunocytochemistry	29

2.14	Quantifying the number of cytokine secreting cells using ELISpot.....	30
2.15	RNA sequencing gene analysis	30
2.16	Perfusion of the mice	31
2.17	Intracerebral single injections and infusions	31
2.18	Intraperitoneal injections	32
2.19	Preparation of brains for flow cytometry	33
2.20	Immunohistochemistry	33
2.20.1	Immunohistochemistry of intracerebral infused brains.....	34
2.20.2	Immunohistochemistry of intraperitoneal injected mice.....	35
2.20.2.1	Immunohistochemistry and Congo red staining	35
2.20.2.2	Immunofluorescence and confocal imaging	36
2.20.2.3	Quantification of Mac-2, CD68 and MHC II stainings	37
2.21	Cell sorting from brains by flow cytometry for gene expression analysis	37
2.22	Statistics.....	39
3	Results	40
3.1	Characterization of microglia in the 5XFAD mouse model.....	40
3.1.1	Impairment of microglial phagocytic activity in 5XFAD is reversible.....	40
3.1.2	LPS alters phagocytic activity of adult microglia isolated from 5XFAD mice .	43
3.1.3	Higher reactivity of microglia in AD environment is reversible	46
3.1.4	Cultured microglia from 5XFAD mice show a decreased proliferation activity compared to the age matched WT mice	49
3.1.5	9 months old 5XFAD mice have no monocyte and neutrophil infiltrates in the brain	50
3.1.6	Microglia in the brains of 5XFAD mice respond to intracerebral injected LPS	52
3.2	Amyloid beta (A β) plaque-associated microglia priming in transgenic mouse models of Alzheimer's disease	55
3.2.1	A β deposition increases in APP23 mice with ageing.....	55

3.2.2	Signs of priming in A β plaque-associated microglia of APP ^{swe} PS1dE9 and 5XFAD mice	56
3.2.3	The genes involved in the immune recognition and phagocytosis are highly expressed in APP23 and 5XFAD mice	59
3.2.4	A β plaque-associated microglia priming and ageing-associated priming are two distinct processes.....	60
3.2.5	MHC II ⁺ microglia in 5XFAD mice reveal gene expression signature of priming	61
3.2.6	Systemic LPS injection leads to morphological changes of microglia	64
3.2.7	Microglia in the vicinity of A β plaques have an enhanced inflammatory response to systemic LPS challenges	66
3.2.8	LPS leads to the production of IL-1 β by microglia surrounding A β plaques	68
3.3	Noradrenergic control over innate immune cell activities in the CNS.....	73
3.3.1	All the cultured microglia express β 2AR.....	73
3.3.2	Not all the TRIF-dependent genes are rescued from the inhibition upon β 2AR activation.....	74
3.3.3	Activation of β 2AR in the CNS inhibits infiltration of immune cells from the periphery.....	76
3.3.4	Activation of β 2AR in the CNS does not decrease gliosis.....	78
3.3.5	The population size of microglia producing TNF α and CCL5 is altered by β 2AR activation.....	80
3.3.6	The amount of CCL5 released from each cell but not the percentage of CCL5 producing cells is decreasing by β 2AR activation	82
3.3.7	PKA mediates the downstream signalling from β 2AR to TLR4	83
3.3.8	Epac has no influence on β 2AR-induced inhibition of TNF α production	85
3.3.9	Activation of PKA after β 2AR activation is increased by LPS	85
3.3.10	Inhibition of TLR4-induced genes by β 2AR is not microglia specific	86
3.3.11	β 2AR activation alters activation of STAT and IRF proteins.....	87

4	Discussion	89
4.1	Functional properties of microglia in 5XFAD mouse model	89
4.1.1	Unaltered phagocytic activity of 5XFAD vs. WT microglia	89
4.1.2	Release activity of microglia isolated from 5XFAD and WT mice	91
4.1.3	Proliferation.....	93
4.1.4	Infiltration of immune cells to the brains of 5XFAD mice	94
4.2	Amyloid beta (A β) plaque-associated microglia priming in transgenic mouse models of Alzheimer's disease	96
4.2.1	Microglia surrounding A β plaques reveal signs of priming.....	97
4.2.2	Systemic inflammation increases the inflammatory response of primed microglia.....	99
4.3	Noradrenergic control on the activity of innate immune cells in the CNS.....	101
4.3.1	Effect of β 2AR signalling on TLR4 signalling	101
4.3.2	<i>In vivo</i> studies of β 2AR activation	103
4.3.3	Population size of TNF α and CCL5 producing cells	104
4.3.4	PKA mediates the downstream signalling from β 2AR to TLR4	105
5	Summary and conclusions.....	109
6	References	111
	List of Abbreviations.....	134
	List of Figures	137
	List of Tables.....	139
	Acknowledgement.....	140
	Curriculum vitae (CV)	142

Abstract

Microglia, resident macrophages of the CNS, execute various functions: they participate in oligodendrogenesis, neurogenesis, learning and behavior, phagocytose harmful material as well as tissue debris and mount crucial innate immune responses upon CNS infection and damage (Hanisch & Kettenmann, 2007). Ageing and associated neurodegenerative processes can impair these functions. In Alzheimer's disease (AD), microglia are incapable to clear the toxic amyloid β peptide ($A\beta$). This may lead to a massive accumulation and deposition of the peptide. Additionally, in an AD environment, microglia seem to be activated, leading to excessive production of inflammatory mediators, such as pro-inflammatory cytokines and chemokines, which can further damage the vulnerable CNS circuitry. The main focus of this study was to investigate if these changes in microglia properties are reversible in a healthy environment. Furthermore, microglial priming (described as their exaggerated response to an inflammatory stimulus compared with stimulus-naïve microglia; Norden & Godbout, 2013) was studied in mouse models of AD. Using 3, 6 and 9 months old 5XFAD mice, as an animal model of AD we could mainly show that the activity of microglia to phagocytose or produce pro-inflammatory factors does not differ from microglia derived from wild-type (WT) mice *ex vivo*. However, we observed a dramatic age-dependent decrease in both of these activities independent of the genotype. These data demonstrate that microglial alteration in AD environments -described in former studies- are reversible, depending on the environment. In addition, we studied the hyper-sensitivity of microglia in the vicinity of $A\beta$ plaques. Characterization of these microglia in APP23, APPswePS1dE9 and 5XFAD mice revealed expression of microglial activation/priming markers such as Mac-2, CD68 and MHC II. Isolation of MHC II positive and -negative microglia from whole brains of 9 months old 5XFAD and WT mice also showed significant changes towards pro-inflammatory characteristics in MHC II positive microglia compared to the MHC II negatives. In addition, immunohistochemical analysis of systemic LPS-induced inflammation in 5XFAD mice led to overexpression of Mac-2, CD68, MHC II and IL-1 β exclusively in the vicinity of $A\beta$ plaques. In contrast, LPS-induced priming and inflammation was absent in plaque free regions. These data indicate that microglia in the vicinity of $A\beta$ depositions are primed.

In the third part we determined how the activation of beta 2 adrenergic receptors (β 2ARs) in LPS-stimulated microglia influences the pro-inflammatory response of microglia. This

investigation was based on previously observed anti-inflammatory effects of the adrenergic system on macrophages including microglia and its positive effects on AD. In the investigations, *ex vivo* or *in vivo*, microglia were treated with LPS and salbutamol (β 2AR agonist) simultaneously and the subsequent microglial production of pro-inflammatory cyto-/chemokines and microglia-induced infiltration of immune cells from the periphery was analyzed. We observed that the production of some but not all pro-inflammatory proteins are inhibited by salbutamol. For instance, the production of TNF α is almost completely inhibited. In contrast, the production of CCL5 is almost not inhibited. Previous studies on microglia lacking the mediator protein TRIF suggested that TLR4 signalling through the TRIF pathway is a supporting path to escape from the inhibitory effects of salbutamol. Our current data concerning involvement of specific TRIF dependent genes and also data from mRNA sequencing experiments in microglia treated with LPS alone or combined with salbutamol proved involvement of the TRIF pathway as an escaping route. Moreover, flow cytometry analyses of mice treated with LPS alone or combined with salbutamol revealed significant decreases in infiltration of immune cells in the brain. Using immunohistochemistry we additionally showed that expression of Iba-1 and GFAP on microglia and astrocytes are not affected by salbutamol. These data clearly show selective effects of the adrenergic system on pro-inflammatory factors in microglia. Reduced recruitment of immune cells from the periphery by activation of the adrenergic system is possibly an important factor in improving AD inflammation.

1 Introduction

1.1 Microglia

Microglia are myeloid glial cells in the central nervous system (CNS) making up 10-15% of all the CNS cells. Due to their similarities- in appearance and function- to tissue macrophages they are considered to be resident tissue macrophages in the brain and spinal cord (Banati, 2003). Microglia are distributed heterogeneously in the CNS tissue and depending on their neighbouring environment they can have various specialized functions and densities (Banati, 2003). A number of studies on microglia indicate that these cells are specialized mononuclear phagocytes and, accordingly, share many characteristics with other myeloid cells such as expression of Fc (fragment crystallisable) and complement receptor, CD11b and F4/80 epitopes expression and also antigen presentation molecules (major histocompatibility complex class I & II (MHC I & II); Harry, 2013).

1.1.1 Origin

It is generally known that microglia cells originate from the yolk sac during the embryogenesis (around day 9 in rodents; Takahashi et al, 1996). Establishment of the microglia population is done by invading embryonic macrophages (erythromyeloid precursors) that are generated during an early 'primitive' wave of haematopoiesis in the yolk sac to the mesenchyme of the brain (Ginhoux et al., 2010). Transcription factors PU.1- and interferon regulatory factor 8 (IRF-8) play fundamental roles in this invasion and differentiation (Kierdorf et al., 2013). Therefore, the microglia compartment in the brain is established before birth. In spite of embryonic macrophage origin, under physiological conditions maintenance of adult microglia population is independent of adult haematopoiesis and primarily occurs by longevity and limited self-renewal (Bruttger et al., 2015).

1.1.2 Homeostasis and defense function

Microglia cell function is very plastic. In the ramified form- which has been called resting stage- they are constantly motile. Their long processes monitor the environment and interact closely with other cell types like neurons, astrocytes and oligodendrocytes in the CNS (reviewed by Hanisch & Kettenmann, 2007). It has been estimated that they are able to monitor the complete brain parenchyma every few hours (Davalos et al., 2005).

A number of studies has shown that microglial monitoring is important for brain homeostasis and surveillance (Nimmerjahn et al., 2005). Support of oligodendrogenesis and neurogenesis, learning and behaviour have been also suggested to be (at least partly) under microglial control (Butovsky et al., 2006; Chen et al., 2010; Ziv et al., 2006). Involvement of soluble growth factors released from microglia during developmental microglia–neuron crosstalk has been also suggested (Michell-Robinson et al., 2015). It has been shown that microglia in neurogenic areas behave differently than those in non-neurogenic regions (Goings et al., 2006; Marshall et al., 2014). Paolicelli *et al.*, (2011) illustrated that microglia support synaptic maturation by actively engulfing synapses during postnatal development. The authors suggested that synaptic abnormalities found in some neurodevelopmental disorders could be due to deficits in microglia function.

1.1.3 Pattern-recognition receptors in microglia

Since microglia cells are part of the innate immune system, they are first line of defence against pathogens which enter the brain and cause infectious diseases. They are able to phagocyte exogenous material like bacteria and other pathogens. Under physiological conditions microglia continuously phagocytose excessive endogenous material, for instance non-functional synapses, myelin and apoptotic debris. This leads to elimination of phagocytosed material and subsequent presentation of their antigens to other immune cells (Newton & Dixit, 2012).

To perform clearance, microglia express sensors that recognize pathogens and other foreign molecules. For this surveillance microglia make use of pattern-recognition receptors (PRRs) (Akira et al., 2006). PRRs recognize pathogen-associated molecular patterns (PAMPs) and damage/danger associated molecular patterns (DAMPs). PAMPs and DAMPs involve infectious and non-infectious materials, respectively. PAMPs are for example various components of bacterial cell walls like lipopolysaccharide (LPS), lipopeptides, peptidoglycans (PGN) and flagellin, and nucleic acids derived from bacteria, viruses, fungi and parasites (Akira et al., 2006). DAMPs include intra- or extracellular proteins such as released heat shock proteins, protein fragments derived from the extracellular matrix, misfolded proteins and adenosine triphosphate (ATP) (Kono & Kenneth, 2008; Heneka et al., 2015).

The two best known examples of PRRs are Toll-like receptors (TLRs) and Nod-like receptors (NLRs; Newton & Dixit, 2012).

1.1.3.1 Toll-like receptors in microglia

Toll-like receptors (TLRs) consist of extracellular, transmembrane and cytoplasmic domains. The extracellular parts contain variable members of leucine-rich-repeat (LRR) motifs which mediate recognition of PAMPs and DAMPs.

The cytoplasmic parts of TLRs are called Toll–interleukin 1 (IL-1) receptor (TIR) domains (Bowie & O’Neill, 2000) and are essential for downstream signal transduction (Figure 1).

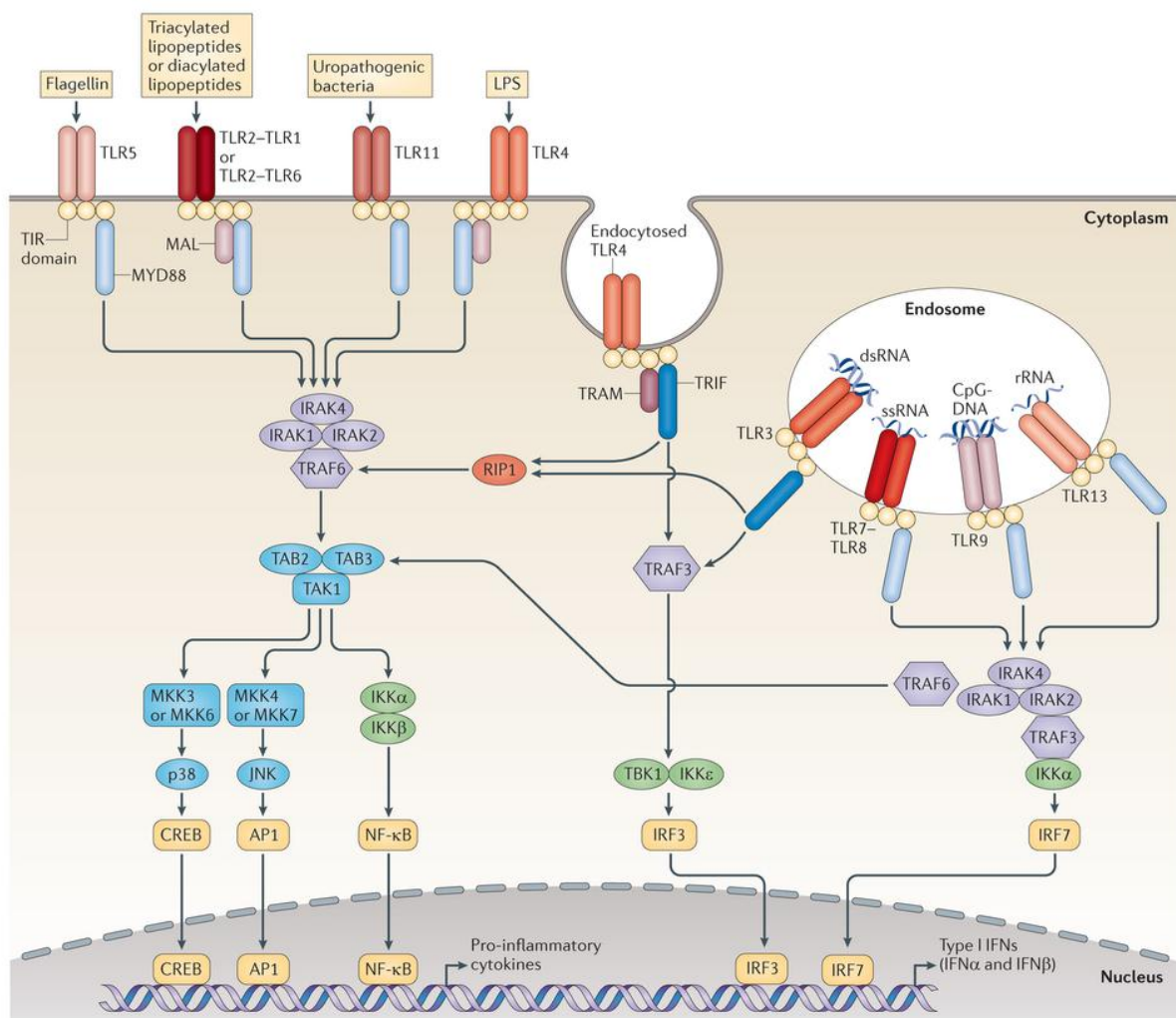


Figure 1: Drawing of mammalian TLR signalling pathways.

The picture illustrates locations and ligands of TLRs. While TLR4, TLR5, combination of TLR1-2 and TLR2-6 are located on the cell surface, TLR3, TLR7, TLR8 and TLR9 are localized in the endosomes. TLR4 have both possibilities to be located at the plasma membrane and the endosomes. Following binding of ligands to the respective TLRs, their Toll–IL-1-receptor (TIR) domains engage TIR domain-containing adaptor proteins (either myeloid differentiation primary-response protein 88 (MYD88) in addition to MYD88-adaptor-like protein (MAL), or TIR domain-containing adaptor protein inducing IFN β (TRIF) with TRIF-related adaptor molecule (TRAM)). Endocytosis of TLR4 is essential for switching signalling from MyD88 to TRIF pathways. Signalling molecules then interact with IL-1R-associated kinases (IRAKs) and the adaptor molecules TNF receptor-associated factors

(TRAFs) leading to the activation of the mitogen-activated protein kinases (MAPKs), JUN N-terminal kinase (JNK), p38 and, eventually, transcription factors such as nuclear factor- κ B (NF- κ B), the interferon-regulatory factors (IRFs), cyclic AMP-responsive element-binding protein (CREB) and activator protein 1 (AP1). TLRs signalling mainly lead to production of pro-inflammatory cytokines or the induction of type I interferons (IFN). Abbreviations: LPS, lipopolysaccharide; dsRNA, double-stranded RNA; rRNA, ribosomal RNA; ssRNA, single-stranded RNA; IKK, inhibitor of NF- κ B kinase; MKK, MAP kinase kinase; TAB, TAK1-binding protein; TAK, TGF β -activated kinase; RIP1, receptor-interacting protein 1; TBK1, TANK-binding kinase 1 (taken from O'Neill et al., 2013).

The TLR family consist of 10 members (TLR1–TLR10) in human and 12 members (TLR1–TLR9, TLR11–TLR13) in mouse (Akira et al., 2006). Depending on their localization and ligands, TLRs are divided into two groups: the first group, composed of TLR1, TLR2, TLR4, TLR5, TLR6 and TLR11, is expressed on the cell surfaces and recognizes primarily microbial membrane components. The second group, which is composed of TLR3, TLR7, TLR8 and TLR9, is expressed solely in intracellular compartments such as the endoplasmic reticulum (ER), lysosomes, endosomes and endolysosomes and recognize microbial nucleic acids (Botos et al., 2011).

Recognition of PAMPs and DAMPs by TLRs leads to recruitment of TIR domain-containing adaptor proteins such as myeloid differentiation primary response gene 88 (MyD88) and TIR-domain-containing adapter-inducing interferon- β (TRIF). These adaptor proteins initiate signalling cascades, which eventually activate mitogen-activated protein kinases (MAPK) or transcription factors such as activator protein 1 (AP-1), nuclear factor kappa-light-chain-enhancer of activated B cells (NF- κ B) and interferon regulatory factors (IRFs). TLR signalling ultimately gives rise to a diverse cellular responses including production of pro- and anti-inflammatory cytokines and chemokines, effector molecules and interferons (INFs) (Kawasaki & Kawai, 2014).

All the TLRs use either MyD88- or TRIF-mediated signal transduction pathways with exception of TLR4, which is capable of using both pathways. Moreover, TLR4 complex, containing myeloid differentiation factor-2 (MD-2) and its co-receptor CD14, is able to recognize both PAMPs and DAMPs (Regen et al., 2011).

1.1.3.2 Nod-like receptors in microglia

Apart from TLRs -which are mainly membrane bound-, cytoplasmic Nod-like receptors (NLRs) represent another type of PRRs. Upon NLR activation by PAMPs and DAMPs,

cytosolic protein complexes- named inflammasomes- assemble and subsequently mediate inflammasome signalling.

In general, inflammasome complexes consist of three main components: a cytosolic PRR such as NLR family containing pyrin domain (NLRP), caspase-1 and an adaptor protein apoptosis-associated speck like protein (ASC), which contains a caspase activation and recruitment domain (CARD). Activation of NLRPs leads to recruitment of ASC, which results in the interaction of ACS with pro-caspase-1 and facilitates its conversion to caspase-1. Caspase-1 is necessary for maturation of pro forms of interleukin (IL)-1 β , IL-18, and IL-33 into their active forms. These interleukins then initiate inflammatory responses. Therefore, inflammasomes play a crucial role in inflammation and inflammatory processes (reviewed by Singhal et al., 2014).

1.1.4 Microglial role in pathology

Under healthy conditions, microglia show a ramified phenotype and produce anti-inflammatory and neurotrophic factors (Streit, 2002). However, in response to pathogens or after tissue damage microglia switch to an activated phenotype, which promotes inflammation and recruitment of peripheral immune cells (Wyss-Coray & Mucke, 2002; Baik et al., 2014). In general, this reaction is self-limiting upon elimination of infection and tissue damage. Nevertheless, sustained stimuli (infectious or endogenous factors such as protein aggregates) can lead to a persistence of inflammation, resulting in continuous production of cytotoxic molecules (Akiyama et al., 2000) for instance pro-inflammatory cytokines and chemokines, reactive oxygen species (ROS) and nitric oxide (NO). Together with ongoing inflammasome activity these factors worsen the tissue damage as observed in neuroinflammatory and neurodegenerative diseases such as Alzheimer's disease (AD), Parkinson's disease (PD), multiple sclerosis and Huntington's disease (reviewed in Glass et al., 2010 and Singhal et al., 2014b).

Chronic low grade inflammation as observed upon ageing and neurodegenerative diseases leads to microglia priming (Norden & Godbout, 2013). Primed microglia are more susceptible to pro-inflammatory stimuli, which may result in an exaggerated inflammatory response.

Secondary pro-inflammatory stimuli can arise either from the CNS or systemic inflammations. For example, in the result of microglia priming, in animals with age-related or

neurodegenerative pathology, LPS provokes a higher pro-inflammatory response in the brain (Sierra et al., 2007). Similarly, high baseline of the pro-inflammatory cytokine tumor necrosis factor alpha (TNF α) due to a systemic infection leads to four-fold increase in the rate of cognitive decline over a 6-month period among mildly to severely affected Alzheimer's disease patients (Holmes et al., 2009).

1.2 Alzheimer's disease

Alzheimer's disease (AD) is a chronic neurodegenerative disorder with a slow progression (Hampel et al., 2010). AD is the most frequent type of dementia and is the fourth common cause of death in the aged population. By estimation more than 35 million cases of AD exist worldwide (Goedert M, 2006; Querfurth HW, 2010). It has been estimated that after an age of 65, the occurrence of age-related AD almost doubles every 5 years (Qiu et al., 2009). The early hallmarks of AD include loss of short-term memory, difficulties in performing daily life activities leading to withdrawal from social life. Besides, progressive deterioration in memory, attention and language are considered as behavioural symptoms (Zhao et al., 2014).

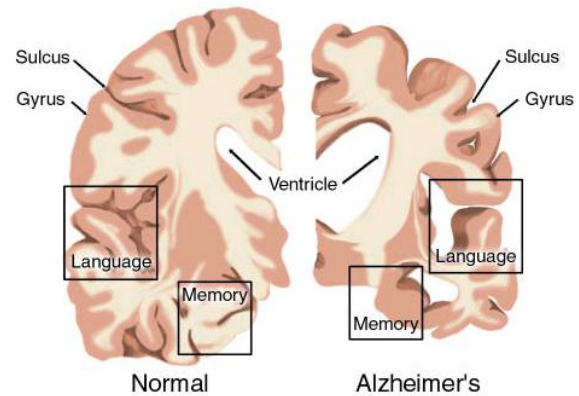
Typically, AD initiates with a preclinical stage and progresses to three common clinical stages: mild (early stage), moderate (middle stage) and severe (late stage). Preclinical stage refers to the onset of brain changes before any symptom appears and can last for even 15 years. In the mild stage of AD, the patient is still capable of performing daily activities in spite of having slight memory gaps, for instance, forgetting words or the locations of objects. With disease progression patients with moderate stage of AD require higher levels of care. The severe stage which is the final stage of the disease, includes incapability of proper responses to their environment due to worsening of memory and cognitive skills (Lyketsos et al., 2011).

1.2.1 Pathology

AD is described by a loss of neurons and synapses in both cortical and subcortical regions of the brain leading to an atrophy of the affected regions, eventually brain shrinkage and increase in ventricle sizes (Figure 2). The most degenerated regions in AD are frontal, temporal and parietal lobes, hippocampus (Wenk, 2003) and locus coeruleus (Heneka et al., 2010).

Figure 2: Schematic picture of brain atrophy in AD.

The picture compares a normal brain with an atrophic brain at late stages of AD. Degenerated regions involve mainly memory and language skills (taken from <http://www.forbes.com>).



1.2.2 Onset and risk factors

Although AD mainly involves people over 65 years, it is not exclusively an age-related disease (Ritchie et al., 1992). Regarding the onset of the disease, AD is divided into two types: early- and late-onset, named familial and sporadic, respectively. Familial AD (FAD) consists of only about 5% of all AD cases. Genetically, FAD is an autosomal dominant disorder and occurs as the result of mutations in amyloid precursor protein (APP) or presenilin (PSEN1 or PSEN2) genes.

In contrast, sporadic type of AD (SAD) consists of 90-95% of AD cases, which is not solely influenced by genetic contributions. So far, ageing, trisomy of chromosome 21 and allele $\epsilon 4$ of apolipoprotein E4 (ApoE4- $\epsilon 4$) have been introduced as the main risk factors for SAD. Among other non-genetic SAD risk factors, severe head injuries, smoking, cerebrovascular diseases, diabetes and hypertension have been suggested (reviewed in Querfurth HW, 2010; Chen CS et al., 2011). Recent AD studies have identified novel risk factors. New techniques in genome sequencing and polymorphism studies have illustrated the contribution of the immune system in the disease progression. Thus, a number of genes which play a role in phagocytic activity of immune cells such as cluster of differentiation 33 (CD33), triggering receptor expressed on myeloid cells 2 (TREM2) and TYRO protein tyrosine kinase-binding protein (TYROBP; also known as DAP12) have been identified as new AD-associated factors (Karch & Goate, 2014; Zhang et al., 2013)

1.2.3 Neuropathological hallmarks

AD is characterized by two main neuropathological hallmarks: the extracellular amyloid plaque formed by aggregated and deposited amyloid β ($A\beta$) peptides and intracellular neurofibrillary tangles (NFTs), consisting of aggregated hyperphosphorylated microtubule-

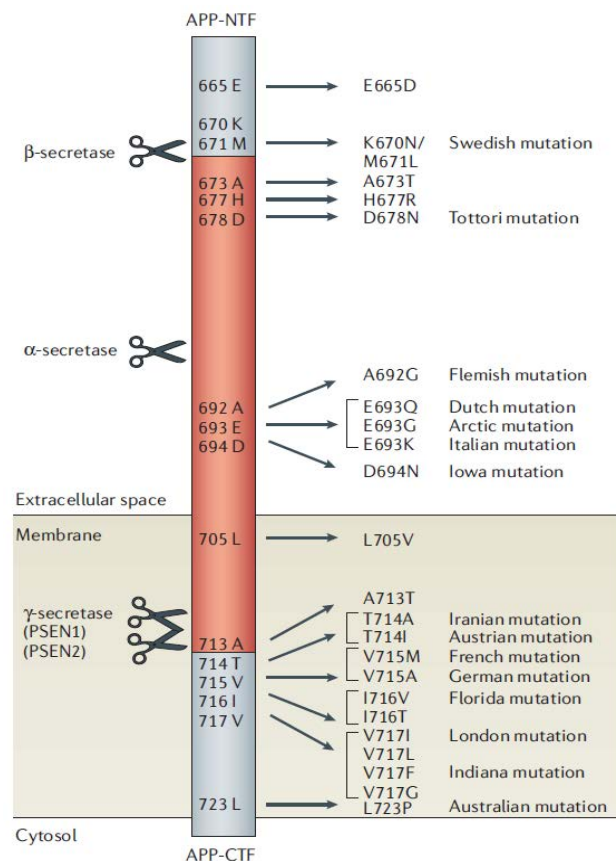
associated tau proteins. According to the distribution of NFTs in the brain of AD patients, Braak and Braak classified the AD pathology into six stages: at the stages I and II NFTs are mainly limited to transentorhinal areas, at the stages III and IV limbic regions such as the hippocampus are involved as well. The two last stages (V and VI) describe the most extensive state of the pathology where extensive involvement of neocortical regions can be observed (Braak and Braak, 1991).

1.2.3.1 A β production and contribution to AD pathology

A β peptide is generated from its precursor protein, APP. APP is a transmembrane glycoprotein containing 695, 751 or 770 amino acids (Figure 3). It is expressed in most tissues with exception of APP695 which is found mainly in neurons. Any mutation in the *APP* can affect its processing and, therefore, A β production (Zhang et al., 2011).

Figure 3: Schematic picture of amyloid precursor protein (APP).

Shown in the picture, APP is a transmembrane protein. Excision regions by the secretases enzymes on the APP and selection of its known mutations are illustrated (taken from Van Dam & De Deyn, 2006). NTF, N-terminal fragment; CTF, C-terminal fragment.



APP can be physiologically processed, where APP is initially cleaved by α -secretase enzyme within the A β sequence to release soluble APP α (sAPP α). Remaining C83 within the membrane will be cleaved by γ -secretase and P3 protein will be released. This type of processing is called the non-amyloidogenic pathway (Kojro & Fahrenholz, 2005).

To generate A β , APP has to undergo a pathogenic (so-called amyloidogenic) pathway. In this pathway APP is firstly cleaved at the extracellular domain (β -secretase cleavage) by β -secretase enzyme leading to release of sAPP β and a remaining 99 amino acid fragment (β -CTF or C99) in the membrane. C99 will be subsequently cut within the transmembrane region by γ -secretase to release A β . Depending on the γ -secretase cleavage site, various A β sequences of different lengths (such as 40, 42 or 43 amino acids) will be generated (Figure 4; O'Brien & Wong, 2011).

γ -secretase, which is a highly hydrophobic catalytic enzyme consists of four subunits: presenilin 1 or 2 (PSEN 1 or PSEN 2), Aph-1a or b, nicastrin and pen-2. While mutations in *APP* leads to more A β production, mutations in *PSEN* cause a higher ratio of A β_{42} to A β_{40} which results in a increasing toxicity due to higher aggregating potentials of longer A β peptides (Wolfe, 2007).

Monomeric forms of A β protein (more prominently A β_{1-42}) tend to self-aggregate and undergo oligomerization: forming dimers, tetramers and higher molecular weight oligomers which are still soluble. A β oligomers lose their solubility with on-going aggregation and form β -sheet structures and fibrils. This process will be continued until A β assemblies deposit in form of plaques (Figure 4; O'Brien & Wong, 2011).

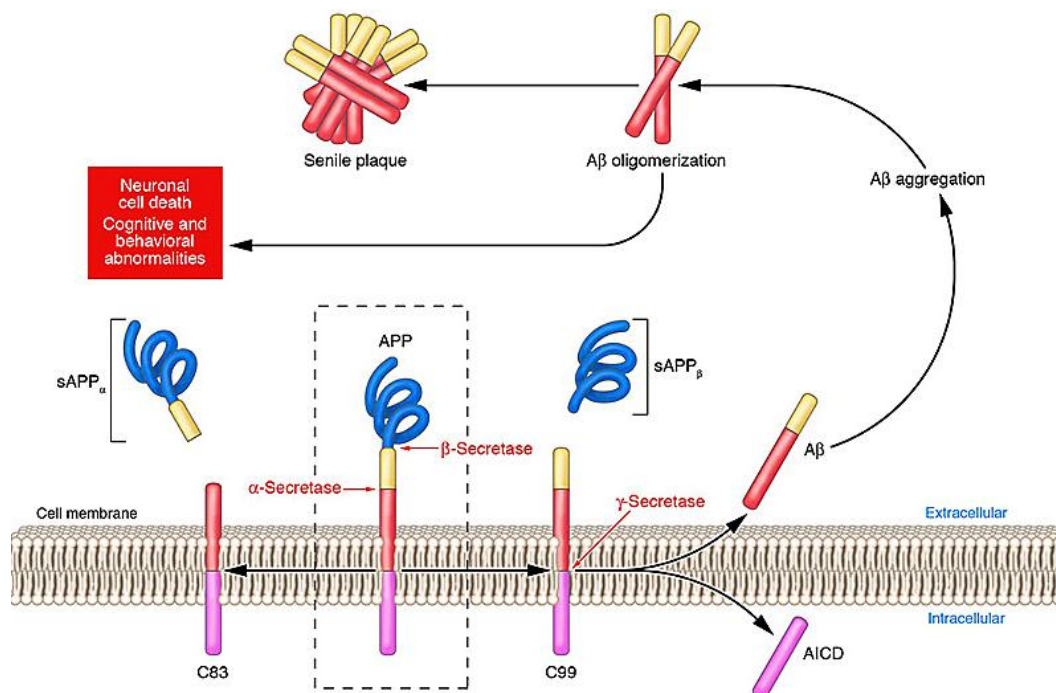


Figure 4: Schematic representation of APP processing and A β oligomerization.

In the amyloidogenic pathway the transmembrane protein APP is cleaved by β - and γ -secretases leading to production of monomeric A β proteins. Unstable monomers self-aggregate to form oligomers and senile plaques, where, oligomers having the most toxicity effect among other aggregates (taken from www.bioscience.org).

For many years it was believed that plaques are the main cause of AD. However, recent studies have not shown a correlation between number of plaque deposits and severity of the disease. In contrast, levels of soluble A β oligomers have a higher correlation to the AD course (reviewed by Wirths et al., 2004; Larson ME, 2012). It has been shown that pathological concentrations of A β oligomers trigger an overstimulation of extrasynaptic NMDA receptors leading to Ca²⁺ upregulation, mitochondrial dysfunction, synaptic disruption, dysregulation of synaptic neurotransmission, abnormal neuronal network activity and finally neuronal loss (reviewed by Palop & Mucke, 2010; Bayer & Wirths, 2011).

1.2.3.2 Tau phosphorylation and contribution to AD pathology

Tau protein is abundant in both the central and the peripheral nervous system. Generally, phosphorylated tau protein stabilizes axonal microtubules in the CNS, supporting neurite outgrowth and cytoplasmic transport. Under certain conditions, tau protein may become hyperphosphorylated, which reduces its binding affinity to microtubules, leading to its intraneuronal aggregation and accumulation. Hyperphosphorylated aggregated tau protein complexes form NFTs (Avila et al., 2004). Accumulation of tau protein in dendrites or dendritic spines affect neuronal cell communication, causing and worsening neurodegeneration (Hoover et al., 2010).

1.2.4 Alzheimer's disease transgenic mouse models

So far various transgenic AD mouse models, based on mutations within the APP gene have been generated. One of the most used APP-based AD mouse models is 5XFAD.

1.2.4.1 5XFAD mouse model

The 5XFAD transgenic (tg) mouse contains five genetic mutations that have been associated with familial Alzheimer's disease. 5XFAD mouse model, which was generated in 2006 by Oakley and colleagues (Oakley et al., 2006), co-expresses mutant human *APP* (*hAPP*) and human *PSEN1* genes simultaneously under neuronal thymocyte differentiation antigen 1 (Thy-1) promoter. *hAPP* and *PSEN1* in this model carry three and two mutations,

respectively: Swedish (K670N/M671L), Florida (I716V) and London (V717I) in *APP*; M146L and L286V in *PSENI*.

Tg-5XFAD is a rapid transgenic AD amyloid mouse model and is one the most aggressive AD mouse models. In this model, as expected, the mutations in *hAPP* lead to additive production of A β - in general- whereas the mutations in *PSENI* result in higher A β ₁₋₄₂ production. Showing amyloid plaques and gliosis already at 2 month of age, neuron loss, memory impairment and, more interestingly, accumulation of intraneuronal A β ₁₋₄₂ before plaque formations are the characteristics of this model. Further studies have shown age dependent motor deficits, reduced anxiety and axonal degeneration in this mouse model (Jawhar et al., 2012).

1.2.4.2 APP/PS1 (APP^{swe}PS1^{dE9}) mouse model

APP^{swe}PS1^{dE9} transgenic mouse model has been described previously (Jankowsky et al., 2004). In brief, it expresses a chimeric mouse/human APP695 gene carrying the Swedish double mutations, K670M/N671L (Mo/HuAPP^{swe}) in addition to human presenilin-1 (PSEN-1) gene with an exon-9 deletion mutation (PS1^{dE9}).

Overexpression of human APP protein leads to abundant A β deposition in this AD mouse model. Both mutations in *APP* and *PSENI* are associated with the early-onset of Alzheimer's disease. This mouse develops beta-amyloid deposits in the brain by 6-7 months of age and, subsequently, shows spatial learning deficits and reduced anxiety at 7 month of age (Reiserer et al., 2007). Other characteristics of this model include impaired contextual memory early as 6 months of age (Kilgore et al., 2010), affected nest-building and burrowing as well as age-dependent decline in cognitive behavioral (Janus et al., 2015).

1.2.4.3 APP 23 mouse model

The APP23 mouse model expresses the human APP751 gene containing the Swedish double mutations, associated with early-onset familial AD, under the Thy-1 promoter (Sturchler-Pierrat et al., 1997). This mouse model develops extensive β -amyloid pathology. A β deposits are first observed at six months of age which increase in size and number with age of animals and eventually this transgenic mouse develops extensive β -amyloid pathology. Deficits in spatial memory have been observed in the Morris water maze at three months, becoming more severe with age (Van Dam et al., 2003).

These characteristics make these three mouse models very useful to investigate other features of AD such as the CNS inflammation. Specifically, the early formation of amyloid deposits in these mouse models separate AD pathology from ageing and allow for distinguishing the effect of ageing and amyloid beta on microglia.

1.3 Adrenergic system

The adrenergic system is a part of the autonomic nervous system's fight-or-flight response and consists of two neurotransmitters adrenaline and noradrenaline (NA). The main source of NA in the CNS is the locus coeruleus (LC) which is located in the brain stem. Long neural projections of the LC can innervate major brain regions as well as the spinal cord to provide them with NA (Swanson & Hartman, 1975).

So far different roles for NA have been investigated, such as attention and focus, emotion and depression, learning, memory and cognition (Benarroch, 2009). Besides its role as a neurotransmitter, NA has anti-inflammatory properties.

1.3.1 Effect of noradrenergic signalling on microglia

NA has several strong effects on microglial functions. For example it suppresses the proliferation of microglia (Fujita et al., 1998) and the production of pro-inflammatory cytokines and molecules such as Tumor necrosis factor alpha (TNF α), NO, IL-1 β , IL-6 (Dello Russo et al., 2004) and IL-12p40 (Prinz et al., 2001). It promotes migration of microglia and production of anti-inflammatory cytokines (Gyoneva & Traynelis, 2013). On the other hand, it seems that NA primes microglia and leads to higher cytokine production when it is used prior to the LPS stimulation (Johnson et al., 2013).

It has also been shown that adrenergic receptor (AR) stimulation suppresses microglial activation and leads to attenuation of cognitive deficits in hippocampus after LPS induced systemic inflammation (http://www.neurology.org/content/82/10_Supplement/P1.248).

1.3.2 Effect of noradrenergic system on cognition and AD symptoms

Since 1975 it has been proposed that NA affects learning (Bias et al., 1975). Besides, alterations in NA have been linked to cognitive and neuropsychiatric symptoms seen in normal ageing, AD or other dementias. In particular, AD is not only about dementia but also about physiological and behavioural changes. Mood, attention and motivation which are-

high extend- impaired in AD, could be the result of degenerated adrenergic neurons in LC (Sara, 2009). Other symptoms of AD such as psychotic phenomena, aggression and depression correlate with NA reduction in brains of AD patients (Forstl et al., 1994; Weinshenker, 2008).

In addition, increasing amyloid beta phagocytosis by microglia after β -AR activation has been indicated. This gives increasing importance to this receptors and their agonists. Since in neurodegenerative diseases such as AD, one of the features that exacerbates the disease progression is ongoing inflammation by overactivation of the innate immune system in the CNS, suppression of this system could be beneficial. By now, it is well proved that the LC region and amount of noradrenaline in the brain of AD patients and some of AD tg mice have been dramatically reduced. It is believed that this reduction occurs even before the disease symptoms. However, it is not well clarified if reduction of the noradrenergic system activity is initiating the AD but these studies suggested a potential role of the noradrenaline system in the disease treatment (Iversen et al., 1983; Bondareff et al., 1987; Matthews et al., 2002; Heneka et al., 2010).

1.4 Adrenergic receptors

It has already been known that a variety of neurotransmitters can regulate morphology and functions of macrophages including microglia. Neurotransmitters are released from synapses of neurons and bind to their receptors on the postsynaptic membrane and are used for cell-cell communication. Neurons are not the only cells which have neurotransmitter receptors. Immune cells such as microglia possess them as well. Microglia have receptors for most known neurotransmitters. In particular, they express plenty of adrenergic receptors (ARs) (Tanaka et al., 2002).

The adrenergic receptors (or adrenoceptors) are a class of G protein-coupled receptors (GPCR). There are two main groups of adrenergic receptors: α (α_1 , α_2) and β (β_1 , β_2 , β_3). Both groups are linked to adenylate cyclases. Binding of agonists to the adrenergic receptors leads to intracellular production of the second messenger cyclic adenosine monophosphate (cAMP) from adenosine triphosphate (ATP) by adenylate cyclases.

cAMP is a signal transducer which activates either protein kinase A (PKA, cAMP-dependent protein kinase) or Exchange proteins activated by cAMP (Epac). Activated PKA can directly

phosphorylate target proteins to increase or decrease their activities. Alternatively, it can directly activate the transcription factor cAMP response element-binding protein (CREB) which binds to certain DNA sequences called cAMP response element (CRE) being usually located upstream of genes, within the promoter or enhancer sites. Therefore, binding of CREB to CRE regions modifies transcription of downstream genes and, eventually, synthesis of the proteins (reviewed by Scanzano & Cosentino, 2015).

1.5 Aims of the thesis

Project 1 (Characterization of microglia in the 5XFAD mouse model)

It has been known that inflammatory processes -due to the microglial overactivation- play important roles in Alzheimer's disease (AD) progression. Besides, impairment of phagocytic activity of microglia leads to accumulation of A β peptides which in return, by binding to the microglial pathogen recognition receptors, initiate innate immune responses (reviewed by Heneka et al., 2015).

To investigate whether these microglial alterations in an AD environment are permanent or temporary, the present PhD project aimed at investigating the tissue influences on microglial properties and to determine whether the cells still have the capacity to perform normal outside the diseased brain, suggesting that their functional impairment could be corrected.

Therefore, the current study consisted of three main characterizations of microglia isolated from 3, 6 and 9 months old 5XFAD mice and aged-matched WT controls:

- The phagocytic capacity of these microglia for myelin, E. coli and A β peptides.
- The activity to produce cyto-/ chemokines after being treated with a battery of TLRs agonists.
- Their proliferation rate with or without LPS treatment.
- Their TLR4 activity in terms of effects on phagocytosis, production of pro-inflammatory cyto-/ chemokines and recruitment of immune cells from the periphery.

Project 2 (Amyloid beta (A β) plaque-associated microglia priming in transgenic mouse models of Alzheimer's disease)

Recent studies on microglia in a close distance to A β depositions have revealed overexpression of activation markers on these cells. Also, in both human and AD transgenic mice, exposure of these microglia to various secondary stimuli led to an enhanced inflammatory reaction described as being primed (reviewed by Perry & Holmes, 2014). To study the A β -associated microglia priming in mouse models of AD, the current project aimed

at investigating three well-established AD mouse models, APP23, APPswePS1dE9 and 5XFAD compared to aged matched WT mice.

Main questions in this project included:

- Expression status of immune cells activation markers (Mac-2, CD68 and MHC II) on microglia close or far from the A β plaques.
- Gene expression analysis of MHC II negative and positive microglia from the 5XFAD mouse model.
- Effect of systemic LPS injection on microglial activation close or far from A β plaques.

Project 3 (Noradrenergic control over innate immune cell activities in the CNS)

Anti-inflammatory roles of the adrenergic system in neuroinflammatory diseases such as AD have been observed. In general, improvements in the AD pathology by activation of this system indicate a likely direct effect on the inflammation and immune cells which results in inhibition of pro-inflammatory factors production (reviewed by Scanzano & Cosentino, 2015). Previous studies showed a selective effect of beta 2 adrenergic receptor (β 2AR) signalling on inhibition of pro-inflammatory cyto-/ chemokines (master's thesis of Stefanie Riesenber; doctoral thesis of Tommy Regen). The present project aimed to further investigate the effect of β 2AR activation on microglial activity and answer the question how some pro-inflammatory proteins or genes are able to escape from the inhibitory effect of β 2AR signalling.

The key questions consisted of:

- Investigation of β 2AR signalling on TRIF dependent genes.
- *In vivo* investigation of β 2AR activation on LPS stimulated microglia in terms of activation and immune cells recruitment from the periphery.
- Analysing the activity of cAMP pathways (PKA and Epac).
- Studying the gene expression analysis of β 2AR signalling on LPS-stimulated microglia, *ex vivo*.

2 Materials and methods

2.1 Animals

Neonatal C57BL/6J wild type (WT) mice were provided by the central animal facility of the University Medical Center Göttingen. Neonatal NMRI mice were obtained from department of Physiology at the University Medical Center Göttingen. Adult C57BL/6J WT mice were either from the breeding of hemizygote 5XFAD and WT mice or purchased from Charles Rivers.

2.1.1 5XFAD

The 5XFAD mouse model has been previously described (Oakley et al., 2006). In summary, it is a double transgenic APP/PS1 model that co-expresses five familial AD mutations in *human- (h) APP* and *hPSEN1* which are expressed under control of a neuron-specific murine Thy-1 promoter: APP695 carrying Swedish, Florida, and London mutations and PSEN1 carrying the M14 6L and L28 6V mutations.

Two Hemizygote 5XFAD male mice which were backcrossed on C57BL/6J for more than 10 generations were kindly provided by Prof. Dr. Thomas A. Bayer to be routinely crossbred with WT females to establish the mouse line. All the mice were housed and handled according to guidelines for animal care at the central animal facility of University Medical Center of Göttingen, Germany. *In vivo* experiments were approved by the animal ethical committee of University of Göttingen (Ausnahmegenehmigung nach § 9 Abs. 1 Satz 4 Tierschutzgesetz). For the experiments male and female 5XFAD and the WT littermates from three different ages (3, 6 and 9 month old) were used (N=5-6).

2.1.2 APP23

APP23 mice express the human APP751 gene containing the Swedish double mutations, associated with early-onset familial AD, under the Thy-1 promoter. The mice were backcrossed to C57/BL6 for more than 6 generations, and genotypes were identified by PCR. Experiments were carried out according to the European Council Directive (86/609/EEC) and were approved by the local Ethical Committee on Animal Experimentation. Male heterozygous APP23 and the WT littermates were recruited from different ages, 6 months old (APP23 N=20; WT N=20), 16 months old (APP23 N=9; WT N=10), 20 months old (APP23 N=14; WT N=20), 24 months old (APP23 N=11; WT N=10).

2.1.3 APP/PS1 (APP^{swe}PS1^{dE9})

APP^{swe}PS1^{dE9} transgenic mice express a chimeric mouse/human APP⁶⁹⁵ gene recruiting the Swedish double mutations, K670M/N671L, (Mo/HuAPP^{swe}; line C3-3) and human presenilin-1 (PSEN-1) gene with an exon-9 deletion mutation (PS1^{dE9}; line S-9; Jankowsky et al., 2004). Transgenic mice and WT littermate pairs were housed under standard conditions. Experimental procedures were approved by the animal ethical committee of the Royal Netherlands Academy of Arts and Sciences. For immunohistochemistry and immunofluorescence, transgenic and WT animals were studied at the age of 18 months old (APP^{swe}PS1^{dE9} N=3; WT N=3).

2.2 Genotyping of 5XFAD mice

2.2.1 Isolation of mouse tail DNA

A small piece of mouse tail was immersed into 500 µl of lysis buffer (containing 100 µM Tris pH 8.5, 5 mM EDTA, 200 mM NaCl and 0.2% SDS) and incubated overnight at 55°C in a thermomixer (Eppendorf, Germany) with continuous agitation (500 g). It was centrifuged for 10 min at 200 g at RT. Supernatant was collected and mixed well with 500 µl of ice-cold 2-propanol, followed by 10 min centrifugation at 200 g. Afterwards, supernatant was discarded and the pellet was washed once with 750 µl 70% ethanol. Remaining pellet was dried using a vacuum (Eppendorf) for 20 minutes and resuspended in 35 µl H₂O. DNA concentration was assessed with a spectrophotometer (Nanodrop, Peqlab; Biotechnologie GmbH).

2.2.2 Polymerase chain reaction (PCR)

To screen for hemizygote animals, only *hAPP* sequence was amplified, since mutated *hAPP* and *PSEN1* are co-expressed simultaneously in 5XFAD mice. Following *hAPP* primers used: Forward 5'-GTAGCAGAGGAGGAAGAAGTG-3' and Reverse 5'-CATGACCTGGGACATTCTC-3'. PCR was performed with conditions described in Table 1 by Master cycler (Eppendorf).

Table 1: PCR conditions

Temperature	Duration	Number of repeats
94°C	3 min	1 x
94°C	45 s	} 29 x
61°C	1 min	
72°C	1min	
72°C	5 min	1 x
4° C	∞	

2.3 Microglial primary culture and harvests

All microglia cultivations were carried out in Dulbecco's modified Eagle's medium (DMEM, Life technologies/Gibco, Karlsruhe, Germany), including 10% fetal calf serum (FCS, Invitrogen/Gibco), 100 U/ml penicillin and 100 µg/ml streptomycin (both Biochrom, Berlin, Germany) as complete DMEM.

2.3.1 Neonatal microglial culture

P0/P1 WT C57BL/6J mice were quickly decapitated by scissors. The skulls were removed and the brains were kept in Hanks balanced salt solution (HBSS, Biochrom, Berlin, Germany) on ice. Subsequently, removal of meninges and blood vessels was performed under an inverted microscope, and brains were transferred to a clean HBBS. The brains were washed three times with 10 ml of fresh cold HBBS. After the last wash the salt was removed and 100 µl of 2.5% Trypsin (Biochrom) per brain was added. Brains were shortly vortexed with half speed and incubated for 5 min in a water bath at 37°C twice. Trypsin digestion was stopped by adding 1 ml complete DMEM. To remove excessive DNA, 40 µl of 0.4 mg/ml DNase (CellSystem, St.Katherine, Switzerland) per brain was added. Brains were thoroughly resuspended and incubated at 37°C for 2-3 min. Large pieces of tissue were mechanically separated using pipetting force and were centrifuged for 10 min at 200 g at 4 °C. After centrifugation, the medium was removed and the remaining pellet was resuspended in 1 ml complete DMEM per brain. To culture the cells in flasks, the flasks were previously coated with 10 ml Poly-L-Lysin (PLL, Invitrogen/Gibco) and incubated for 20 min at RT. Then, three times washed with sterile ddH₂O and one time with complete DMEM. Cells resuspended in 15 ml DMEM were added to 75 cm² flask. Flasks were incubated at 37°C, 5% CO₂. Next day cells were washed thrice with pre-warmed phosphate-buffered saline (PBS;

Life Technologies/Gibco) and once with complete DMEM. 15 ml of fresh complete DMEM was added to the flask and incubated at 37°C with 5% CO₂, an additional change of medium was performed on the following day. One week after brain preparation, cells received 5 ml conditional L929 medium mixed with 10 ml complete DMEM to stimulate microglial growth. For each Microglia harvest, flasks were gently shaken for about 30 min at 37°C to detach microglia from the surface. Freed microglia were washed with fresh DMEM and resuspended in a small volume of DMEM (depending on size of cell pellet). Cells were counted with a cell counting machine (cellometer™ Auto T4; Nexcelom Bioscience) and plated in the desired densities.

2.3.2 Adult microglial culture

3, 6 or 9 months old WT C57BL/6J and 5XFAD mice were anesthetized with Isoflorane (100%; Obvie[®]) and decapitated. Brains were isolated and divided into cerebral hemispheres, brain stem and cerebellum. Meninges and blood vessels were removed from each part and the parts were, subsequently, cut into small pieces (~1 mm³) and washed with HBSS. Enzymatic treatments and further washings were performed as described for preparation of neonatal microglia (refer to 2.3.1). To produce single cell suspensions, cells were additionally passed through cell strainers (Falcon[®]) with 40 µm pore size. Cells were seeded into 75 cm² tissue culture flasks which contained a 100% confluent monolayer of astrocytes from neonatal NMRI mice, which was shown to be necessary for an appropriate growth supply of the cultured adult microglia. The adult microglia were harvested every 7 days following conditional L929 medium stimulation.

2.4 Astrocyte culture

To prepare pure astrocyte cultures, neonatal NMRI mice were used. Cells were prepared as described in neonatal microglia cultures (refer to 2.3.1), but in contrast, a week after the preparation, cells were incubated with complete DMEM containing 200 µg/ml dichloromethylenedisphosphonic acid disodium salt (Clodronate; Sigma-Aldrich, Taufkirchen, Germany) for 48 hours at 37°C, 5% CO₂ to eliminate myeloid cells. Afterwards, cells were shaken at about 260 rpm for minimum of 12 hours to get rid of dead myeloid cells. Then, flasks were washed once with pre-warmed complete DMEM and incubated for less than 4 days to serve for adult microglia culture preparation.

2.5 L929 mouse fibroblast culture

L929 fibroblasts were cultured in complete DMEM and passaged every 2 weeks (1:5). 14 days later supernatants were collected and stored at -20°C for further usage to stimulate microglial proliferation. After 30 passages, fresh L929 cultures were established.

2.6 Bone marrow derived macrophages (BMDMs) preparation

8-12 weeks old WT C57BL/6J mice were sacrificed by cervical dislocation. The bodies were disinfected with 70% ethanol and femurs were extracted by sterile scissors and forceps. The residual muscle tissue was removed by paper tissues soaked with 70 % ethanol and the femurs were flushed using syringe with Pluznik medium (DMEM with L-Glutamine; Invitrogen/Life Technologies) containing 10 % FCS (Invitrogen/Gibco), 5% horse serum (Sigma-Aldrich), 1% sodium pyruvate (Sigma-Aldrich), 1% 5 mM β 2-mercaptoethanol (Sigma), 100 U/ml penicillin and 100 μ g/ml streptomycin. Bone marrow from two femurs were plated on one 10 cm-petri dish (Sarstedt, Nümbrecht, Germany) with 10 ml Pluznik medium and incubated at 37°C and 5% CO₂. A day after, cells in medium were collected into 50 ml tubes, centrifuged 10 min at 200 g at 4°C and resuspended in 40 ml of Pluznik medium. The resulting cell suspension was divided to four parts and each part was plated on 10-cm petri dish and medium was exchanged three days later. Differentiated BMDMs were harvested on day 7 by addition of 4 mM Trypsin/EDTA, followed by incubation at 37°C for 10 min. Cells were washed with complete DMEM, and plated in 96-well plates at a density of 1.5×10^4 cells per well. Cells were incubated over night at 37°C, 5% CO₂ and stimulated on the next day.

2.7 *Ex vivo* microglia and BMDMs stimulation

Various compounds (described in Table 2) were dissolved and diluted in complete DMEM and added to cells for respective experiments.

Table 2: Constituents used for *ex vivo* stimulations

Stimuli	Function	Catalogue No.	Provider
Smooth chemotype LPS, Escherichia coli, serotype O55:B5 (S-LPS)	TLR4 agonists	ALX-581-013	Enzo Life Sciences/Alexis
Rough chemotype LPS, E.	TLR4 agonists	ALX-581-007	Enzo Life

Materials and methods

coli, serotype R515 (Re-LPS)			Sciences/Alexis
Bovine plasma Fibronectin	TLR4 agonists	F-1141	Sigma
Mouse plasma Fibronectin	TLR4 agonists	MFBN	Molecular Innovations
Pam3CSK4	TLR1/2 agonist	165-066-M002	Enzo Life
			Sciences/Alexis
Poly (I:C), TLRgrade™	TLR3 agonist	ALX-746-021	Enzo Life
			Sciences/Alexis
Poly (A:U)	TLR3 agonist	P1537	Sigma
MALP-2	TLR6/2 agonist	APO-54N-018	Enzo Life
			Sciences/Alexis
CpG ODN, TLRgrade™	TLR9 agonist	764-020	Enzo Life
			Sciences/Alexis
Recombinant mouse interferon- γ (IFN γ), carrier-free		485-MI/CF	R&D Systems
IL-4, carrier-free		404-ML/CF	R&D Systems
IL-10		417-ML/CF	R&D Systems
HJC0197	Epac 1&2 inhibitor	C 136	Biolog
ESI-09	Epac 1&2 inhibitor	B 133	Biolog
ESI-05	Epac 2 inhibitor	M 092	Biolog
8-pCPT-2'-O-Me-cAMP	Epac activator	C 041	Biolog
N6-Benzoyl-cAMP	PKA activator	B 009	Biolog
Forskolin	Adenylyl cyclase activator	F686	Sigma
Salbutamol	β 2-adrenoceptor agonist	S8260	Sigma
ICI 118,551 hydrochloride	β 2-adrenoceptor antagonist	I127-5MG	Sigma

LPS, lipopolysaccharide; TLR, toll-like receptor; IL-, interleukin-; Epac, exchange factor directly activated by cAMP; PKA, protein kinase A.

IIR PKI (Cell-permeable PKA inhibitor) was kindly provided by Prof. Dr. Viacheslav Nikolaev (University Medical Center Göttingen, Germany).

Depending on experiments incubation time varied. Regardless of the stimulation protocol, all cells were incubated at 37°C with 5% CO₂.

2.8 Cyto- and chemokine measurement in the supernatants of cells

Microglia and BMDMs were cultured with density of 1.5×10^4 /well in 96 well-plate (Cellstart^R, Greiner bio-one) and were incubated with respective stimuli and kept for 18 h at 37°C with 5% CO₂. Then, supernatants were collected and stored at -20°C until assayed. The soluble factors in the supernatants were quantified by enzyme-linked immunosorbent assay (ELISA) test systems. CCL3 (macrophage inflammatory protein, MIP-1a), CCL5 (regulated upon activation normal T-cell expressed and presumably secreted, RANTES), CXCL1 (keratinocyte-derived chemokine, KC), CXCL2 (macrophage inflammatory protein 2, MIP-2) and Interleukin (IL-) 6 were measured using DuoSet[®] ELISA Development Kits (R&D Systems). For CCL2 (monocyte chemoattractant protein, MCP-1) measurement, ELISA Kits from R&D Systems and BioLegend (San Diego, CA, USA) were used. Tumor necrosis factor α (TNF α) and interferon β (IFN β) levels were measured using an ELISA kit from BioLegend (San Diego, CA, USA). Total IL-12p40 (including monomeric p40) amounts were defined by an ELISA kit from eBioscience (San Diego, CA, USA). All the assays were performed according to the manufacturer's instructions. Absorbance was measured at 450 nm and also 540 nm as reference wavelength by a microplate reader (Bio-Rad). Results were calculated by a Microsoft Excel program (macro) which was developed by Dr. Jörg Scheffel and optimized by Ulla Gertig at the Institute of Neuropathology, University Medical Center Göttingen.

2.9 Cell harvest and preparation for flow cytometric analysis

Microglia were cultured in 12 well-plates (Cellstart, Greiner bio-one). Regarding different experiments, cells were treated with stimuli or phagocytic compounds and incubated at 37°C and 5% CO₂. Afterwards, microglia were harvested. To harvest the cells they were washed once with complete DMEM and once or twice with PBS. Then, they were incubated with 300 μ l of 0.05%/0.02% Trypsin/EDTA (Biochrom) for 3-5 min at 37°C and 5% CO₂. Trypsin effect was stopped by adding 600 μ l of complete DMEM and cells were scraped off the plate by cell scraper (Sarstedt). Cells were collected in 2 ml microcentrifuge tubes and kept on ice. Cells were centrifuged at 800 g at 4°C for 10 min and washed with FACS buffer (PBS containing 2% FCS, 0.1 % NaN₃ and 0.01 M EDTA pH 8.0). Fc receptors on the cells were blocked by anti- CD16/CD32 antibody (BioLegend) for 10 min at 4°C. Complement receptor, CD11b, MHC I and intracellular cytokines were stained by specific antibodies for 20 and 45 min in the dark, respectively (Table 3). Excessive antibodies were washed away by FACS buffer and cells were resuspended in 170 μ l FACS buffer, transferred to FACS tubes and

recorded by a flow cytometer (FACS Canto II). The data were analysed by Flowjo V10 (Tree Star, Ashland, OR, USA).

2.9.1 E. coli phagocytosis

Adult microglia with a density of 2×10^5 /well were incubated with 10 ng/ml Re-LPS for 24 h. Cells were washed and treated with 2×10^6 cfu/ml E. coli-DsRed (a pathogenic strain DH5 α ; kindly gifted by S. Hammerschmidt, Ernst Moritz Arndt University Greifswald, Germany; Sørensen et al., 2003) in DMEM with 10% FCS and 100 μ g/ml ampicillin (Sigma-Aldrich) for 2 h at 37°C and 5% CO₂. Afterwards, non-phagocytosed E. coli was eliminated by replacing the medium with DMEM containing 100 μ g/ml gentamicin (Sigma) for 1 hour. Cells were harvested and stained for FACS analysis as explained in chapter 2.9. CD11b positive cells which contained DsRed fluorescent were considered as E. coli-phagocytic microglia.

2.9.2 Myelin phagocytosis

Adult microglia were plated with a density of 2×10^5 cells/well. Cells were incubated with 10 ng/ml Re-LPS for 24 h before 5 μ g Rhodamine- or DyLight 550-conjugated mouse myelin was added to the cells for another 2 h of incubation. Afterwards, cells were washed, harvested and recorded as described in chapter 2.9. The percentage of myelin-phagocytosing microglia was calculated from CD11b positive cells.

Myelin was purified from freshly isolated 8-12 weeks old WT mice brains, as previously described (Norton & Poduslo, 1973) and labelled by Antibody labelling kit (Thermo scientific).

2.9.3 Amyloid beta phagocytosis

Microglia isolated from adult WT and 5XFAD mice were plated with a density of 2×10^5 cells/well. Cells were incubated with monomeric forms of HiLyte FlourTM 647-labelled A β ₁₋₄₀ or A β ₁₋₄₂ (250 nM) for two hours. Subsequently cells were washed, harvested and recorded as defined in chapter 2.9. The percentage of A β -phagocytosing microglia was calculated from CD11b positive cells.

2.9.4 MHC I expression

Microglia (2×10^5 per well) were treated with Re-LPS, Salbutamol or combination of both in complete DMEM for 24 h at 37°C and 5 % CO₂. Then, the stimuli were removed, cells were washed and harvested. In addition to CD11b, microglia were stained simultaneously with anti-mouse MHC class I antibody (BioLegend). Cell staining and flow cytometric analysis was performed as explained in chapter 2.9. For data analysis, mean fluorescent intensity (MFI) of MHC I signal was calculated from CD11b positive population.

2.9.5 Intracellular cyto- and chemokine staining for flow cytometry analysis

Microglia with a density of 3×10^5 per well were stimulated with indicated stimuli for 3 h at 37°C and 5 % CO₂. To block cyto- and chemokine release, a protein transport inhibitor, monensin, (BioLegend) was added to the cells for additional 5 h. Next, microglia were proceeded for extracellular CD11b staining as described in the section 2.9. Excessive CD11b antibody was washed away by 1 ml PBS. To fix and permeabilize the cells, they were resuspended in 200 µl Cytofix/Cytoperm™ solution (BD Biosciences) while slightly vortexing and kept for 20 min at 4°C in the dark and washed with 1 ml saponin buffer (0.1% Saponin (Sigma) in PBS). Intracellular Fc receptors were blocked using anti- CD16/CD32 antibody (BioLegend) in saponin buffer for 5 min at RT and subsequently cells were incubated with Phycoerythrin- (PE-) conjugated anti-mouse CCL5 (RANTES) monoclonal antibody or Alexa Fluor® 488 conjugated anti-mouse TNFα monoclonal antibody (both BioLegend) for 45 min in the dark. After the incubation time cells were washed with 1 ml of saponin buffer, resuspended in 170 µl of FACS buffer and recorded and analyzed as mentioned in section 2.9. Percentage of CCL5 (RANTES) and TNFα producing microglia were calculated from CD11b positive population.

Table 3: Antibodies used for flow cytometry analysis of cultured microglia

Antibody	Catalogue No./ Clone	Provider	Final dilution (in FACS buffer)	Final dilution (in Saponin buffer)
Anti-mouse CD16/CD32	101310/93	BioLegend	1:100	-
APC anti-mouse CD11b	M1/70/101212	BioLegend	1:200	-

Pacific Blue anti-mouse CD11b	M1/70/ 101224	BioLegend	1:200	-
eFluor [®] 450 anti-mouse CD11b	M1/70/ 48-0112-82	BioLegend	1:200	-
Alexa Fluor [®] 647 anti-mouse MHC I	34-1-25/ 114712	BioLegend	1:200	-
PE anti-mouse CCL5	2E9/ 149104	BioLegend	-	1:200
Alexa Fluor [®] 488 anti-mouse TNF α	MP6-XT22/ 506313	BioLegend	-	1:200

2.10 Cells proliferation assessment

Microglia from adult WT and 5XFAD mice were cultured with the density of 15×10^4 cell/well in 96 well-plates and were stimulated with Re-LPS (0.1 ng/ml and 10 ng/ml) for 24 hours (37°C, 5% CO₂). The supernatants were discarded and the proliferation of the cells was evaluated by an ELISA-based cell proliferation kit (R&D) according to the manufacturer's instructions.

2.11 Cell viability assessment

To check the toxicity of microglial stimuli, upon collecting the supernatants from cells, a solution of 10% water-soluble Tetrazolium salts (WST-1) reagent (Roche Applied Science) in complete medium was added to the cells, incubated for 3h at 37°C with 5% CO₂ and, subsequently, the amount of produced formazan (result of Tetrazolium salts reduction) was measured at 450 nm with reference wavelength of 655 nm by a microplate reader (Bio-Rad).

2.12 PKA activity assay

To determine activity of PKA inside the cells, a PKA kinase activity kit (Enzo life science) was used according the manufacturer's instructions. Neonatal microglia were plated in 6 well-plate (CellstartR, Greiner bio-one) with a density of 8×10^5 cells per well. Cells were incubated with Re-LPS, Salbutamol, Forskolin, 6-Bnz-cAMP, IIR-PKI (for detailed information refer to Table 2) for 20 min at 37°C, 5% CO₂. For IIR-PKI 30 min pre-incubation was applied. To prepare cell lysates, after the stimulation time, cells were washed once with pre-warmed PBS and incubated with 350 μ l cell lysis buffer (20 mM Tris-HCL (pH 7.5), 150

mM NaCl, 1 mM Na₂EDTA, 1 mM EGTA, 1% Triton, 2.5 mM sodium pyrophosphate, 1 mM β -glycerolphosphate, 1 mM Na₃VO₄, 1 μ g/ml leupeptin; Cell Signaling Technology) for 5 min on ice. Cells were scraped and centrifuged at 14,000 g at 4°C for 10 min. Supernatants were collected and stored at -80°C till assayed. Total protein concentration in the lysates was determined using micro BCATM Protein Assay kit (Thermo scientific) following the manufacturer's protocol.

2.13 Immunocytochemistry

5×10^4 microglia in complete medium (Gibco) were plated on PLL (Invitrogen/Gibco) pre-coated cover slips (Thermo Scientific) and incubated at 37°C with 5% CO₂. The next day, cells were washed once with pre-warmed PBS and fixed with ice-cold methanol (100%, Merck) for 5 min at -20°C. Cells then were washed three times with PBS, with gentle shaking for 5 min between each washing step. Cells were permeabilized and blocked with PBS-0.3% Triton-X100 (Thermo Scientific) containing 5% goat serum for 45 min at RT. Cells were incubated with 0.5% Beta 2 Adrenergic receptor (β 2AR) antibody in PBS-0.03% Triton-X100 containing 2.5% goat serum and 0.5% anti- CD16/CD32 antibody overnight at 4°C in the dark. The following day, cells were washed three times with PBS-0.03% Triton-X100 with gentle shaking for 5 min between the steps. 1% secondary antibody in PBS containing 2.5% goat serum and 0.03% Triton-X100 was added to the cells and incubated for 45 min at RT in the dark. Staining was continued with three times washings as mentioned above and cell nuclei were labelled with 0.1% DAPI in PBS for 2-3 min at RT. Cells were washed three times with PBS as above, dipped in deionized water and the cover slips were mounted on object slides (Thermo Scientific) by a fluorescent mounting medium (Dako). Pictures were taken by a fluorescent microscope (Olympus Bx51) using software cellSens Dimension 1.7 (Olympus Life Science).

Table 4: Antibodies used for Immunocytochemistry analysis

Antibody	Catalogue No.	Provider
Anti-mouse CD16/CD32	101310	BioLegend
Rabbit-anti-mouse Cy3-labelled β 2AR	bs-0947R-cy3	Bioss
Anti-Rabbit Alexa Fluor [®] 488-labelled IgG antibody	A11034	Life Technologies

2.14 Quantifying the number of cytokine secreting cells using ELISpot

In order to study percentage of cells which produce CCL5 (RANTES), mouse CCL5 Enzyme-Linked ImmunoSpot (ELISpot) kit (R&D Systems, USA) was used. The experiments were performed according to the manufacturer's instructions. In brief neonatal were plated on capture antibody-pre-coated 96 well-plates at a density of 1,000 cells per well in complete medium containing indicated stimuli (Re-LPS, Salbutamol or both). Cells were incubated at 37°C with 5% CO₂ for 24 hours. Afterwards, supernatants were removed and cells were washed four times with a washing buffer (0.05% Tween® 20 in PBS). Detection antibody was added to the wells and incubated overnight at 4°C. Wells were washed as described above and then kept with Streptavidin-AP for 2 h at RT in the dark followed by washing. For color development BCIP/NBT^R (R&D Systems) was added to wells and incubated for 15-30 min at RT. The plate was rinsed once with deionized water, the flexible plastic underdrain was removed and the plate was dried at 37°C. The spot number and area were analyzed by an automated ELISpot reader (AELVIS). The data were further analyzed by GraphPad Prism® 6 software.

2.15 RNA sequencing gene analysis

Microglia cells with a density of 8×10^5 were plated in a 6 well-plate (CELLSTAR, Greiner bio-one) in complete DMEM and incubated at 37°C with 5% CO₂. The next day, cells received medium or indicated stimuli solutions at the respective concentrations (10 ng/ml Re-LPS, 100 µM salbutamol, and a combination of both) and incubated for 3 h (37 °C and 5 % CO₂). Afterwards, cells were washed once with 1 ml pre-warmed PBS. 1 ml Qiazol[®]Lysis reagent (QIAGEN) was added, cells were scraped, cell suspensions were collected and incubated for 5 min at RT and finally frozen at -20°C. The RNA sequencing gene analysis (Illumina) from frozen samples was performed in collaboration with Microarray and Deep-Sequencing Facility (Transkriptomeanalyselabor, TAL, Göttingen; Dr. Gabriela Salinas-Riester). In brief, total RNA was sequenced using the TruSeq RNA Sample Preparation Kit (Illumina, Cat. N°RS-122-2002) starting from 500 ng. Accurate quantization of cDNA libraries was performed by QuantiFluor dsDNA System (Promega). The size range of final cDNA libraries was 300-320 bp and was determined by application to the Fragment Analyzer (Advanced Analytical). cDNA libraries were amplified and sequenced by the cBot and HiSeq2000 from Illumina (SR; 1×50 bp; 5- 6 GB ca. 30-35 million reads per sample).

Sequence images were transformed with Illumina software BaseCaller to bcl files, which were demultiplexed to fastq files with CASAVA v1.8.2. Quality check was done via fastqc (v. 0.10.0, Babraham Bioinformatics).

Bioinformatics analysis was performed by Dr. Thomad Lingner as followed: Sequences were aligned to the genome reference sequence of *Mus musculus* (GRCm38/mm10). Alignment was performed using the STAR alignment software (Dobin et al., 2013; version 2.3.0e) allowing for 2 mismatches within 50 bases. Subsequently, conversion of resulting SAM files to sorted BAM files, filtering of unique hits and counting was conducted with SAMtools (Li et al., 2009; version 0.1.18) and HTSeq (Anders, et al., 2014; version 0.6.1p1). Data was pre-processed and analyzed in the R/Bioconductor environment (<http://www.bioconductor.org>) using the DESeq2 package (Simon Anders & Huber, 2010; version 1.8). The data was normalized and tested for differentially expressed genes based on a generalized linear model likelihood ratio test assuming negative binomial data distribution. Candidate genes were filtered to a minimum of 2-fold change and FDR-corrected p-value < 0.05. Gene annotation was performed using *Mus musculus* entries from Ensembl (<http://www.ensembl.org>) via the biomaRt package (Durinck et al., 2005, version 2.18.0). GO and KEGG enrichment analysis on candidate genes was conducted with the Goseq package (Young, et al., 2010; version 1.2) using standard parameters. Identifiers of mouse genes relevant for cAMP and TLR pathways were extracted using the KEGG database.

2.16 Perfusion of the mice

To anesthetize adult mice they were injected intraperitoneally (i.p.) with 180 and 200 μ l 14% chloralhydrate (Merck) for females and males, respectively. After loss of consciousness, the chest was opened and through the left ventricle transcatheterial perfusion was applied. When brains were prepared for FACS analysis, mice were perfused with 1x PBS. For immunohistochemistry analysis in addition to PBS, 4% Paraformaldehyde (PFA) in PBS (pH 7.4) was used. To prepare brain lysates 0.09% NaCl (B. Braun) was used.

2.17 Intracerebral single injections and infusions

6 and 9 months old WT and 5XFAD mice from both genders were anesthetized i.p. by a combination of ketamin/xylazin (Medistar/Riemser) and following loss of consciousness heads were fixed on a stereotactic frame (model 900, David Kopf Instruments). To avoid eye dryness, eyes were covered with an eye and nose crème (Bepanthen[®]; Bayer). A rostral-

caudal excision was applied, a hole in the skull was placed by a 0.5 mm round-headed drill (Hager & Meisinger GmbH) at the position of 0.5 mm rostral and 1.5 mm right from the bregma. For the single injection (stab wounds) 1 µl of freshly prepared 1 mg/ml or 0.01 mg/ml S-LPS (ALX-581-013, Alexis Biochemicals) solution was placed in a syringe (1.0 µL Neuros Model 7001 KH SYR, Hamilton) which later got fixed on the stereotactic manipulator. The needle was inserted in the brain at depth of 3 mm from the skull surface and the stimuli was injected within 3 min. Upon removal of the syringe the skin was sutured or glued by Histoacryl[®] glue (B.Braun).

For long term infusions (24 or 72 hours) 8-12 weeks old WT female mice were anesthetized and prepared for the surgery as mentioned above. Freshly prepared 1 mg/ml Re-LPS (ALX-581-013, Alexis Biochemicals), 100 µM β2AR agonist Salbutamol (SB; Sigma-Aldrich), 100 µM β2AR antagonist ICI 118,551 hydrochloride (ICI; Sigma), combinations of Re-LPS with SB or ICI were placed in the micro-osmotic pumps (model 1007D, 0.5 µl/h) and were connected to cannulas of the Brain Infusion Kit 3 (both Alzet). Cannulas were fixed to the skull by Loctite 454 Adhesive Gel (Alzet). The pumps were placed under the skin on the back side the mice and the excision was sutured. Mice were injected with a pain killer (Rimadyl, 5 µg/10 g bodyweight; Pfizer, Germany) and placed in clean cages on heating plates with 37°C till the next day.

In case of 72 hours deliveries, 2 days before the surgery mice were provided with the pain killer Novaminsulfon (Metamizol; Ratiopharm, Germany) in their drinking water.

After the indicated period of time, mice were sacrificed and perfused, as described in chapter 2.16 and used for flow cytometry analysis or immunohistochemistry.

2.18 Intraperitoneal injections

12 months old WT and 5XFAD, male and female, mice were injected by freshly prepared LPS (Lipopolysaccharides from Escherichia coli 0111:B4; Sigma-Aldrich) in PBS at amount of 1 mg/kg of the weight in 200 µl volume. 200 µl PBS was injected in control mice. 10 h later, mice were perfused with NaCl as mentioned in chapter 2.16. Brains were used for immunohistochemistry and gene expression analysis.

2.19 Preparation of brains for flow cytometry

Following perfusion of mice with PBS (described in section 2.16) brains were isolated and kept in HBSS without Mg^{2+} and Ca^{2+} (Sigma-Aldrich) on ice. Further procedure was performed using the Neuronal Tissue Dissociation Kit (T) (Miltenyi Biotec, Germany) in combination with the gentleMACS™ Dissociator (Miltenyi Biotec) according to the manufacturer's instructions. Using two different Percoll™ (GE Healthcare Life Sciences, Germany) dilutions, 37% and 70%, in complete DMEM leukocytes were isolated as followed: single cell suspensions were resuspended in 37% Percoll and placed on the 70% percoll solution and centrifuged at 500 g at 4°C for 25 min without acceleration and brake forces. The interphase layer containing immune cells was carefully collected and washed with FACS buffer (centrifuged for 10 min at 300 g at 4°C). Fc receptors were blocked by anti-mouse CD16/CD32 antibody for 10 min at 4°C and stained with 50 µl antibody mixtures against CD11b, Ly-6C, Ly-6G, CD45 diluted in FACS buffer (Table 5). Subsequently, the cells were washed with FACS buffer and resuspended in 300 µl FACS buffer and recorded by a FACS CantoII (BD Bioscience). Data were analyzed by FlowJo (Tree Star, Ashland, OR, USA).

Table 5: Antibodies used for flow cytometry analysis of brain

Antibody	Catalogue No./ Clone	Provider	Final dilution (in FACS buffer)
Anti-mouse CD16/CD32	101310/ 93	BioLegend	1:50
Pacific Blue anti-mouse Ly-6G	127612/ 1A8	BioLegend	1:33
PerCP anti-mouse CD45	103130/ 30-F11	BioLegend	1:50
APC anti-mouse Ly-6C	128016/ HK1.4	BioLegend	1:50
PE anti-mouse CD3	100308/ 145-2C11	BioLegend	1:50
FITC anti-mouse/human CD11b	101206/ M1/70	eBioscience	1:33

2.20 Immunohistochemistry

Two different approaches were performed for Immunohistochemistry.

2.20.1 Immunohistochemistry of intracerebral infused brains

Mice were perfused with PBS and paraformaldehyde (PFA; 4%), as described in section 2.16 and decapitated. Skins were removed from the skull and the head was transferred into 4% PFA in PBS (pH 7.4) for post-fixation (2-3 days at 4°C). PFA was replaced by PBS and stored at 4°C until further preparation. Brains were carefully removed, and cut into two coronal parts at the position of infusing needle. Brain sections were dehydrated overnight through a series of graded alcohol/xylene/paraffin by an automated tissue processor (EXCELSIOR ES, Thermo Scientific) and then embedded in the paraffin. Dehydrations and embeddings were kindly performed by Uta Scheidt at the department of Neuropathology, UMG.

Paraffin embedded sections were sliced at a thickness of 3 µm by a sliding microtome (SM 2000R, Leica) and stained. For staining, dried sections on object slides were deparaffinized by incubating them for 5 min in 100%, 95% and 85% Xylol, and 70% alcohol and eventually distilled water. Sections were rinsed twice in PBS-Tween 20 (PBS-T, 0.02%) and incubated in Hydrogen peroxidase (2%, diluted in 60% methanol) for 60 min and rinsed once in PBS-T for 10 min. Unspecific binding was blocked by Blocker A (combination of 2% bovine albumin, 0.3% milk powder and 0.5% donkey normal serum in PBS-T) for 60 min. Primary antibodies, diluted in Blocker A were added to the sections and incubated overnight at RT followed by three washing steps by PBS-T (each 10 min). Subsequently, sections were incubated with secondary biotinylated antibodies (diluted in 2 parts PBS-T and 1 part Blocker A) for 60 min. Three washing steps were applied as described above. Following incubation with extravidin peroxidase (1:2000 in PBS-T) and three washings, sections were kept for 5 min in Tris-HCL and DAB/Nickel (20 mg ammonium nickel (II) sulfate, 100 µl DAB [2mg DAB in 100µl distilled water] and 2.5 µl H₂O₂ in 5 ml Tris-HCl) was used for the color development. Sections were rinsed once in Tris-HCL for 5 min, twice in PBS-T and PBS, (10 min each), and finally in distilled water. Tissue was dehydrated in graded alcohol series and mounted with Entellan[®] (Merck). Pictures were taken by Leica SM 2000R microscope and were analysed by ImageJ software.

Slicing and staining of the sections were generously accomplished by Katja Reimann at the Paul-Flechsig-Institute for Brain Research (Medical faculty of Leipzig University).

Table 6: Antibodies used for immunohistochemistry analysis of intracerebral infused mice

Primary Antibody	Catalogue No.	Host	Provider	Final dilution
Iba-1	019-19741	Rabbit	Wako	1:800
Mac-3	10850	Rat	BioLegend	1:200
GFAP	Z0334	Rabbit	Dako	1:600
Secondary Antibody				
anti-Rabbit	711-065-152	Donkey	Dianova	1:1000
anti-Rat	712-065-150	Donkey	Dianova	1:1000

2.20.2 Immunohistochemistry of intraperitoneal injected mice

Mice were perfused with NaCl as explained in the section 2.16. Brains were cut sagittally into two parts. One half was kept in 4% PFA, overnight at 4°C and was processed the next day as followed: tissue was transferred to 1% PFA for 2-3 days. The PFA was replaced by 25% sucrose in PBS for 1 day at 4°C. Subsequently, brains were frozen at -50°C in a cryostat, and sectioned at 14 µm or 40 µm thickness for immunohistochemical or immunofluorescence stainings, respectively. Sectioning and staining of the brain samples from intraperitoneal injected mice were performed by Zhuoran Yin (Department of Neuroscience, University medical center Groningen, the Netherlands).

2.20.2.1 Immunohistochemistry and Congo red staining

Sections were fixed by 4% paraformaldehyde in PBS for 10 min and three times rinsed by PBS. The sections were pre-incubated in 0.3% H₂O₂ for 30 min and blocked by 10% normal goat serum (NGS) in PBS+0.3% Triton-X100 (Merck, Darmstadt, Germany) for 30 min followed by primary antibodies incubation diluted in PBS+0.3% Triton-X100+1% NGS, overnight at 4°C. Biotinylated goat anti-rabbit (1:400, Vector BA1000), or biotinylated rabbit anti-rat (1:400, Vector BA4001) was used as the secondary antibody. To determine the protein expression the avidin-biotin-peroxidase method (Vectastain ABC kit, Vector Laboratories, PK-6100) or AEC substrate chromogen solution (DAKO, K4009) with DAB (105H3705, Sigma) were used. To visualize amyloid fibrils Cresyl violet or Congo red staining was performed on Iba1, Mac-2, MHC II, CD68, IL-1β or ASC immuno-stained sections according to a standard protocol (Puchtler et al., 1967). After Congo red staining, the apple green birefringence could be observed under polarized light microscopy.

Table 7: List of antibodies used for immunohistochemistry analysis of intact or intraperitoneal injected mice

Primary Antibody	Catalogue No.	Host	Provider	Final dilution
Iba-1	019-19741	Rabbit	Wako	1:1000
IL-1 β	500-P 51	Rabbit	PeptoTech	1:750
Mac-2	CL8942AP	Rat	Cedarlane	1:1000
MHC II	14-5321	Rat	eBioscience	1:100
CD68	MCA1957GA	Rat	AbD Serotec	1:200
ASC	AL177	Rabbit	Adipogen	1:200
4G8	800701	Mouse	BioLegend	1:500
CD11c	14-0114	Armenian Hamster	eBioscience	1:100
Dectin-1	MCA2289	Rat	AbD Serotec	1:100
Lamp2	ab37024	Rabbit	Abcam	1:100
Trem2b	MAB17291	Rat	R&D	1:100
Secondary Antibody				
anti-rabbit	BA1000	goat	Vector Laboratories	1:400
anti-rat	BA4001	rabbit	Vector Laboratories	1:400
anti-mouse	BA2000	horse	Vector Laboratories	1:400
anti-hamster	6060-02	goat	Southern Biotechnology	1:100

2.20.2.2 Immunofluorescence and confocal imaging

For immunofluorescence staining, sections were rinsed shortly in PBS and blocked by 10% normal goat serum in PBS+0.3%Triton X-100 for 1h at RT. Sections were incubated overnight at 4°C with primary antibodies (refer to Table 7) diluted in 1% normal goat serum in PBS+0.3% Triton X-100. The next day, the free floating brain sections were rinsed by PBS thrice and incubated with the secondary antibodies for 2 hours. Three times washings with PBS were applied and the sections were incubated in Hoechst (1:1000, Fluka) for 10 min and eventually mounted on StarFrost® glass slides and embedded in Mowiol (Calbiochem, the Netherlands).

Confocal images were acquired with a Leica Sp8 confocal microscope with LASAF software. The z-maximum-intensity projection function of ImageJ was used to optimize the appearance of microglia processes.

Table 8: List of secondary antibodies used for immunofluorescence staining

Secondary Antibody	Catalogue No.	Host	Provider	Final dilution
anti-rabbit Alexa 488	A21070	chicken	Molecular Probes	1:400
anti-rat Cy3	712-165-150	donkey	Jackson Immuno Research	1:700

2.20.2.3 Quantification of Mac-2, CD68 and MHC II stainings

Brain sections of 20 months old WT and APP23 mice i.p. injected with PBS or LPS were stained with Mac-2, CD68 and MHC II as mentioned in 2.20.2. For each staining the area covered by DAB positive cells was measured. To compare PBS- with LPS-treated mice, the whole cortical area ($6.69 \pm 3.36 \text{ mm}^2$) was defined as total area. To analyze PBS and LPS effect in ‘plaque-’ and ‘non-plaque’ regions in APP23 mice, the areas containing amyloid plaques were considered as ‘plaque area’ and set as total area ($0.017 \pm 0.001 \text{ mm}^2/\text{area}$) and the regions without plaque depositions were defined as ‘non-plaque area’ and set as total area ($0.017 \pm 0.001 \text{ mm}^2/\text{area}$). In each animal 6 ‘plaque areas’ and 3-4 ‘non-plaque regions’ were analyzed. The morphological analysis was performed by TissueFAXS microscope (TissueGnostics GmbH, Austria).

2.21 Cell sorting from brains by flow cytometry for gene expression analysis

The cell sorting method was slightly modified from Raj et al., 2014. In brief, 9 months old WT and 5XFAD (male and female) mice were perfused with NaCl as mentioned in section 2.16 Brains were collected and kept in Medium A (HBSS containing 0.6 % glucose and 15 mM HEPES buffer). Tissue was homogenized with the glass homogenizer (Glass potter, Braun Melsungen, Germany) until a cell suspension was obtained. The suspension was then filtered through a 70 μm cell strainer and centrifuged at 220 g for 10 min at 4°C. Supernatant was discarded and the residual pellet was resuspended thoroughly in 15 ml percoll gradient (22%, GE Healthcare), 77% myelin gradient buffer (5.6 mM $\text{NaH}_2\text{PO}_4 \cdot 2\text{H}_2\text{O}$, 20 mM $\text{Na}_2\text{HPO}_4 \cdot 2\text{H}_2\text{O}$, 140 mM NaCl, 5.4 mM KCl, 11 mM Glucose) and 40 mM NaCl. 3 ml of

PBS was added carefully on top of the suspension and centrifuged at 950 g for 20 min (acceleration of 4, brake of 0) at 4°C. The interface layer containing microglia and macrophages between Percoll and PBS was collected and washed with PBS. Fc receptors on the cells were blocked with anti-CD16/CD32 antibody for 15 min at 4°C. Cells were stained with respective cell surface antibodies (CD11b, CD45, Ly6C and MHC II) and incubated for 30 min on ice. Cells were washed with Medium A and eventually resuspended in Medium A and transferred to FACS tubes with cell strainer. Using 1µl of Propidium Iodide (Sigma) staining, viable cells were sorted by BD FACSAria™ II (BD Biosciences) with 85 and 100 µm nozzle diameter and collected in RLT lysis buffer (QIAGEN) followed by 30 s vortexing. Samples were stored at -80°C till RNA extraction. To extract RNA, RNeasy Plus kit (QIAGEN) was used following the provider's instructions. RNA extraction was kindly performed by Zhuoran Yin (Department of Neuroscience, University medical center Groningen, the Netherlands).

RNA was finally analyzed for over 800 specific microglial gene expression patterns in collaboration with Lundbeck Company (New York, United States).

Table 9: Antibodies used for sorting brain cells

Antibody	Catalogue No./ Clone	Provider	Final dilution (in Medium A)
anti-mouse CD16/CD32	101310/93	BioLegend	1:100
BV421 anti-mouse/human CD11b	101236/M1/70	BioLegend	1:28
FITC anti-CD45	11-0451-85/30-F11	eBioscience	1:250
APC anti-Ly6C	128016/HK1.4	Biolegend	1:133
PE/Cy7 anti-MHC II	107630/M5/114.15.2	Biolegend	1:200

2.22 Statistics

Statistical differences were evaluated either by one- or two-way-Analysis of Variance (ANOVA) followed by Tukey's or Bonferroni's multiple comparison test as indicated. Statistical significances were defined as *: $p < 0.05$, **: $p < 0.01$, ***: $p < 0.001$. All the data were presented as mean \pm SEM. Statistical analysis were performed using the software GraphPad Prism[®] V6.01 (USA). The data obtained from ELISA experiments to characterize microglia of WT and 5XFAD mice were analysed using SPSS software. The General Linear Modeling (GLM) multivariate procedure was used to test null hypotheses about the effects of genotype and age on the means of various groupings of a joint distribution of dependent variables (TNF α , IL-6, IL-12p40, CCL2, CCL3, CCL5 and CXCL1). The analysis was performed for male and female mice separately. The multivariate analysis of variance using Hotelling's trace criterion was provided for combination of the dependent variables and the univariate analysis of variance was provided for each dependent variable. To test for difference of each dependent variable in different age groups, Tukey's test was used. In addition to the testing hypotheses, GLM multivariate produced estimates of parameters, too. The Statistical tests using SPSS software were kindly performed by Nargess Saiepour (University of Queensland, Australia).

3 Results

3.1 Characterization of microglia in the 5XFAD mouse model

3.1.1 Impairment of microglial phagocytic activity in 5XFAD is reversible

One of the known changes of the microglia phenotype associated with AD pathology is the reduced A β phagocytic activity (Hickman, et al., 2008).

To investigate whether this microglial impairment in phagocytosis is consistent in the healthy environment, phagocytic activity of microglia was assessed outside the brain in *ex vivo* cell cultures. Microglial phagocytic activity *in vivo* involves clearing myelin debris, pathogens or misfolded proteins such as A β peptides in the CNS. Accordingly, microglial cultures from 3, 6 and 9 months old WT and 5XFAD male and female mice were prepared and the phagocytosis of myelin, *E. coli* and A β was investigated. The cultures received astrocytic support but were free of other cell types or additional stimulation (Scheffel et al., 2012). Microglia cultivated from the above mentioned groups received fluorescently labelled myelin for 2 hours and subsequently the percentage of microglia phagocytosing myelin was evaluated using FACS analysis (Figure 5B). Figure 5C compares cells from male WT with male 5XFAD cells at the investigated ages. No differences were observed between WT and 5XFAD microglia. However, comparing different ages irrespective of genotype shows a significant reduction of phagocytic activity of microglia at 9 months of age by the WT and 5XFAD mice (p value WTs: 3 vs 9, 0.0004; 6 vs 9, < 0.0001; 5XFADs 3 vs 9, 0.009; 6 vs 9, < 0.0001). Comparing WT and 5XFAD female mice (Figure 5D) shows a similar outcome (p value WTs: 3 vs 9, 0.003; 6 vs 9, < 0.003; 5XFADs 3 vs 9, 0.0003; 6 vs 9, < 0.003).

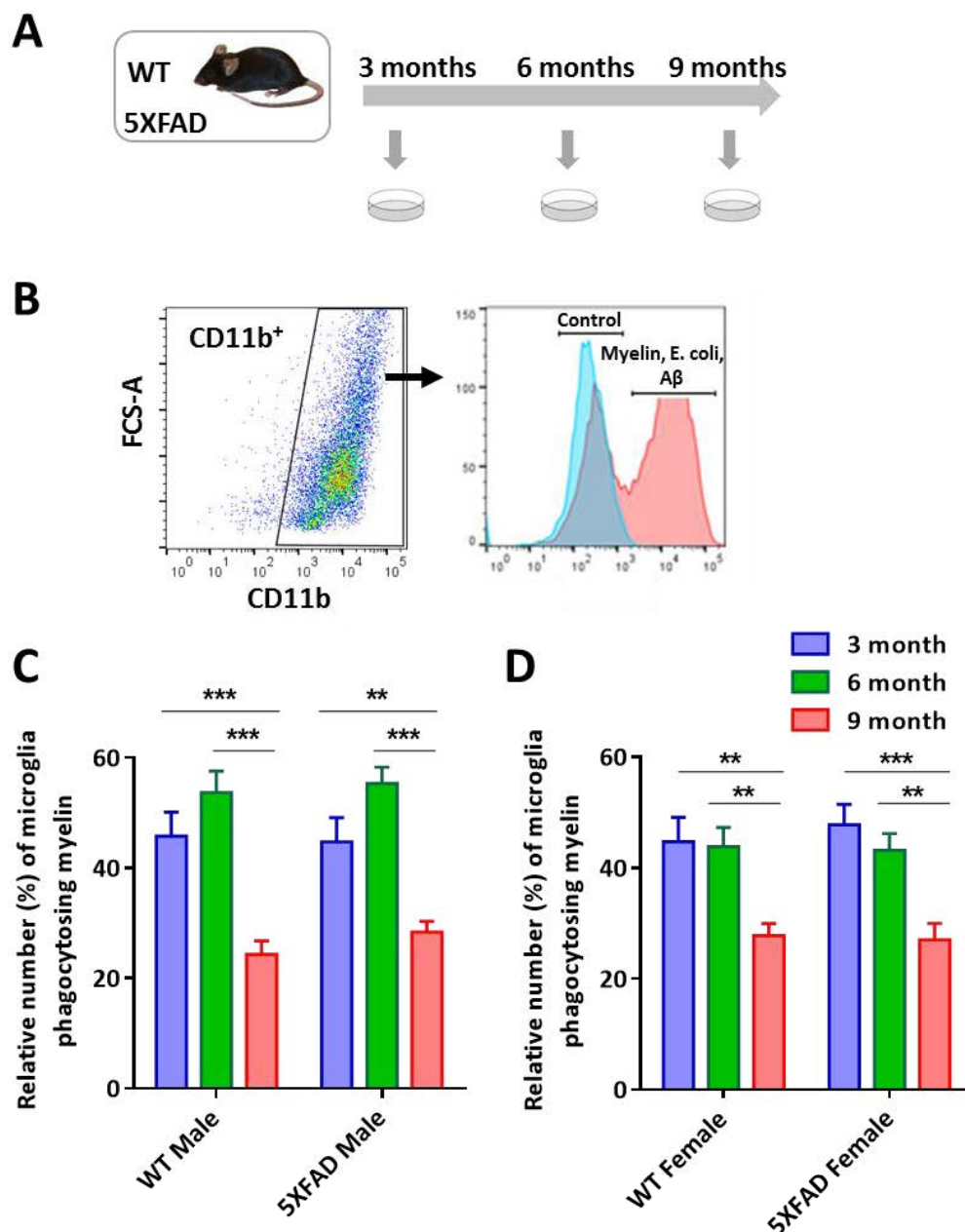


Figure 5: Ex vivo myelin phagocytosis assessment by adult microglia.

(A) Experimental design for myelin phagocytosis. Microglia from 3, 6 and 9 months old male and female WT and 5XFAD mice were cultured (2×10^5 cells were plated in 12 well-plate). After their attachment to the surface, Rhodamine- or DyLight 550-labelled myelin ($10 \mu\text{g/ml}$) was added to the cells for 2 hours. (B) A representative example of flow cytometry data evaluation. The percentage of the myelin positive population was calculated from CD11b^+ cells (microglia). (C) Percentage of microglia isolated from WT and 5XFAD male mice which phagocytosed myelin. (D) Microglia from female WT and 5XFAD mice that phagocytosed myelin. Data are mean \pm SEM, $N=5$. (Two-way ANNOVA followed by Tukey's post-hoc test; *, $p < 0.05$, **, $p < 0.01$, ***, $p < 0.001$)

Microglia- as other macrophages- are professional phagocytic immune cells and are able to recognize entering pathogens to the CNS with a high sensitivity. Thus, in the next approach we studied phagocytosis of *E. coli* by microglia isolated from the same mice (Figure 6).

Fluorescently labelled *E. coli* were added to the microglia cell cultures and incubated for 2 hours. Evaluation of the microglia positive for *E. coli* by flow cytometry analysis is depicted in Figure 5B. Figure 6A shows no significant differences between male WT and 5XFAD *E. coli*-positive microglia at the three different ages. Nevertheless, comparing different ages in each genotype reveals a significant reduction of phagocytic microglia at 9 months of age compared to younger ages (p value WTs: 3 vs 9, 0.008; 6 vs 9, < 0.02; 5XFADs 3 vs 9, 0.008; 6 vs 9, < 0.006). Figure 6B depicts the outcome for the female groups. As in males, there is no difference between the two genotypes but the percentage of phagocytosing microglia drops dramatically at 9 months of age compared to 3 and 6 months mice (p value WTs: 3 vs 9, 0.04; 5XFADs 3 vs 9, 0.02; 6 vs 9, < 0.03).

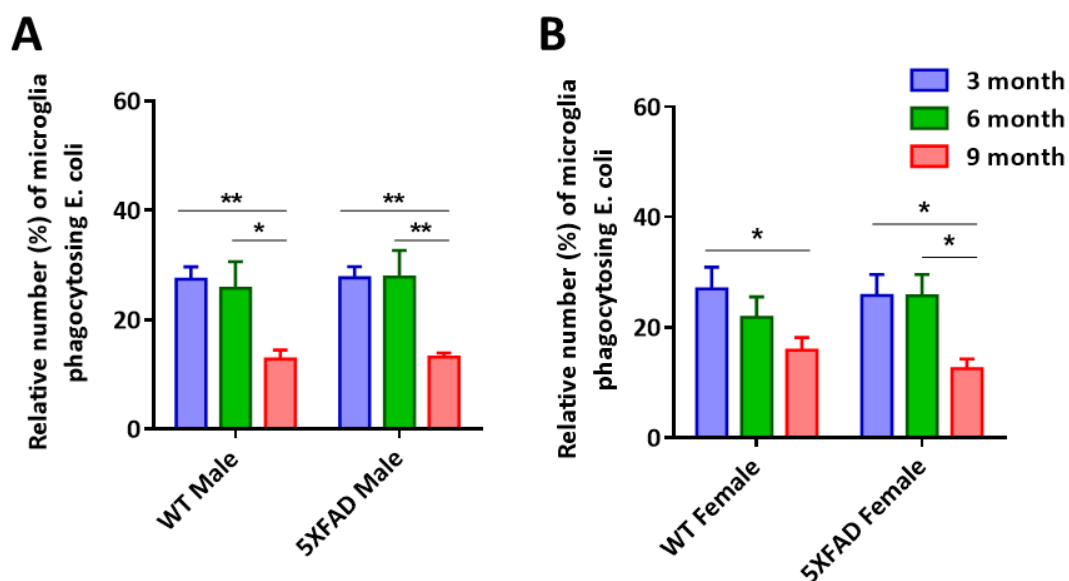


Figure 6: *E. coli* phagocytosis assessment by adult cultured microglia.

Microglia cultures (2×10^5 cells in 12 well-plate) were prepared from 3, 6 and 9 months old WT and 5XFAD mice. *E. coli* phagocytosis was investigated by addition of Ds-Red labelled *E. coli* (2×10^6 CFU) in complete DMEM with ampicillin instead of streptomycin and penicillin to the cells for 2 hours. Percentage of *E. coli* positive population was calculated from CD11b⁺ cells (microglia). (A) Percentage of microglia cells isolated from WT and 5XFAD male mice which phagocytosed *E. coli*. (B) Microglia from female WT and 5XFAD mice phagocytosing *E. coli*. Data are mean \pm SEM, N=5. (Two-way ANNOVA followed by Tukey's post-hoc test; *: p<0.05, **: p<0.01, ***: p<0.001)

In AD pathology microglia are responsible for A β phagocytosis as well. Thus, we investigated phagocytic activity of microglia isolated from 3 and 6 month old female WT and 5XFAD mice for monomeric forms of A β ₁₋₄₀ and A β ₁₋₄₂ peptides (Figure 7). Due to the limited number of mice, 9 months old mice could not be studied in this approach. Fluorescently labelled A β peptides were added to the cells for two hours and subsequently the percentage of cells that phagocytosed A β ₁₋₄₀ (Figure 7A) and A β ₁₋₄₂ (Figure 7B) was evaluated using flow cytometry analysis. As shown by the data, microglia isolated from 5XFAD and WT mice have the same phagocytic activity for A β ₁₋₄₀ and A β ₁₋₄₂. No differences can be observed between 3 and 6 months old groups.

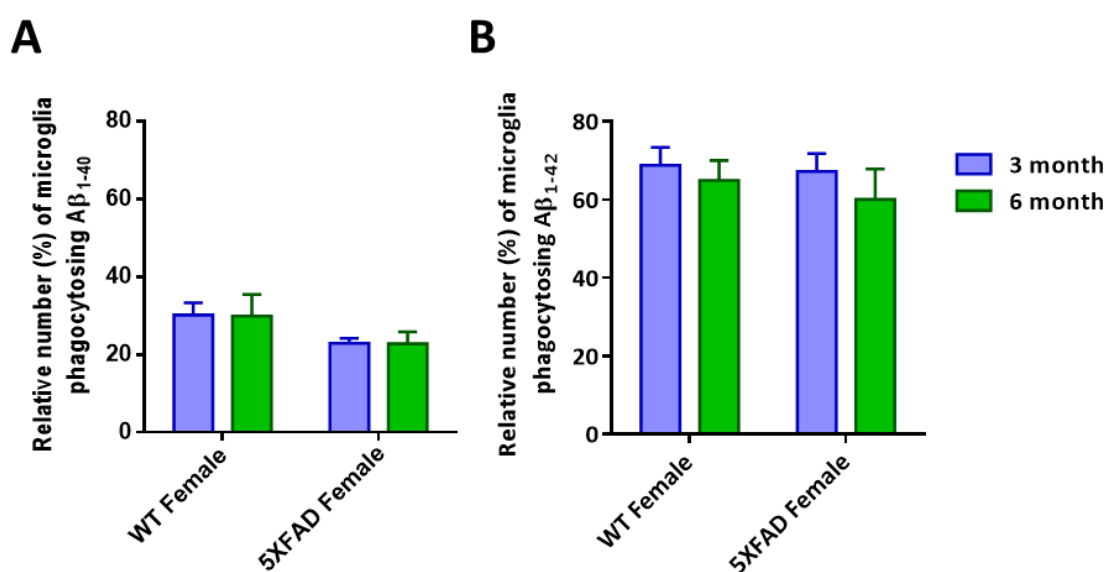


Figure 7: A β phagocytosis assessment by adult cultured microglia.

Adult microglial cultures (2×10^5 cells/well in a 12-well plate) were prepared from 3 and 6 months old female WT and 5XFAD mice. Cells received a monomeric form of HiLyte FlourTM 647-Labelled A β ₁₋₄₀ or A β ₁₋₄₂ in complete DMEM (both 250 nM) for 2 hours. The percentage of microglia positive for A β ₁₋₄₀ (A) and A β ₁₋₄₂ (B) was assessed from CD11b⁺ cells (microglia). Data are mean \pm SEM, N=5. (Two-way ANNOVA followed by Bonferroni's post-hoc test; *: p<0.05, **: p<0.01, ***: p<0.001)

3.1.2 LPS alters phagocytic activity of adult microglia isolated from 5XFAD mice

Previous studies have shown that stimulation of microglia with LPS (TLR4 agonist, one of the TLRs involved in AD (reviewd by Walter et al., 2007) results in alterations of their phagocytic activity. These changes, however, vary for different phagocytic materials. For instance, microglia stimulated with LPS show decreased myelin phagocytosis (Regen et al., 2011) but increased E. coli phagocytosis (Ribes et al., 2009). Thus, to study the effect of LPS

on phagocytosis in 5XFAD mice compared to WT mice we assessed the microglial response to LPS in terms of myelin and *E. coli* phagocytic activity (Figure 8).

Microglia were isolated from three different ages of WT and 5XFAD mice as mentioned in 1.1.1. Myelin (Figure 8B-C) and *E. coli* (Figure 8D-E) phagocytosis in microglia were evaluated after 24 hours after pre-incubation with LPS. The data were normalized to their respective groups without LPS stimulation (Figure 5 and Figure 6). As shown in Figure 8B and C, myelin phagocytosis decreased upon LPS pre-stimulation in both genotypes and genders. Moreover, there were no significant differences between WT and 5XFAD groups in the studied ages (Figure 8B). Female mice (Figure 8C) show a similar sensitivity to LPS compared to male mice.

An increased *E. coli* phagocytic activity by adult microglia upon pre-stimulation of LPS was observed (Figure 8D-E: values were normalized to *E. coli* phagocytosis without pre-stimulation). In the male groups, WT and 5XFAD microglia show no significant differences (Figure 8D). However, these data show a tendency of an age-dependent increase of *E. coli* phagocytosis in both genotypes upon LPS stimulation. Figure 8E compares WT and 5XFAD female mice. Both groups show similar responses to LPS and it seems that microglia isolated from 9 months old mice of both genotypes tend to be more responsive to LPS.

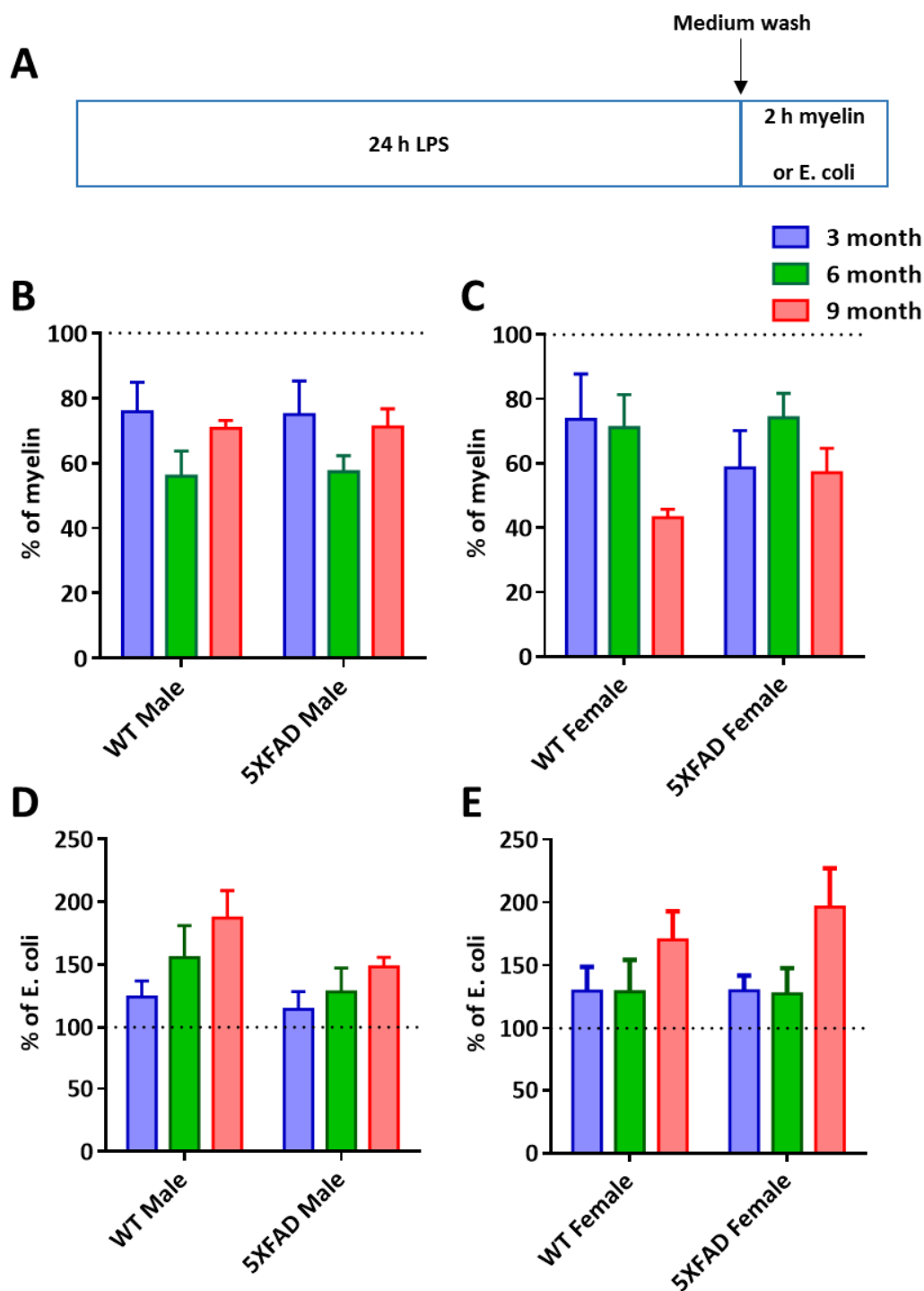


Figure 8: LPS pre-incubation effects on myelin and *E. coli* phagocytosis by adult microglia.

Microglia cultures (2×10^5 cells/well) were prepared from 3, 6 and 9 months old WT and 5XFAD male and female mice. (A) Experimental design. Cells were incubated with LPS (rough type, 10 ng/ml) for 24 hours. Cells were washed with the complete medium before addition of phagocytic compounds (myelin or *E. coli*). (B and C) Myelin (10 μ g/ml) was added to the cells isolated from males and females, respectively. Myelin-positive microglia were detected by flow cytometry analysis. (D) Male and (E) female microglia received *E. coli* (2×10^6 CFU) for 2 hours. Dotted lines indicate 100% and refer to the myelin or *E. coli* phagocytosis without LPS pre-stimulation. Data from each age, genotype and gender are normalized to their respective groups without LPS stimulation (Figure 5 and Figure 6).

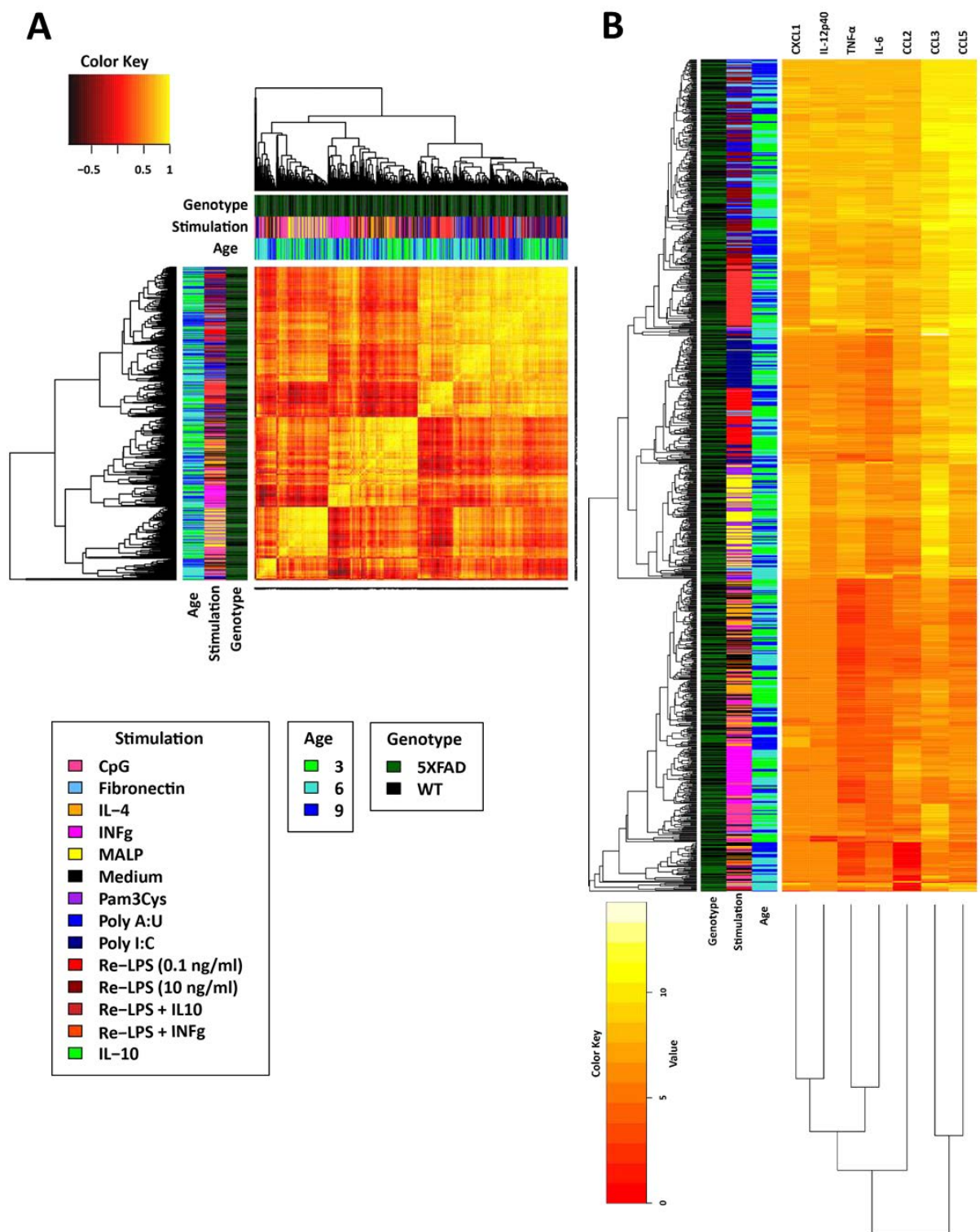
Data are mean \pm SEM, N=5. (Two-way ANNOVA followed by Tukey's post-hoc test; *: $p < 0.05$, **: $p < 0.01$, ***: $p < 0.001$). h, hour.

3.1.3 Higher reactivity of microglia in AD environment is reversible

It has been shown that microglia in the brains of AD patients and mouse models harbour a hyperreactive phenotype which accompanies an enhanced cyto-/ chemokine production in these cells (reviewed by Heppner et al., 2015). To determine the activity of microglia to produce cyto-/ chemokines in a healthy environment, microglia were isolated from 3, 6 and 9 months old 5XFAD and age matched WT control mice from both genders and were stimulated with a large battery of pro- and anti-inflammatory stimuli for 18 hours. The stimuli included LPS, Fibronectin, Pam3CSK4, Poly (I:C), Poly (A:U), MALP-2, CPG ODN, $INF\gamma$, IL-4, IL-10 and combination of LPS with IL-10 or $INF\gamma$. Control groups from both genotypes received only culture medium. Subsequently, the amount of a selection of secreted pro-inflammatory cyto-/ chemokines (TNF α , IL-6, IL-12p40, CCL2, CCL3, CCL5 and CXCL1) was measured in the supernatant of the cells, using ELISA (Figure 9).

The data obtained from all the groups were compared together as shown by a correlation heatmap (Figure 9A). The individual expressions of all the groups are depicted in a separated heatmap (Figure 9B). For a better understanding of possible differences between 5XFAD and WT groups, the data from all the stimuli were pooled together and compared for respective cyto-/ chemokines between age groups and between different genotypes. The analyses were performed separately for male and female mice.

With the exception of CCL2 in female mice, the multiple comparison analyses reveal no significant differences between WT and 5XFAD groups. For female mice, CCL2 production upon microglial stimulation is reduced in 3, 6, and 9 months old 5XFAD female mice compared to WT (p value 0.045). Although almost all the cytokines have the tendency for a reduced production in older ages, significant differences can be seen for IL-6 (p values: 3 vs 6, 0.04; 3 vs 9, 0.01), CCL2 (p values: 3 vs 9, < 0.0001 ; 6 vs 9, 0.001), CCL3 (p values: 3 vs 6, < 0.0001 ; 3 vs 9, < 0.0001) for female mice and IL-6 (p values: 3 vs 9, 0.04; 6 vs 9, 0.03) and CCL2 (p values: 3 vs 6, < 0.0001 ; 3 vs 9, 0.001) for males (Figure 9C). All interactions between genotype and age were insignificant (p-values > 0.05).



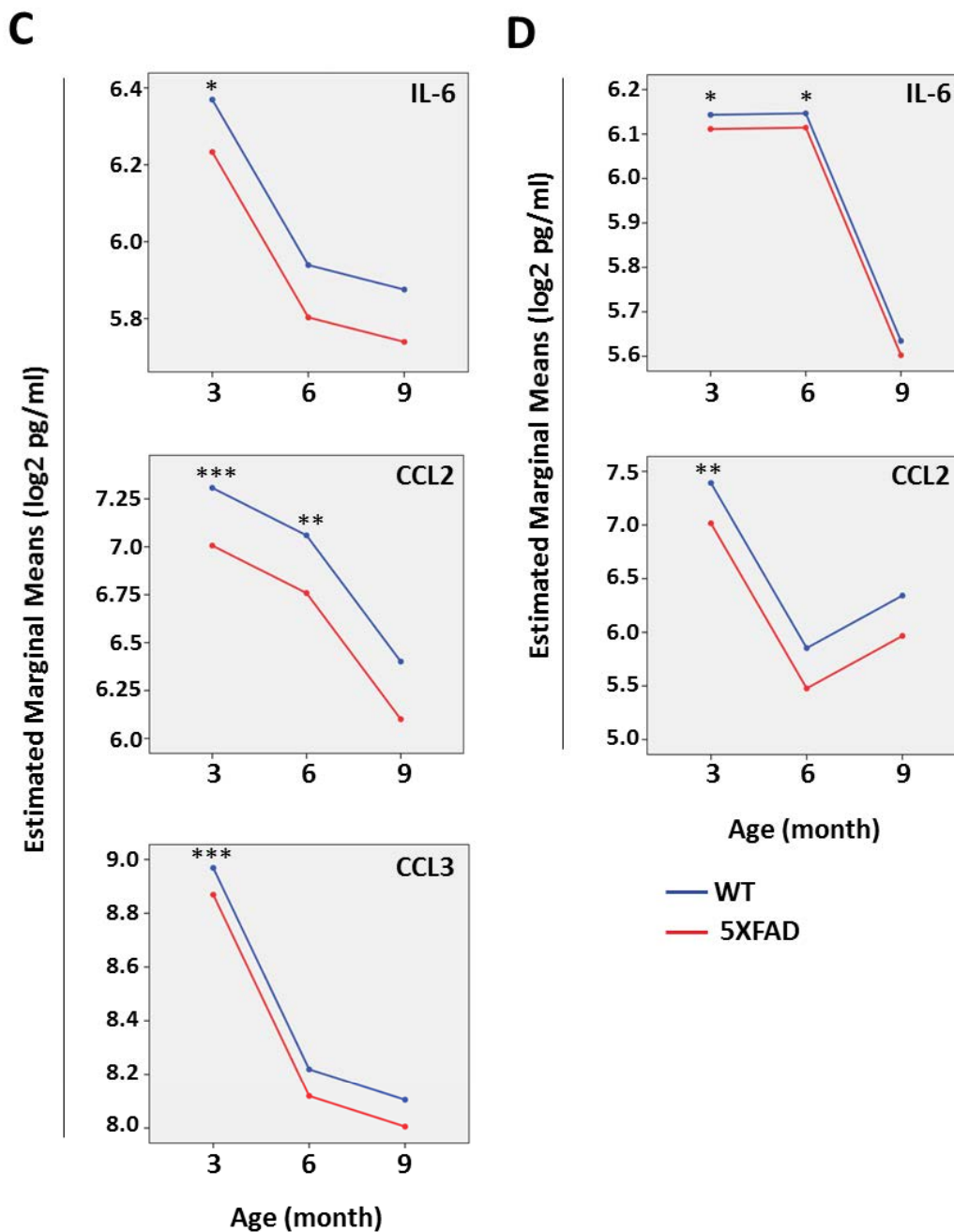


Figure 9: Cyto/ chemokine production by 5XFAD microglia compared with WTs.

Microglia cultures (15×10^4 cells in 96 well-plate) were prepared from 3, 6 and 9 months old WT and 5XFAD mice. Cells received Re-LPS (0.1 ng/ml and 10 ng/ml), Fibronectin (100 μ g/ml), Pam3CSK4 (10 ng/ml), Poly (I:C) (50 μ g/ml), Poly (A:U) (50 μ g/ml), MALP-2 (10 ng/ml), CPG ODN (5 μ g/ml), $\text{INF}\gamma$ (10 ng/ml), IL-4 (10 ng/ml), IL-10 (10 ng/ml) and combination of Re-LPS (10 ng/ml) with IL-10 or $\text{INF}\gamma$ (both 10 ng/ml) for 18 hours. Amounts of $\text{TNF}\alpha$, IL-6, IL-12p40, CCL2, CCL3, CCL5 and CXCL1 were measured in the supernatants using ELISA. (A) A heatmap of the correlations between stimulated microglia from WT and 5XFAD mice. (B) A heatmap for the individual expressions of all the groups by respective stimuli. The data obtained from all the stimuli in female (C) and male (D) mice were pooled and analysed for different cyto/ chemokines. The data from 3 and 6 months old are compared with 9 months old. N=5-6. (Multivariate tests Hotelling's Trace followed by Tukey's post-hoc test; *: $p < 0.05$, **: $p < 0.01$, ***: $p < 0.001$)

3.1.4 Cultured microglia from 5XFAD mice show a decreased proliferation activity compared to the age matched WT mice

Microglia as one of the main cell types in touch with A β depositions are believed to have a higher proliferation activity in AD brains. *In vivo* studies have shown, that this enhanced proliferation occurs mainly in the vicinity of A β plaques (Orre et al., 2014; reviewed by Gomez-Nicola & Boche, 2015). To investigate this activity of microglia in the absence of A β peptides or other possible stimulations of an AD environment, we investigated proliferation of microglia isolated from 6 and 9 months old WT and 5XFAD male and female mice *ex vivo*. The proliferation activity was measured within 24 hours by using a BrdU proliferation assay. The proliferation rate was assessed in control medium or after stimulation with LPS (Figure 10). The data show that microglia isolated from adult mice are capable of proliferation. In addition, the data reveal that microglia isolated from 6 and 9 months old male (Figure 10A) or female (Figure 10B) 5XFAD mice have a significantly lower proliferative activity compared to the WT controls (p value males: 6 month, WT vs 5XFAD, 0.001; 9 month WT vs 5XFAD, 0.0007; females: 6 month, WT vs 5XFAD, 0.006; 9 month WT vs 5XFAD, 0.0008). Moreover, the proliferation rate of microglia from female mice decreases with age of animals independent of the genotype (Figure 10B; p value WTs: 6 vs 9, 0.001; 5XFADs 6 vs 9, 0.002).

To investigate the effect of LPS on the proliferation, cells were stimulated with two different concentrations of LPS (low, 0.1 ng/ml and high, 10 ng/ml). LPS stimulation induced a reduction of proliferative activity in adult microglia (Figure 10C). The proliferation rate upon LPS stimulation was normalized to the proliferation under control conditions of each respective group. The data show that both concentrations of LPS lead to a decrease of proliferation to almost 50% of medium control. Nevertheless, no significant differences among the groups have been observed (Figure 10C).

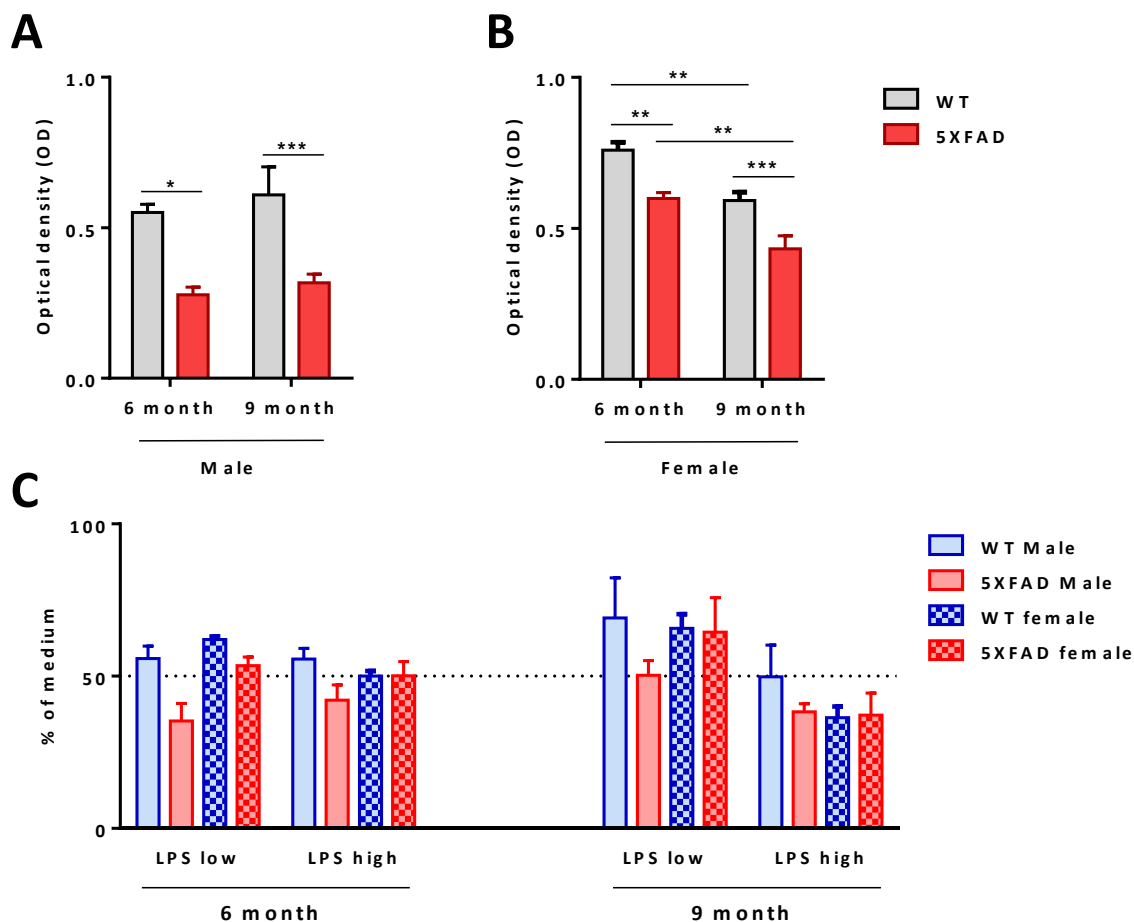


Figure 10: Proliferation rate of cultured adult microglia.

Microglia isolated from 6 and 9 months old male and female WT and 5XFAD mice were cultured and plated with a density of 1.5×10^4 cells/well. Complete medium containing BrdU compound alone was added to the cells isolated from male (A) or female (B) mice for 24 hours. Subsequently, incorporated BrdU in microglia was detected calorimetrically using a specific anti BrdU antibody. (C) Cells were additionally stimulated with two concentrations of LPS (rough type; low, 0.01 ng/ml and high, 10 ng/ml). Data of each group were normalized to their respective values (medium control, A and B) as the percentages. N for 6 months old mice=12 from 2 mice, for 9-month old mice= 12-20 from 3-5 mice. Data are means \pm SEM. (Two-way ANNOVA followed by Bonferroni's post-hoc test; *: $p < 0.05$, **: $p < 0.01$, ***: $p < 0.001$)

3.1.5 9 months old 5XFAD mice have no monocyte and neutrophil infiltrates in the brain

Immune cell infiltration from the periphery to the CNS is one of the extensively discussed issues in the AD context. Infiltrating monocytes and neutrophils (phagocytic cells) are believed to be more functional to clear excessive A β proteins than resident microglia (reviewed by Lai & McLaurin, 2012). However, this hypothesis is under debate. In our study, microglia cultures were prepared from whole brains and the purity of the cultures was tested

by expression of the complement receptor CD11b (Scheffel et al., 2012). CD11b is also expressed on other immune cells including macrophages and neutrophils and therefore it cannot discriminate among these cell types. Thus, to exclude that other possible CD11b⁺ immune cells were added to the cultures, we investigated the putative presence of monocytes and neutrophils in the brains of 5XFAD mice compared to WT mice using CD11b, CD45, Ly6C and Ly6G markers. Since 9 months was the oldest age we used for our *ex vivo* experiments, we have not used animals below 9 months for this experiment. Immune cell infiltrates were assessed using flow cytometry analysis. WT and 5XFAD mice from both genders were transcardially perfused to wash away the immune cells in the blood vessels and subsequently monocytes and neutrophils were detected by specific antibodies. The data demonstrate that the percentage of monocytes (Figure 11B) and neutrophils (Figure 11C) in the brains of 5XFAD mice do not differ from age matched WT mice.

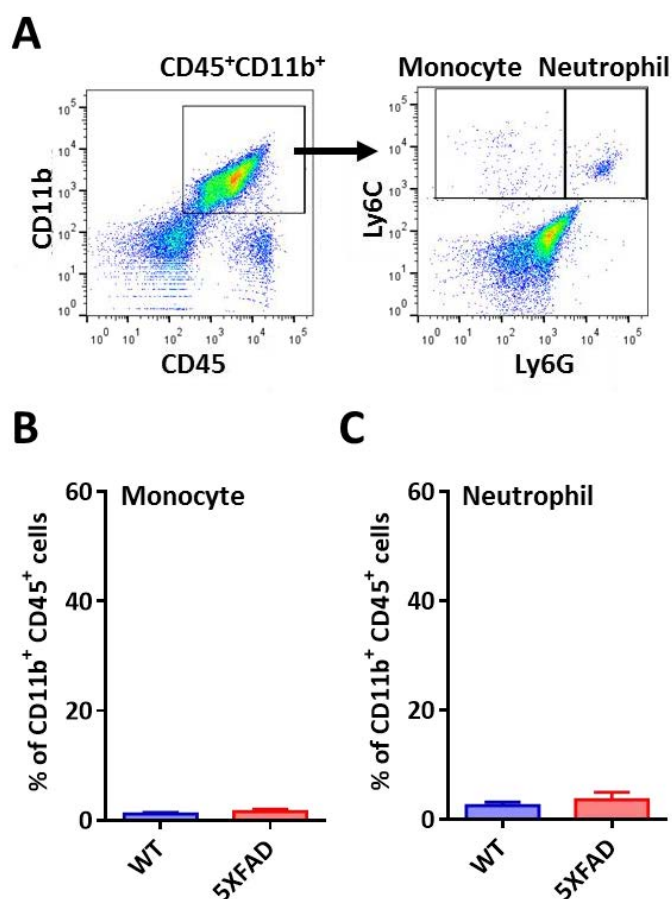


Figure 11: Number of monocytes and neutrophils in the brains of WT and 5XFAD mice.

Intact brains of 9 and 12 month old WT and 5XFAD mice were prepared for immune cells infiltrate assessment. **(A)** An example of sample evaluation by flow cytometry. Percentage of monocytes (CD45⁺, CD11b⁺, Ly6C⁺ and Ly6G⁻) **(B)** and neutrophils (CD45⁺, CD11b⁺, Ly6C⁺ and Ly6G⁺) **(C)** from CD45⁺ and CD11b⁺ population. Data from male and female mice are pooled. N=3. Data are mean \pm SEM. (Mann-Whitney U test; *: $p < 0.05$, **: $p < 0.01$, ***: $p < 0.001$)

3.1.6 Microglia in the brains of 5XFAD mice respond to intracerebral injected LPS

Under pathological conditions, microglia are continuously stimulated by A β exposure. Especially in the 5XFAD mouse model, which develops plaque depositions already at 2 months of age (Jawhar et al., 2012), microglia are exposed to soluble A β stimulation from early on in life, which can affect their response to a secondary stimulation such as infectious materials. LPS (which represents bacterial infection) is one of the strongest PAMPs to activate immune cells including microglia. In particular, in the CNS any appearance of LPS has to be quickly eliminated. One of the reactions of microglia after this harsh *in vivo* stimulation is secreting chemoattractive proteins to recruit other immune cells from the periphery to the infectious site. To investigate how these microglia that were pre-stimulated with A β will respond to LPS in terms of recruiting immune cells from the periphery, two concentrations of LPS (0.01 mg/ml as low and 1 mg/ml as high) were injected in the striatum of 6 and 9 months old WT and 5XFAD mice from both genders. 24 hours after injections, mouse brains were analysed for infiltrating neutrophils and monocytes (Figure 12). Evaluation of neutrophil infiltrates (Figure 12C-D) shows a concentration-dependent increase of neutrophils by increasing LPS concentrations. As shown in Figure 12C there are no significant differences between infiltrating neutrophils in WT and 5XFAD male and female brains at 6 or 9 months of age, indicating that microglia of all groups respond similarly at a low concentration of LPS to recruit neutrophils. Shown in Figure 12D, all groups of WT and 5XFAD mice show the same infiltration rate of neutrophils, except the 9 months old 5XFAD male mice which reveal significantly lower neutrophils compared to age matched controls (p value 0.01). Figure 12E-F compares the infiltration rate of monocytes. Similar to the neutrophil infiltration, LPS injection dose-dependently leads to infiltration of monocytes (Figure 12E to F). Upon injection of a low concentration of LPS, no differences among the groups of 6 and 9 months old WT and 5XFAD have been observed (Figure 12E). The data resulting from injection of high concentration of LPS (Figure 12F) show no significant differences between WT and 5XFAD. 9 months old 5XFAD male mice have significantly higher numbers of monocytes compared to age matched females (p value 5XFAD male vs WT female, 0.005; 5XFAD male vs 5XFAD female, 0.01).

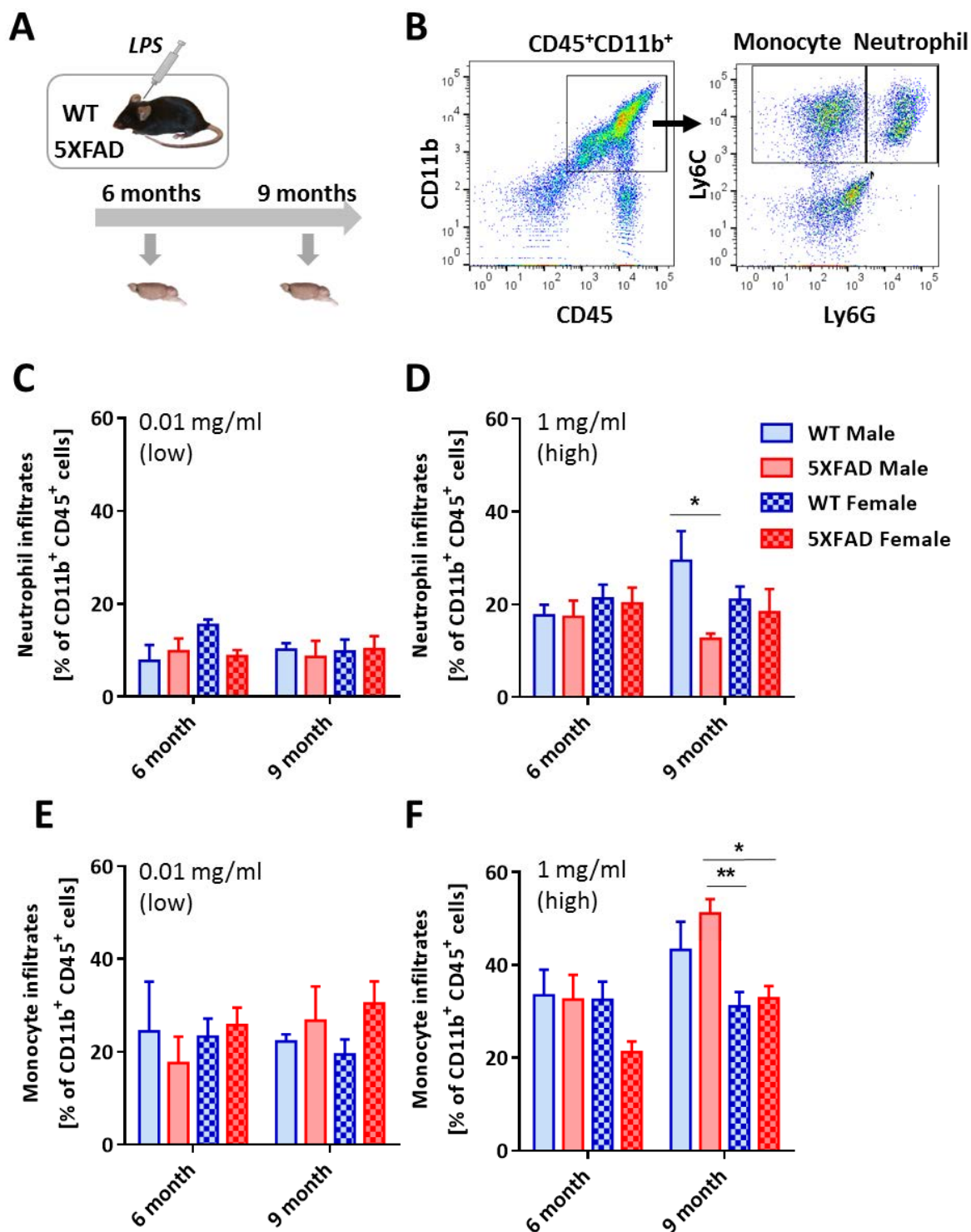


Figure 12: LPS injection into the striatum leads to immune cell infiltration from the periphery to the brain in 5XFAD mice as in WT.

(A) 6 and 9 months old WT and 5XFAD mice were injected with 0.01 mg/ml (10 ng) or 1 mg/ml (1 μ g) LPS (smooth type) in the striatum. 24 hours after the injection brains were isolated and single cell suspensions were prepared. 10,000 CD11b positive cells were recorded using flow cytometry to seek for neutrophils and monocytes infiltrates. (B) An example of brain sample evaluation by flow cytometry. Immune cells in the brain (CD45 and CD11b positive) were evaluated for neutrophils (CD45⁺, CD11b⁺, Ly6C⁺ and Ly6G⁺) and monocytes (CD45⁺, CD11b⁺, Ly6C⁺ and Ly6G⁺). (C)

CD11b⁺ and CD45⁺ population upon 0.01 mg/ml of LPS injection. **(D)** Percentage of neutrophils in CD11b and CD45 positive cells upon 1 mg/ml of LPS injection. **(E)** Percentage of Monocyte infiltrates upon 0.01 mg/ml of LPS. **(F)** Monocytes infiltrated in the brains upon 1 mg/ml of LPS injection. N=4-6. Data are mean ± SEM. (Two-way ANNOVA followed by Tukey's post-hoc test; *: p<0.05, **: p<0.01, ***: p<0.001)

3.2 Amyloid beta (A β) plaque-associated microglia priming in transgenic mouse models of Alzheimer's disease

3.2.1 A β deposition increases in APP23 mice with ageing

APP23 transgenic mice have been shown to form A β plaques after the age of 6 months and the A β plaques increase in size and number with the age of the animals (Sturchler-Pierrat et al., 1997). To detect the amount of dense-core plaques and A β depositions inside and outside the mature plaques at various ages, immunohistochemistry analysis was applied in 6, 16, 20 and 24 months old APP23 mice using Congo red, Thioflavin S (both detecting mature plaques) and an anti-A β antibody (4G8, detecting A β_{17-24} ; Figure 13). A β depositions are not detectable at 6 months of age by any of the stainings (Figure 13A-C). 16, 20 and 24 months old APP23 mice show A β depositions in the cortex and the hippocampus using Congo red, Thioflavin S and 4G8 antibody which increases age dependently (Figure 13A-C). However, A β plaques in thalamus and olfactory nucleus are only detected at 24 months of age (Figure 13A).

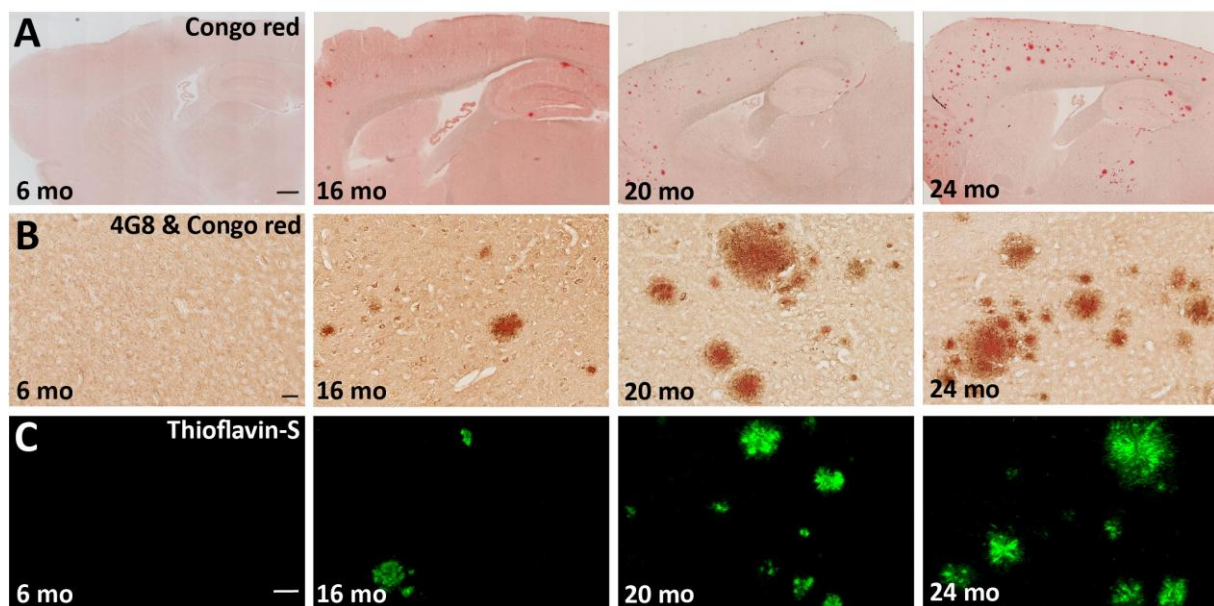


Figure 13: Age-dependent increase of A β plaque depositions in APP23 mouse model.

Age-dependent increase in A β plaque deposition in APP23 transgenic mice at 6, 16, 20 and 24 months old. Sagittal sections of APP23 mice were stained with (A) Congo red and (C) Thioflavin S. (B) Cortical sections of APP23 mice brains from different ages were stained with anti-A β antibody 4G8 and Congo red. Scale bars: A= 500 μ m; B- C= 50 μ m. N=3-5. mo: months.

3.2.2 Signs of priming in A β plaque-associated microglia of APPswePS1dE9 and 5XFAD mice

It has been suggested that microglial priming features can be observed in A β plaque-associated microglia of AD mouse models as well as post-mortem tissues from AD patients (reviewed by Norden & Godbout, 2013). To examine if this priming exists in the microglia in direct contact to the A β plaques, expression of priming markers (Mac-2, CD68 and MHC II) were studied in two well established APP-overexpressing mouse models, APPswePS1dE9 (Figure 14) and 5XFAD (Figure 15). Brain sections of these mice were stained with Congo red (to visualize the plaque depositions) and antibodies against Mac-2, CD68 and MHC II.

In the cortex and thalamus of 18 months old APPswePS1dE9 mice, immunoreactivity with Mac-2, CD68 and MHC II antibodies can be restrictedly seen in microglia in the vicinity of A β plaque depositions and not the plaque-free regions (Figure 14A-C). Moreover, Mac-2, CD68 and MHC II positive cells are co-stained with microglia marker, Iba1 (Figure 14D-F). Investigations of cortex, subiculum, thalamus and pons of 5XFAD mouse brains show Mac-2 positive cells around the A β depositions already at the age of 7.5 months (Figure 15A). The immunoreactivity with Mac-2, CD68 and MHC II is more pronounced at the age of 12 months (Figure 15B-D), however, non-plaque regions lack these positive cells. Co-staining of these cells with the microglia marker, Iba1, can be seen as well (Figure 15E-G).

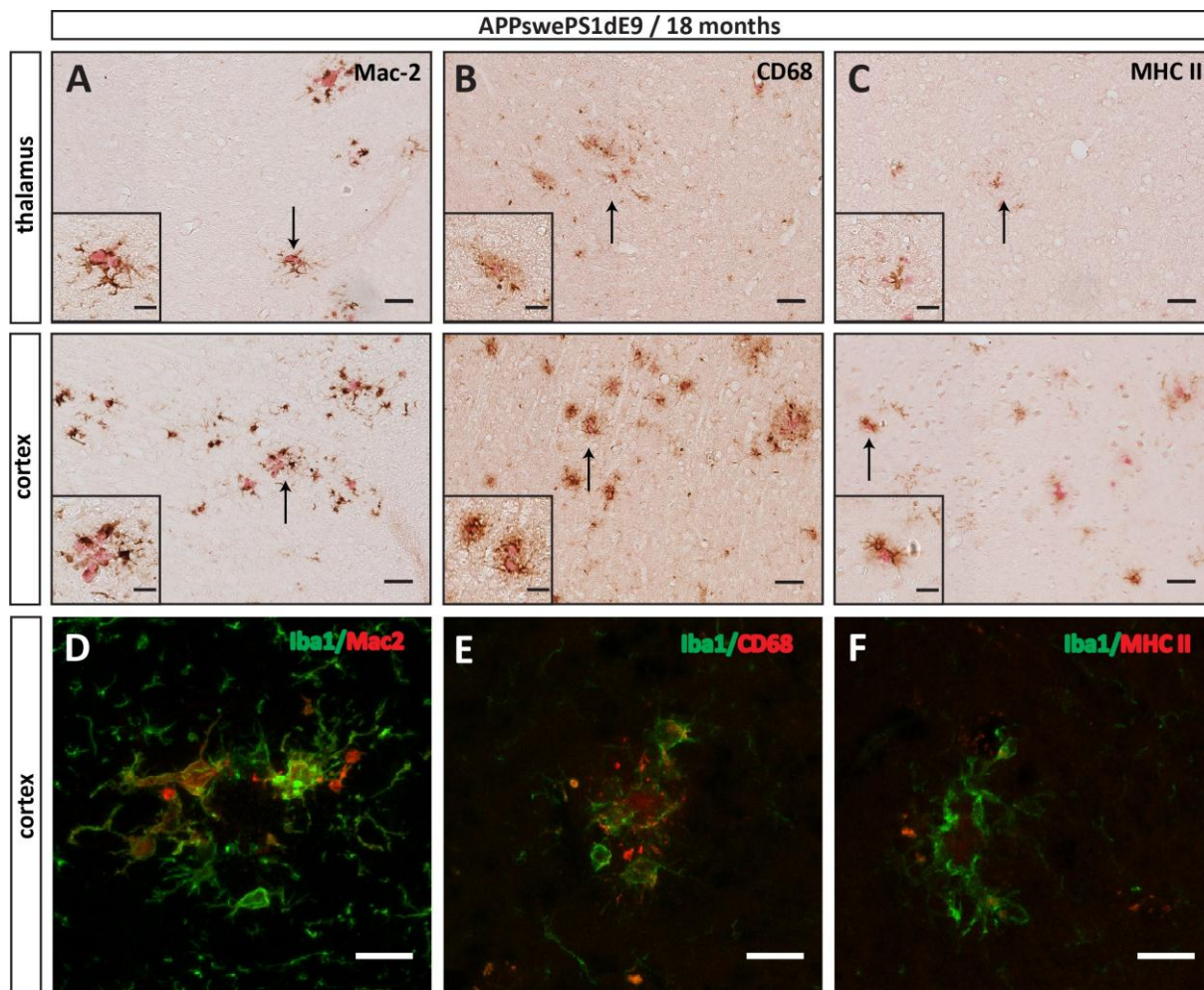


Figure 14: Expression of priming markers on plaque-associated microglia of APPswePS1dE9 mice.

Sections of thalamus and cortex from 18 months old APPswePS1dE9 mice were stained with Congo red to label mature A β plaques and immuno-stained with the microglia priming markers (A) Mac-2, (B) CD68 and (C) MHC II. Immunofluorescence co-staining of microglia marker Iba1 and priming markers (D) Mac-2, (E) CD68 and (F) MHC II. Arrows indicate positive signal for Mac-2, CD68 and MHC II around Congo red positive stainings. Scale bars: A-C= 50 μ m; insets and D-F= 15 μ m. N=3.

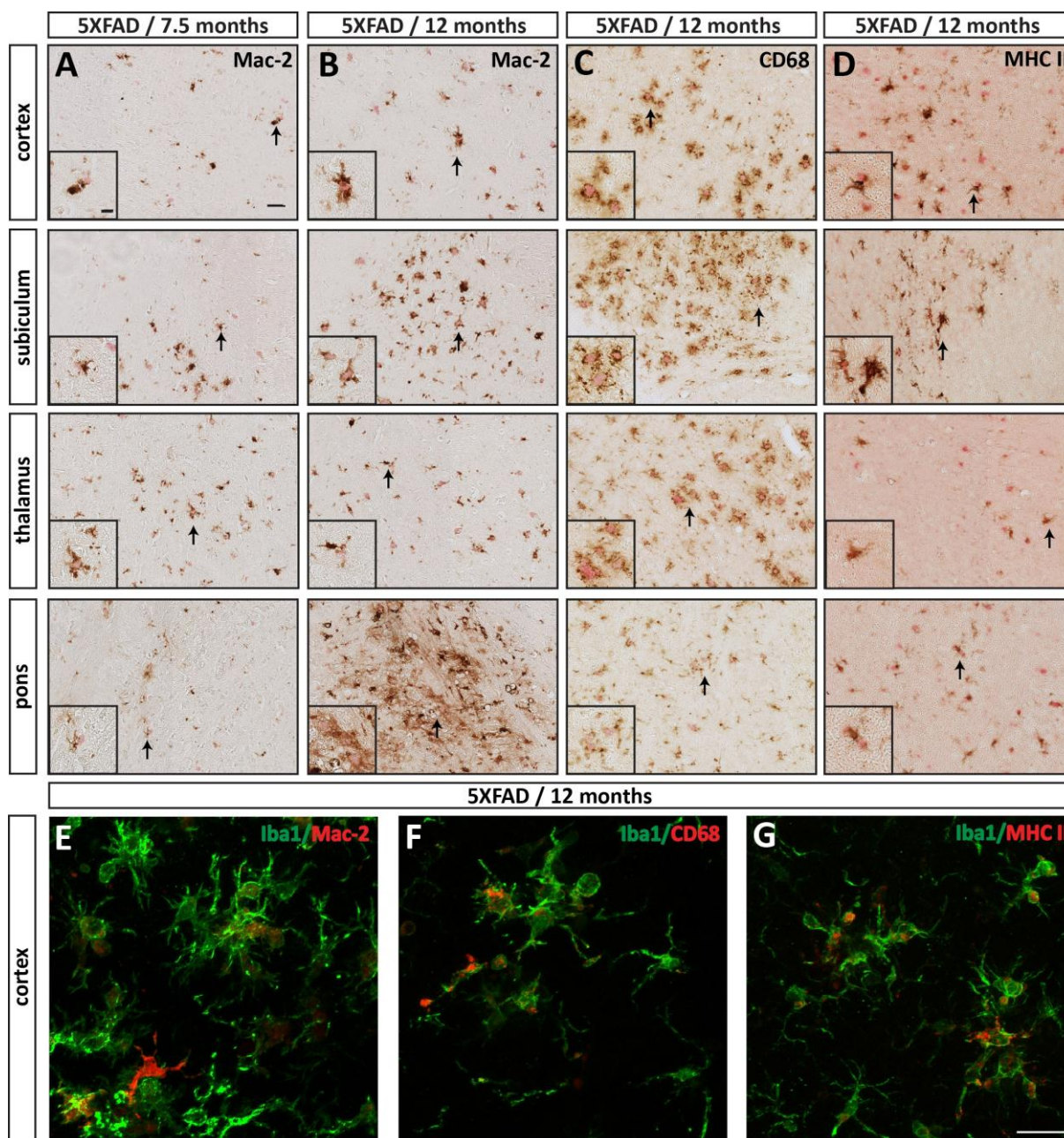


Figure 15: Expression of priming markers on $A\beta$ associated microglia in 5XFAD mice.

Sections of cortex, subiculum, thalamus and pons from 7.5 (A) and 12 months old 5XFAD transgenic mice (B-D) were stained with Congo red and antibodies against the priming markers, (A-B) Mac-2, (C) CD68 and (D) MHC II. Immunofluorescence co-staining of cortical sections of 12 months old 5XFAD mice for the microglia marker, Iba1 and priming markers Mac-2 (E), CD68 (F) and MHC II (G). Arrows indicate positive signal for Mac-2, CD68 and MHC II around Congo red positive stainings. Scale bars: A-D = 50 μ m; insets = 15 μ m; E-G = 20 μ m. N=3-5.

3.2.3 The genes involved in the immune recognition and phagocytosis are highly expressed in APP23 and 5XFAD mice

CD11c, Dectin1, Lysosomal-associated membrane protein 2 (Lamp2) and Triggering receptor expressed on myeloid cells 2 (Trem2) are involved in the immune recognition and phagocytosis of the immune cells. CD11c and Dectin1 have been described to belong to the gene profile of microglia priming (Holtman et al., 2015), Lamp2 is involved in phagosome maturation (Huynh et al., 2007) and Trem2 plays an essential role in the phagocytic activity of immune cells and its mutations have been introduced as risk factors of late onset Alzheimer's disease (LOAD; Guerreiro et al., 2013). To investigate the expression pattern of these proteins in the plaque areas in APP23 and 5XFAD mice, cortical and hippocampal sections of 16 months old APP23 and 12 months old 5XFAD mice were studied. The presence of these proteins in the transgenic mice were compared to the age matched WT controls. Overexpression of all of these proteins can be observed in 16 months old APP23 mice (Figure 16B) compared to WT littermates (Figure 16A). Similar to APP23 mice, 12 months old 5XFAD mice (Figure 16D) show high expression of CD11b, Dectin1, Lamp2 and Trem2 which are lacking in control WT mice (Figure 16C).

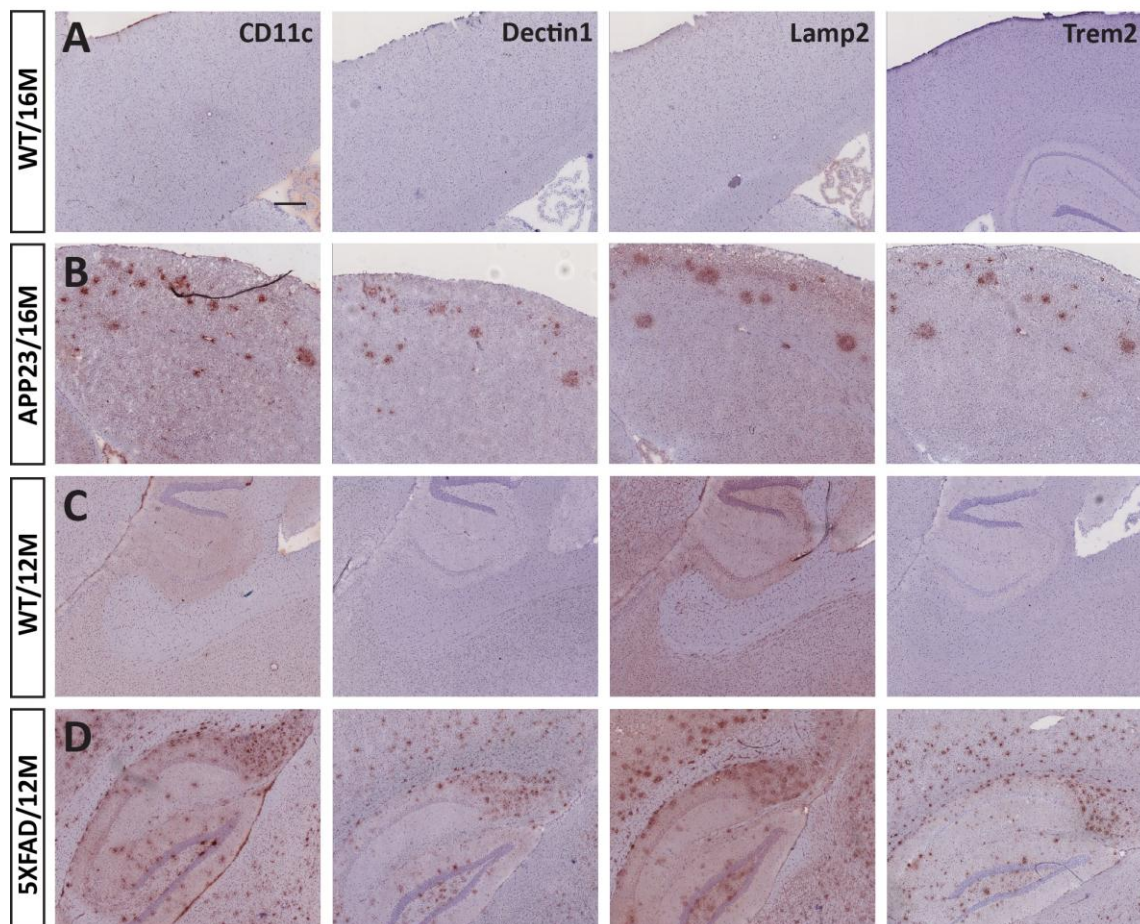


Figure 16: Expression of CD11c, Dectin1, Lamp2 and Trem2 in A β plaque-associated microglia of APP23 and 5XFAD mice.

Immunohistochemical analysis of the cortex and hippocampus sections of 16 months old WT (A), 16 months old APP23 (B), 12 months old WT (C) and 12 months old 5XFAD (D) mice for CD11c, Dectin1, Lamp2, Trem2 and counterstained with cresyl violet. Scale bar= 300 μ m. N=3-5. M: months

3.2.4 A β plaque-associated microglia priming and ageing-associated priming are two distinct processes

In order to distinguish the expression of Mac-2, CD68 and MHC II markers (microglia priming markers) in microglia in the vicinity of A β plaques and to exclude it from the ageing effect, 16 months old APP23 and WT mice were studied. In addition, to investigate ageing-associated microglia priming independent of A β -association, 24 month old WT and APP23 mice were observed. Cortical sections of 16 months old APP23 mice show the expression of these markers by microglia in the vicinity of A β deposits and not in the plaque-free areas (Figure 17A). Appearance of these markers is not observed in 16 months old WT mice (data not shown). Expression of Mac-2 and CD68 but not MHC II is observed in the cortex of 24

months old WT mice (Figure 17B). In 24 months old APP23 mice Mac-2 and CD68 positive cells can be found in both A β -plaque areas as well as non-plaque regions (data not shown). The scheme in the Figure 17C shows that the A β plaque-associated microglia priming occurs prior to the age-associated priming.

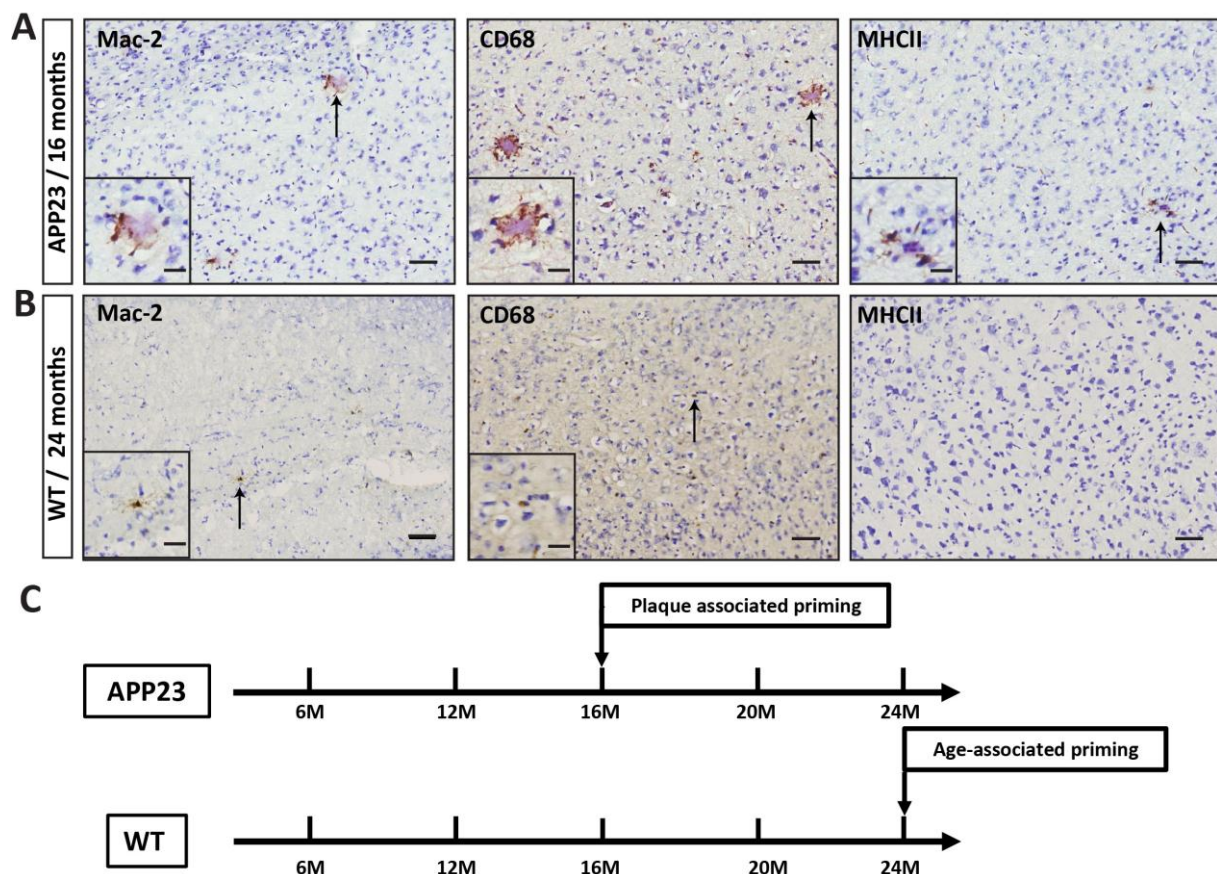


Figure 17: A β -associated microglia priming occurs prior to age-induced microglia priming. Cortical sections of 16 months old APP23 (A) and 24 months of WT (B) mice were stained with microglia priming markers: Mac-2, CD68 and MHC II. The A β plaques are labelled by cresyl violet. (C) In APP23 mice plaque-associated microglia priming is detected at the age of 16 months (16M) at which age-related microglia priming could not yet be detected in WT mice. Age-associated microglia priming was first detected in 24-month-old mice. Arrows indicate positive signal for Mac-2, CD68 and MHC II around dense cresyl violet stainings (senile plaques). Scale bars: A-B= 50 μ m; insets= 15 μ m. N=3-5. M: months.

3.2.5 MHC II⁺ microglia in 5XFAD mice reveal gene expression signature of priming

In the previous experiments we showed that microglia in the vicinity of A β plaques express priming markers such as MHC II. In order to better understand the phenotype of these

microglia, MHC II positive (MHC II⁺) microglia were isolated from 5XFAD mice and age matched WT littermates using flow cytometry sorting. To exclude the ageing effect on the priming -which was shown in section 3.2.4- 9 months old mice were chosen. For the sorting, microglia were selected as CD11b⁺CD45^{intermediate}Ly6C⁻ cells and further sub-gated into MHC II⁺ and MHC II⁻ populations (Figure 18A). Subsequently, the expression of over 800 specific microglial genes of three selected pure populations (WT/MHC II⁻, 5XFAD/MHC II⁻ and 5XFAD/MHC II⁺) were analysed using an OpenArray and compared in a heatmap (Figure 18B).

The expression of many genes is mildly increased in 5XFAD/MHC II⁻ microglia compared to WT/MHC II⁻ (Figure 18C). A more pronounced upregulation/downregulation was observed in 5XFAD/MHC II⁺ microglia in comparison to 5XFAD/MHC II⁻ (Figure 18C). A previous study on the gene analysis of pure microglia isolated from accelerated ageing and neurodegenerative mouse models described “general activated” and “primed” modules (Holtman et al., 2015). In the current study, overexpressed genes belong to both “primed” and “activated” modules in MHC II⁺ microglia. The significantly upregulated genes in the MHC II⁺ population related to the “primed” module include apolipoprotein E (ApoE), C-type lectin domain family 7 member A (Clec7a, Dectin1), integrin alpha (Itgax, Mac-1, CD11c), lectin galactoside binding soluble 3 (Lgals3, Mac-2). Upregulated genes such as secreted phosphoprotein 1 (Spp1, immune modulator), encoding cystatin-F (Cst7, immune regulator) belong to the “activated” module. Other overexpressed genes which have been previously shown to be upregulated in AD mouse models (Orre et al., 2014) include cytochrome c oxidase subunit VIa polypeptide 2 (Cox6a2, mitochondrial respiratory chain), MAM domain containing 2 (Mamdc2, glycosaminoglycan binding), low density lipoprotein receptor (Ldlr, endocytosis, neurotrophin pathway), triggering receptor expressed on myeloid cells 178 (Trem178, negative regulator of macrophage activation) and Trem2, the variant of which was defined as a genetic risk for late onset Alzheimer’s disease (LOAD). TYRO protein tyrosine kinase-binding protein (TyroBp), is significantly upregulated in 5XFAD/MHC II⁻ microglia compared to WT/MHC II⁻ microglia but the difference between 5XFAD/MHC II⁺ and 5XFAD/MHC II⁻ is not significant. Downregulated genes include CD33 (inhibiting phagocytosis) and Myc box-dependent-interacting protein 1 (BIN1, role in endocytosis) (Figure 18D).

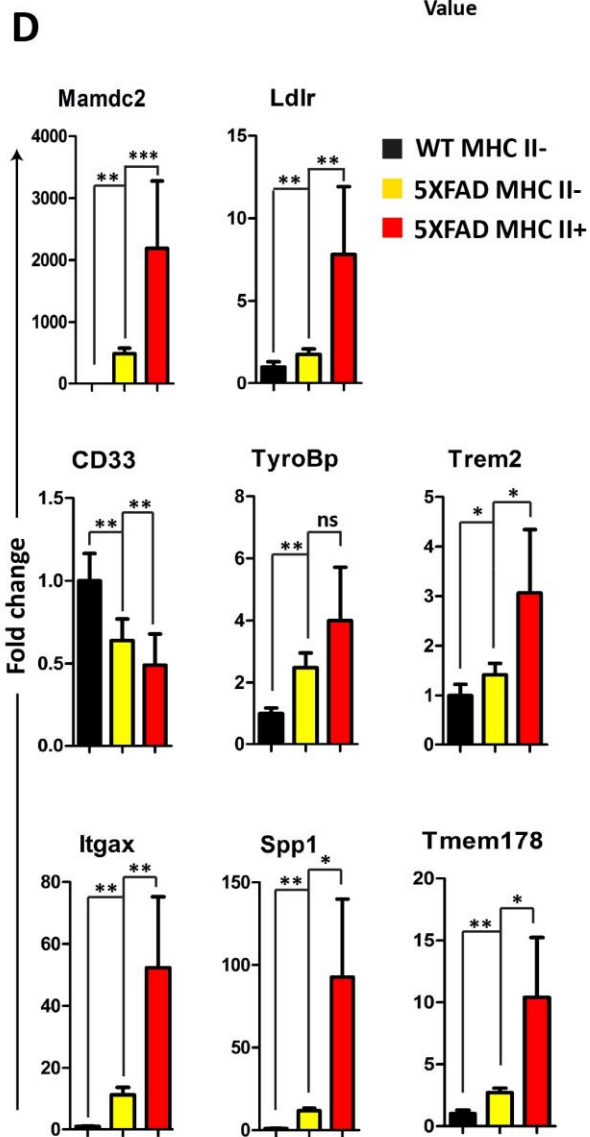
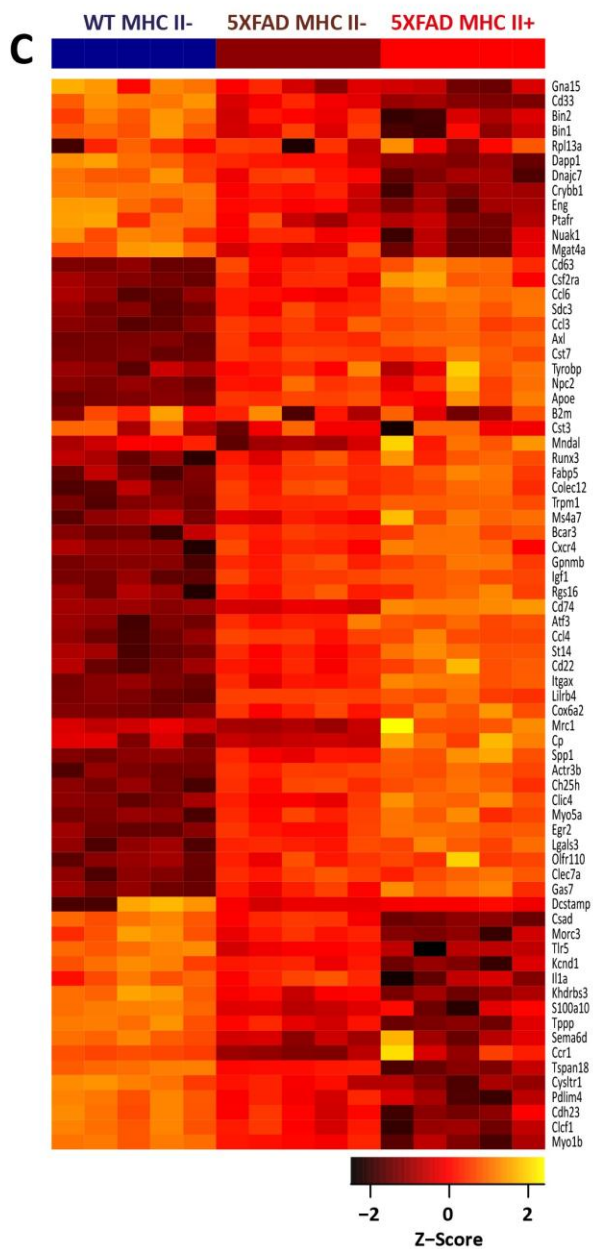
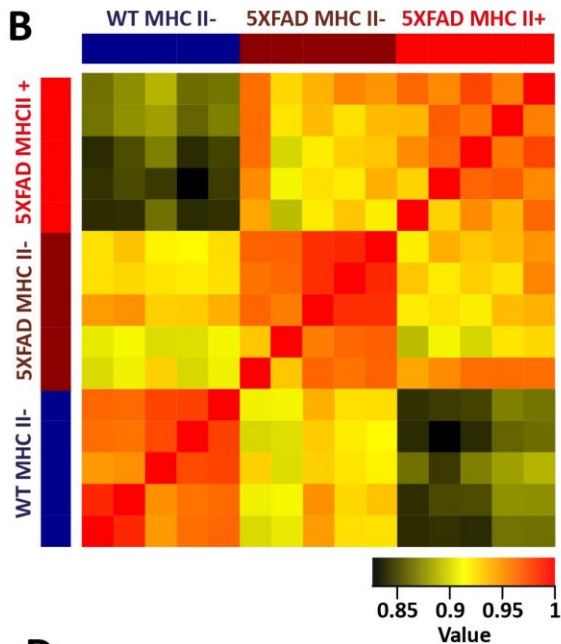
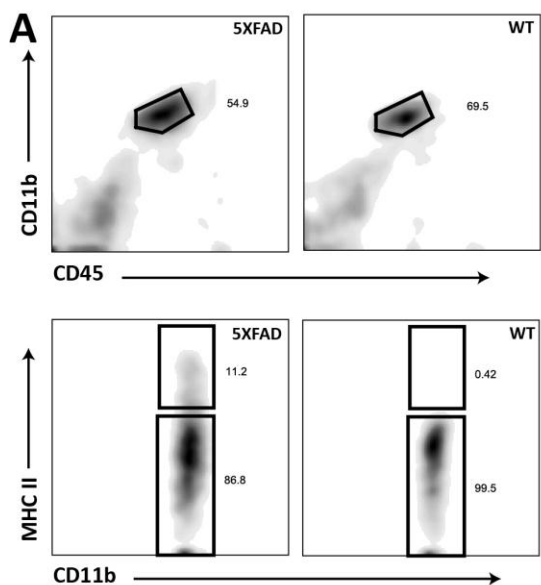


Figure 18: MHC II⁺ microglia from 5XFAD mice have an activated microglial phenotype.

Microglia from 9 months old WT and 5XFAD mice were sorted and analysed for regulation of 842 specific microglial genes related to the inflammatory responses using an OpenArray[®] qPCR platform in collaboration with Lundbeck company (New York, the United states). **(A)** A representative of flow cytometry plots for microglia sorting. Microglia (CD11b⁺CD45^{intermediate}Ly6C⁻) were gated and subsequently sub-gated into MHC II⁺ and MHC II⁻ populations. **(B)** A heatmap of the correlation between every two groups within 5XFAD/MHC II⁺, 5XFAD/MHC II⁻ and WT/MHC II⁻ microglia populations. **(C)** A heatmap of gene expressions in 5XFAD/MHC II⁺, 5XFAD/MHC II⁻ and WT/MHC II⁻ microglia for 72 most differentially expressed genes. The significance threshold for the effect size was set at two fold change and false discovery rate (FDR) adjusted of $p < 0.01$. **(D)** Illustration of selected genes expressions in 5XFAD/MHC II⁺, 5XFAD/MHC II⁻ and WT/MHC II⁻ groups. N=5 from pooled male and female mice. (False discovery rate (FDR), *: $p < 0.05$, **: $p < 0.01$, ***: $p < 0.001$)

3.2.6 Systemic LPS injection leads to morphological changes of microglia

Previous studies have described a stronger pro-inflammatory response in the brain of animals with age-related or neurodegenerative pathology upon LPS injections (Gatti & Bartfai, 1993; Cunningham et al., 2005; Sierra et al., 2007; Ramaglia et al., 2012). To examine the effects of ageing, A β plaque deposition and systemic infection on microglia activation in APP23 and 5XFAD mice, 6, 20 and 24 months old APP23 mice, 12 months old 5XFAD mice as well as aged matched WT mice were injected with LPS (i.p.; 1 mg/kg). 6 hours after LPS injection mice were transcardially perfused and the brains were analysed for morphological changes of the microglia. In the AD transgenic mice microglia far from or in the vicinity of A β plaque depositions were also compared. Control groups of transgenic and WT mice received PBS, instead (Figure 19).

PBS-injected 6 months old WT and APP23 mice show ramified microglia with thin and long processes, whereas LPS injected mice reveal more densely stained microglia (Figure 19A). Microglia in the cortex of 20 months old WT mice or non-plaque regions of APP23 represent a ramified morphology after PBS injection, while microglia in the vicinity of A β plaque depositions have thicker processes and are less ramified. However, LPS injection leads to less ramifications even in WT or non-plaque regions of APP23 mice (Figure 19B). Intermediate loss of ramifications in microglia can be found in 24 months old PBS-injected WT mice and non-plaque areas of 24 months old APP23 mice, as well (Figure 19C). At the age of 20 and 24 months, LPS injection leads to the amoeboid or rod-shaped microglia with short and thick processes in direct contact to the A β plaques (Figure 19B-C). Figure 19D represents microglia morphology in 5XFAD mice compared to WTs. Upon PBS injection, microglia of WT mice or non-A β plaque regions of 5XFAD mice are ramified whereas microglia in the

neighbourhood of A β depositions have thicker processes and show less ramifications. LPS injection results in the shortening and thickness of microglial processes in WT mice and to a further loss of ramifications in microglia surrounding the A β depositions in 5XFAD mice (Figure 19D).

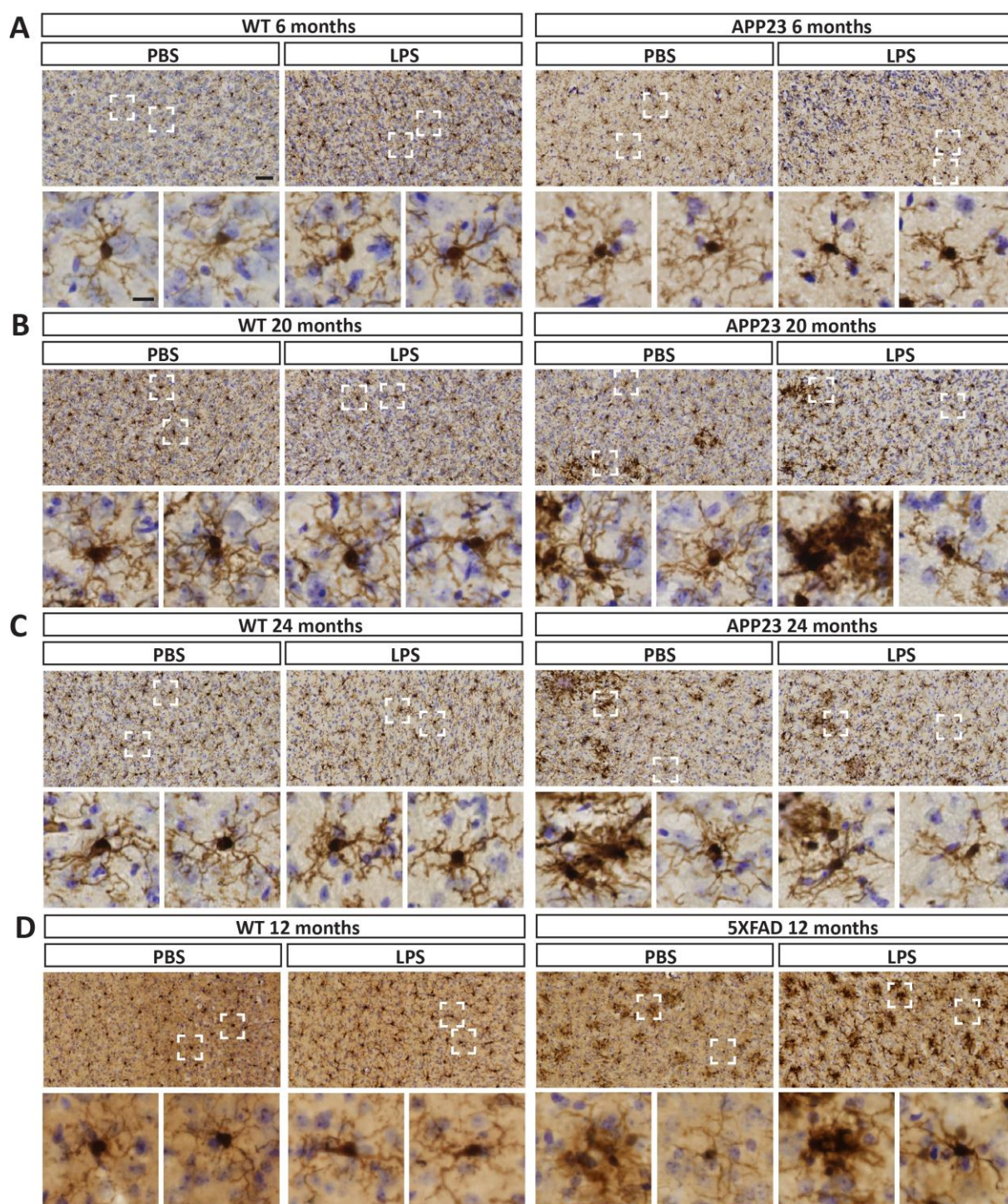


Figure 19: Morphological changes in plaque-associated microglia in APP23 and 5XFAD mice upon LPS injections.

Iba1 and cresyl violet staining of cortical sections of increasing age of WT and APP23 transgenic mice (6, 20 and 24 months old) (A-C) and 12 months old WT and 5XFAD mice (D). Mice were injected with PBS or LPS, i.p. (1 mg/kg of the weight in 200 μ l volume) 6 hours prior to sacrifice. Enlarged images depict microglia in WT mice, non-plaque areas and in the neighbourhood of A β plaque depositions (labelled by cresyl violet, shown in brackets) in APP23 and 5XFAD mice as indicated. Scale bars: A-D: images = 30 μ m, enlarged images = 10 μ m. N= 3-5.

3.2.7 Microglia in the vicinity of A β plaques have an enhanced inflammatory response to systemic LPS challenges

After i.p. LPS injections stronger morphological changes were observed in microglia in the vicinity of A β plaque depositions compared with the microglia remote from the plaques. It has been described that morphological changes in microglia -to some extent- alter their functions. For instance, ramified microglia have been introduced as surveying cells in the CNS whereas amoeboid shapes represent their pro-inflammatory activities (reviewed by Wojtera et al., 2012). To determine the activation state of these less-ramified microglia upon LPS challenges, 20 months old APP23 and WT mice were injected with PBS or LPS, i.p. (1 mg/kg) 6 hours prior to be sacrificed and the cortical regions of the brains were stained with microglial activation markers Mac-2, CD68 and MHC II.

Figure 20A, D and G represent cortical sections of WT and APP23 mice stained with cresyl violet (labelling A β plaques) and Mac-2, CD68 and MHC II, respectively. Upon PBS or LPS injections, the expression of these markers is observed only in microglia surrounding the A β depositions. WT mice (PBS or LPS injected) and non-plaque regions of APP23 mice (PBS or LPS injected) lack Mac-2, CD68 and MHC II staining (Figure 20A, D, G). Since even PBS injected APP23 mice express these proteins (in the microglia surrounding the plaques), for a better understanding of how much expression of these markers are upregulated in microglia after an LPS injection, the stainings were quantified by calculating the ratio of DAB stained areas to the total cortical area. Expression of Mac-2 is very low in WT mice even upon LPS injection. However, PBS injected APP23 mice show a higher expression of Mac-2, which is strongly induced by an LPS challenge (p value 0.001; Figure 20B). For a more detailed study the data were divided into two groups obtained from non-plaque areas and plaque regions (Figure 20C, F, I). Quantification of Mac-2 staining reveal that LPS does not lead to a higher Mac-2 expression on the cells from non-plaque regions, while a significant increase in Mac-2

staining is found in the cells from plaque areas (p value, < 0.0001; Figure 20C). Similar to Mac-2 immunoreactivity, upon LPS injection CD68 and MHC II show a higher expression in APP23 mice compared to LPS-injected WT (p values 0.002 and 0.003) or PBS-injected transgenic mice (p values 0.03 and 0.009; Figure 20E, H). LPS injection leads to a higher expression of these factors in the areas with A β plaques compared to non-plaque areas (p values < 0.0001). Also, in the areas with plaques LPS has a strong effect on expression of these markers compared to PBS injection (p values < 0.0001 and 0.003; Figure 20F, I).

To be sure that the cells expressing these markers are microglia and not astrocytes, immunofluorescent staining for GFAP (astrocyte marker), Iba1 co-stained with Mac-2, CD68 and MHC II was applied on the brain sections. GFAP and Iba1 staining revealed expression of these activation markers only on microglia (data not shown) and not on astrocytes (Figure 21A-C).

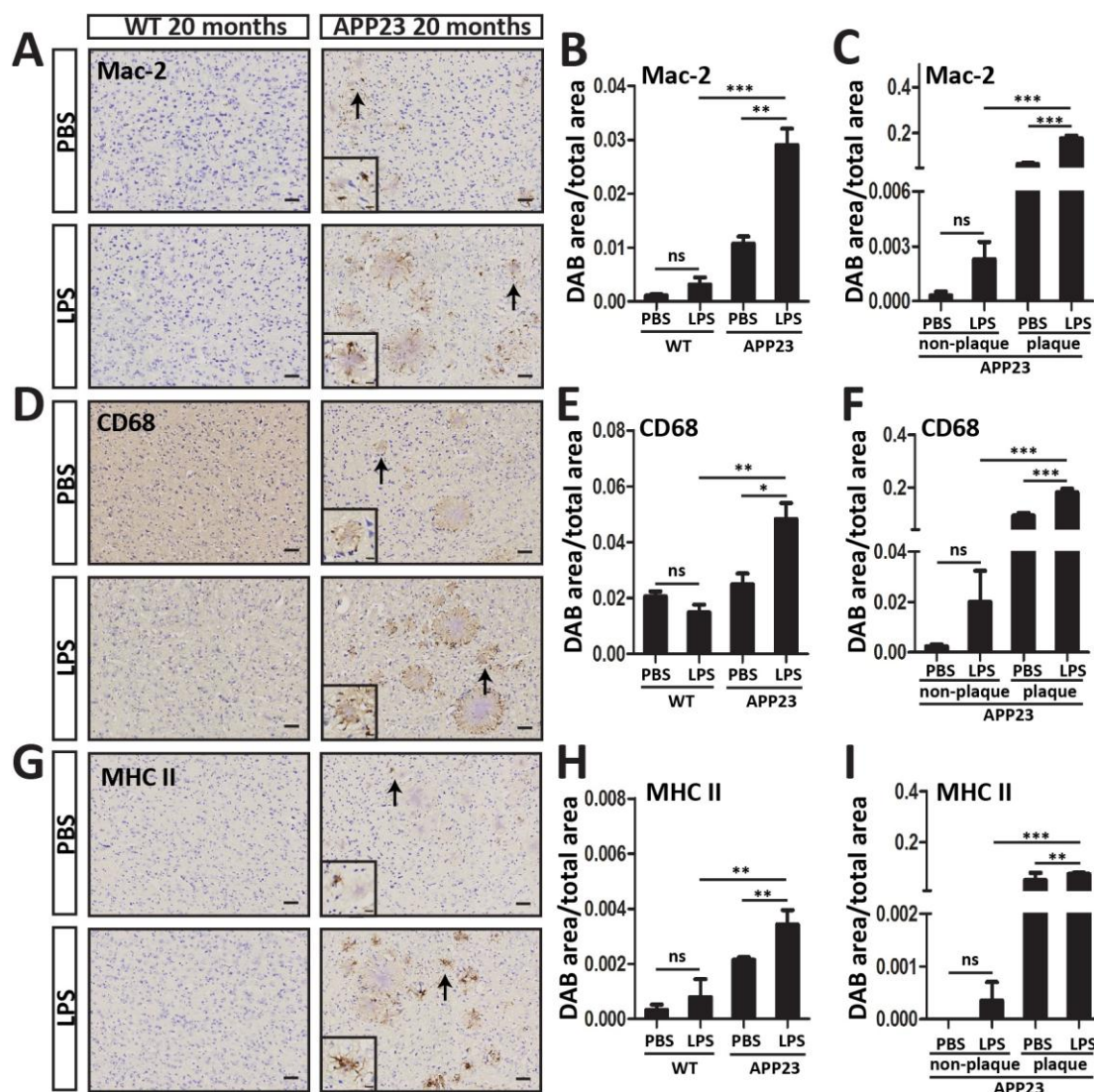


Figure 20: Increased expression of microglial activation markers after peripheral LPS injections.

20 months old WT and APP23 transgenic mice were injected with PBS or LPS (i.p., 1 mg/kg) as indicated. Cortical sections from these mice were stained with (A) anti-Mac-2 (D) anti-CD68, (G) anti-MHC II and cresyl violet (labelling A β depositions). Quantification of Mac-2 (B-C), CD68 (E-F) and MHC II (H-I) expression by dividing the areas covered by DAB to the total area. Comparison between WT and APP23 mice (B, E, H) or non-plaque areas and the plaque covered regions in APP23 mice (C, F, I). (One-way ANNOVA followed by Bonferroni's post-hoc test; *: p<0.05, **: p<0.01, ***: p<0.001) Scale bars: A, D, G = 10 μ m; insets = 10 μ m. Number of plaque areas = 6/ mouse, number of non-plaque areas = 3-4/ mouse, N= 3-5 mice. M: months.

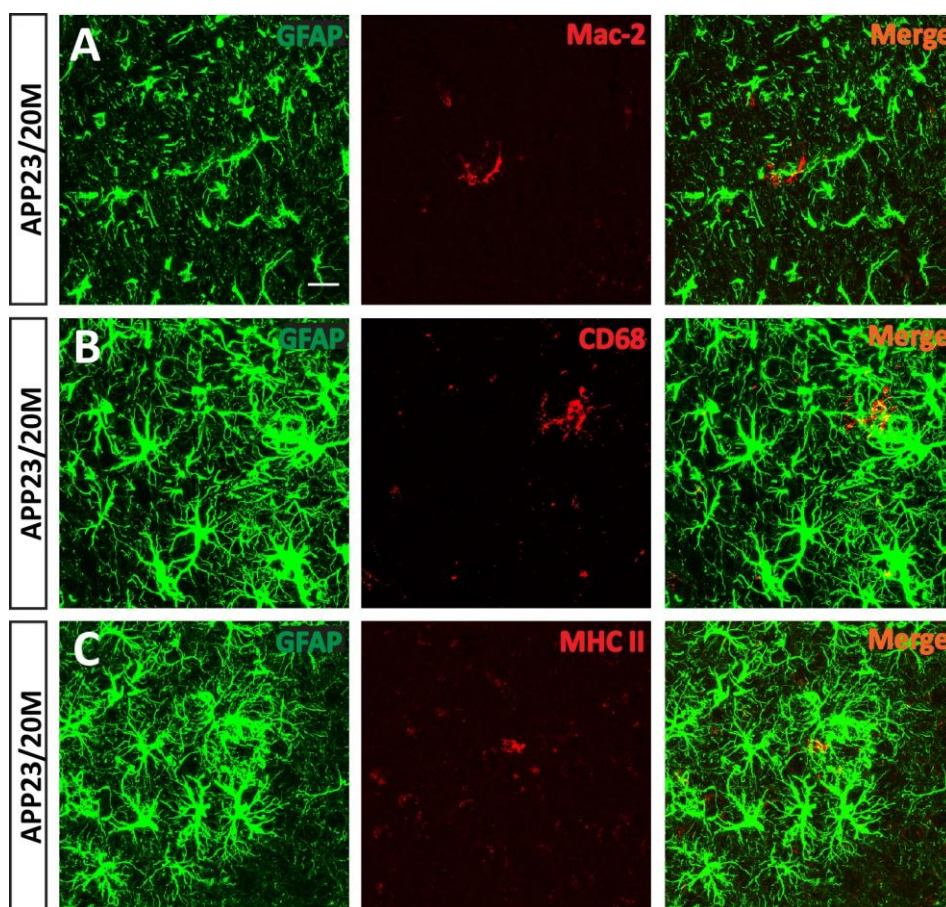


Figure 21: No expression of microglial activation markers on astrocytes.

Immunofluorescence staining of cortical sections of i.p. LPS injected (1 mg/kg) 20 months old APP23 mice for GFAP and (A) Mac-2, (B) CD68 and (C) MHC II. Scale bar = 20 μ m. N=3.

3.2.8 LPS leads to the production of IL-1 β by microglia surrounding A β plaques

Secretion of pro-inflammatory cyto-/ chemokines is one the characteristics of activated immune cells including microglia (Hanisch & Kettenmann, 2007). We observed

morphological changes of microglia as well as expression of activation markers by these cells after i.p. LPS injection mainly in the vicinity of A β plaques. To investigate if these microglia also secrete pro-inflammatory cytokines, we examined production of IL-1 β by these cells. Therefore, 20 and 24 months old APP23 mice and 12 months old 5XFAD mice were i.p. injected with PBS or LPS (1 mg/kg) and were sacrificed 6 hours later. Cortical sections were stained with IL-1 β and Congo red (staining mature A β depositions; Figure 22).

In the PBS injected 20 and 24 months old APP23 mice no microglia IL-1 β expression is observed (Figure 22A, C), neither surrounding the plaques (Figure 22A', C'), nor far from the plaques (Figure 22A'', C''). 20 months old APP23 mice injected with LPS show a high production of IL-1 β in microglia around the A β depositions (Figure 22B, B') but not at plaque-free areas (Figure 22B, B''). LPS injection in 24 months old APP23 mice leads to an abundant production of IL-1 β by the cells in the close vicinity of the plaques (Figure 22D, D') as well as at plaque-free regions (Figure 22D, D''). To confirm the production of IL-1 β by microglia, the sections were stained with Iba1 and IL-1 β . Immunofluorescence stainings of LPS-injected APP23 (20 and 24 months old) and 5XFAD mice reveal co-staining of IL-1 β -expressed cells only with microglia marker, Iba1 (Figure 23A-C).

IL-1 β is among the pro-inflammatory cytokines that requires activation of intracellular inflammasomes. Recruitment of the adaptor protein ASC and its interaction with pro-caspase 1 is essential for this process (reviewed by Singhal et al., 2014). To investigate if the present IL-1 β staining signal is truly the result of a pro-inflammatory response (to LPS), different regions of brain sections from 24 months old LPS-injected APP23 mice were stained with ASC and Congo red. Three tested brain regions of cortex, hippocampus and thalamus show ASC immunoreactivity on the cells which are surrounding the A β plaque depositions (Figure 24A-B).

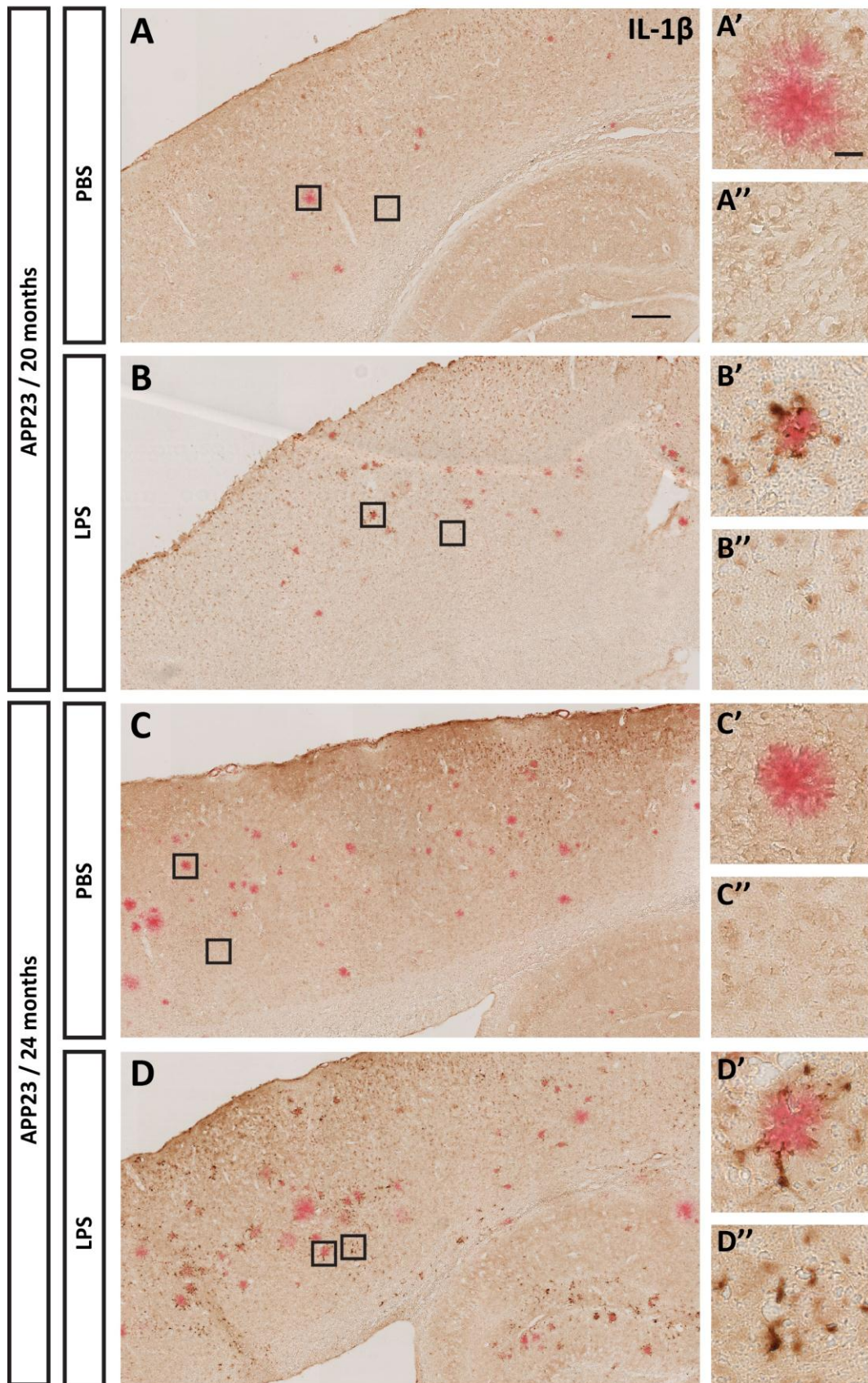


Figure 22: Production of IL-1 β in APP23 mice after i.p. LPS injection.

Cortical sections of LPS injected APP23 mice. 20 and 24 months old APP23 mice were injected i.p. with PBS or LPS (1 mg/kg) 6 hours prior to be sacrificed. The cortical brain sections were stained with antibody against IL-1 β and Congo red (labelling matured A β plaques). Lower magnification of the cortex from PBS injected 20 months old (**A**), LPS injected 20 months old (**B**), PBS injected 24 months old (**C**) and LPS injected 24 months old (**D**) APP23 mice. Higher magnifications show A β plaque areas (**A'**, **B'**, **C'**, **D'**) and non-plaque region (**A''**, **B''**, **C''**, **D''**). Scale bars: A-D = 200 μ m; A'-D', A''-D'' = 20 μ m. N=3-5.

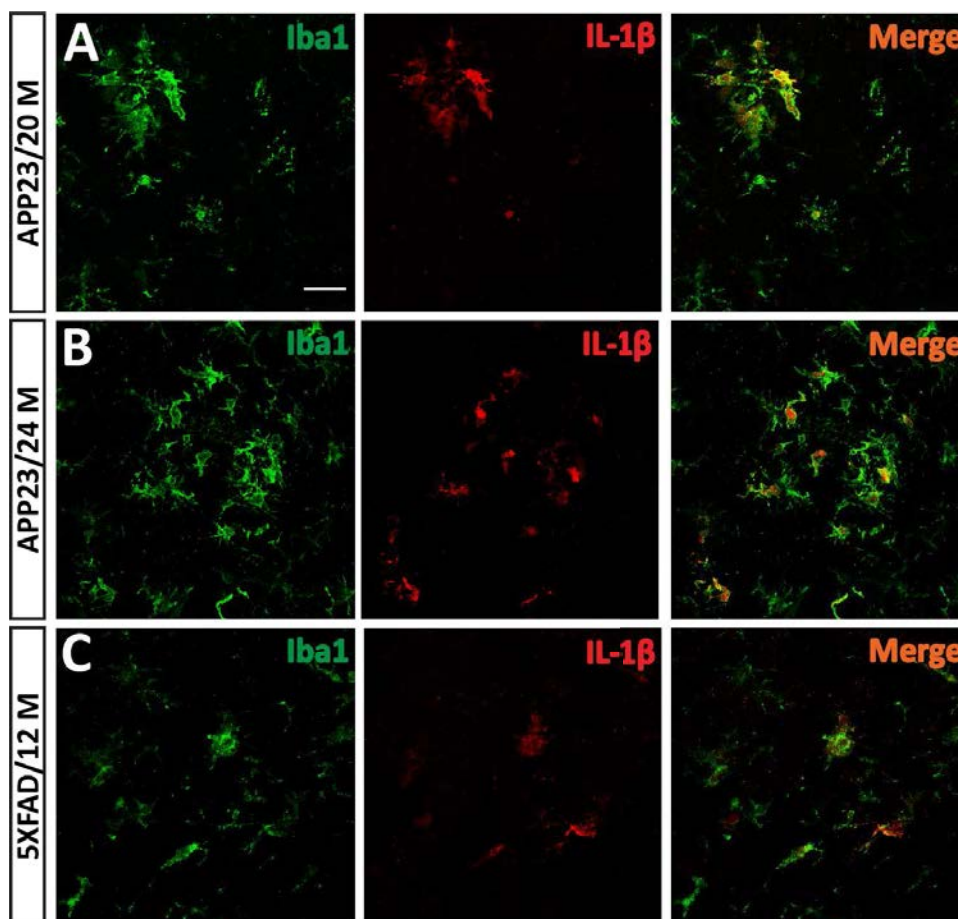


Figure 23: Expression of LPS-induced IL-1 β by plaque-associated microglia in APP23 and 5XFAD transgenic mice.

Immunofluorescence staining of Iba1 and IL-1 β on cortical sections of (**A**) 20 months old, (**B**) 24 months old APP23 and (**C**) pons region of 12 months old 5XFAD mice injected with LPS i.p. (1 mg/kg). Scale bars: 20 μ m. N=3-5. M: months.

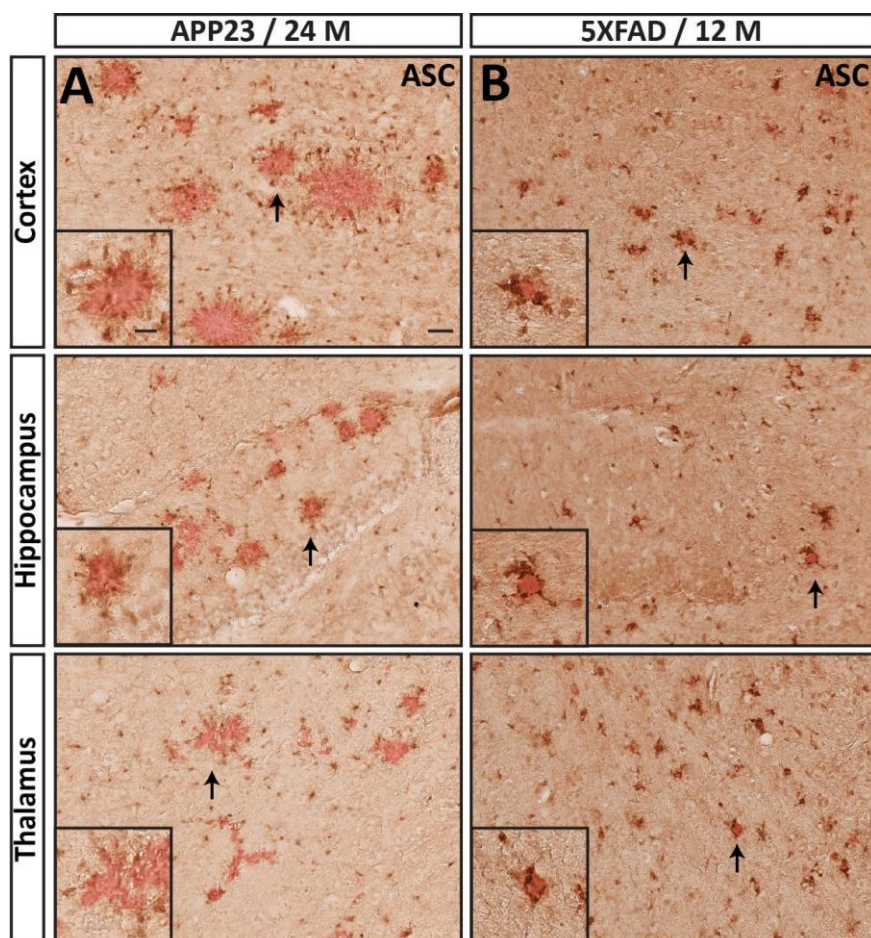


Figure 24: LPS-induced ASC activation by plaque-associated microglia in APP23 and 5XFAD transgenic mice.

Congo red and ASC (inflammasome adaptor protein) staining of cortex, hippocampus and thalamus regions of **(A)** 24 months old APP23 and **(B)** 12 months old 5XFAD mice injected with LPS i.p. (1 mg/kg). Arrows indicate the ASC staining around the congophilic A β plaques. Scale bars: 50 μ m, insets = 15 μ m. N=3-5. M: months.

3.3 Noradrenergic control over innate immune cell activities in the CNS

Earlier studies proposed anti-inflammatory effects of the noradrenergic system by activating the beta 2 adrenergic receptor (β 2AR; reviewed by Scanzano & Cosentino, 2015). Previous own data have shown, that the β 2AR agonist, salbutamol, selectively inhibits the expression of pro-inflammatory cyto- /chemokines, which are produced upon LPS stimulation. Clearly, treatment of LPS-stimulated microglia with salbutamol inhibits a subset of pro-inflammatory cytokines (Figure 25A) while, having no effect on another group of pro-inflammatory cytokines (Figure 25B; see master's thesis of Stefanie Riesenberger; doctoral thesis of Tommy Regen). Among the studied proteins, TNF α and CCL5 are the strongest inhibited and non-inhibited pro-inflammatory factors, respectively. Thus, for further studies we focussed mainly on these two genes.

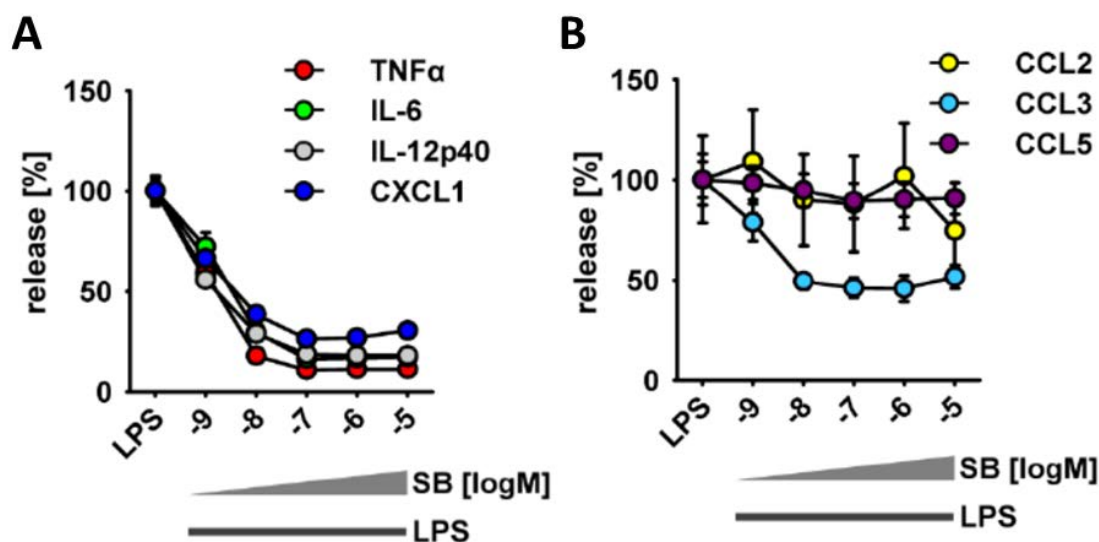


Figure 25: β 2ARs regulate LPS-induced gene expression.

Neonatal mouse microglia were stimulated with LPS (rough type; 10 ng/ml) alone or in combination with increasing concentrations of salbutamol (SB) as indicated. The released cyto- /chemokines were measured in the supernatant of the cells, subsequently. The Data are normalized to LPS stimulation without salbutamol (100%). Inhibited proteins (**A**) and non-inhibited proteins (**B**) are presented. The figure is modified according to Stefanie Riesenberger's master thesis. SB: salbutamol.

3.3.1 All the cultured microglia express β 2AR

Since induction of a group of genes is blocked by β 2AR activation, it was necessary to check whether microglia express β 2ARs. Recent research has shown that microglia behave heterogeneously in terms of the expression of cyto- /chemokines (Scheffel et al., 2012). Thus,

it would be possible that a cytokine-producing subpopulation of microglia lacks β 2AR. We used immunocytochemistry analysis on microglia from neonatal WT mice to study their expression of β 2AR. Figure 26 shows that all microglia show immunoreactivity for anti- β 2AR, indicating that a β 2AR-lacking microglia population does not exist. No signal was observed by anti-rabbit antibody alone (data not shown).

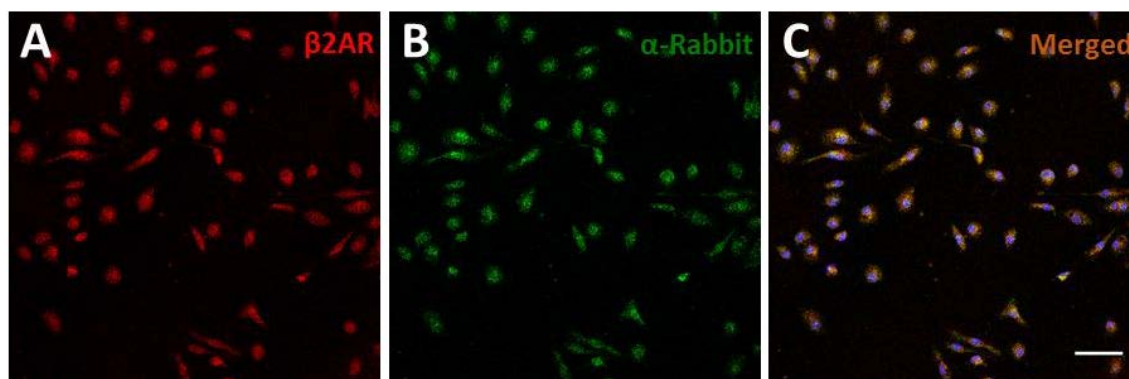


Figure 26: Immunocytochemistry analysis for β 2AR expression on microglia.

Microglia from neonatal WT mice (5×10^4 cells per well in 4-well plate) were stained with (A) Cy3-labelled rabbit anti-mouse anti- β 2AR antibody (Red) and (B) Alexa Flour488-labelled anti-Rabbit antibody (green). The merged photo (C) shows β 2AR expression on all the microglia. The nuclei were staining by Dapi (blue). Scale bar= 50 μ m. β 2AR: beta 2 adrenergic receptor; α : anti.

3.3.2 Not all the TRIF-dependent genes are rescued from the inhibition upon β 2AR activation.

As described earlier (section 3.3, Figure 25), different pro-inflammatory genes behave differently on activation of β 2AR. Gene induction by LPS (through TLR4) stimulation is accomplished through MyD88, TRIF or both adaptor proteins (Figure 1; reviewed by Takeda & Akira, 2004). For instance, TNF α is exclusively MyD88-dependent whereas expression of CCL5 is induced by both MyD88- and TRIF-mediated pathways (doctoral thesis of Tommy Regen). Dr. Tommy Regen in his PhD thesis also showed that CCL5 in microglia deficient in TRIF protein (*TRIF*^{-/-}) is no longer a non-inhibited protein but becomes inhibited (data not shown). According to this finding we questioned whether the TRIF pathway is the non-inhibitory path. If this is the case, all the genes which have the possibility to use this pathway would be non-inhibited. To answer this question, we assessed the induction of two exclusively TRIF dependent genes, MHC I and IFN β upon β 2AR activation using flow cytometry and ELISA, respectively. Data obtained from MHC I expression analysis (Figure 27B) reveal no

inhibition by salbutamol. However, activation of β 2AR by salbutamol leads to a significant reduction of IFN β production compared to its release upon LPS stimulation (p value 0.001; Figure 27C).

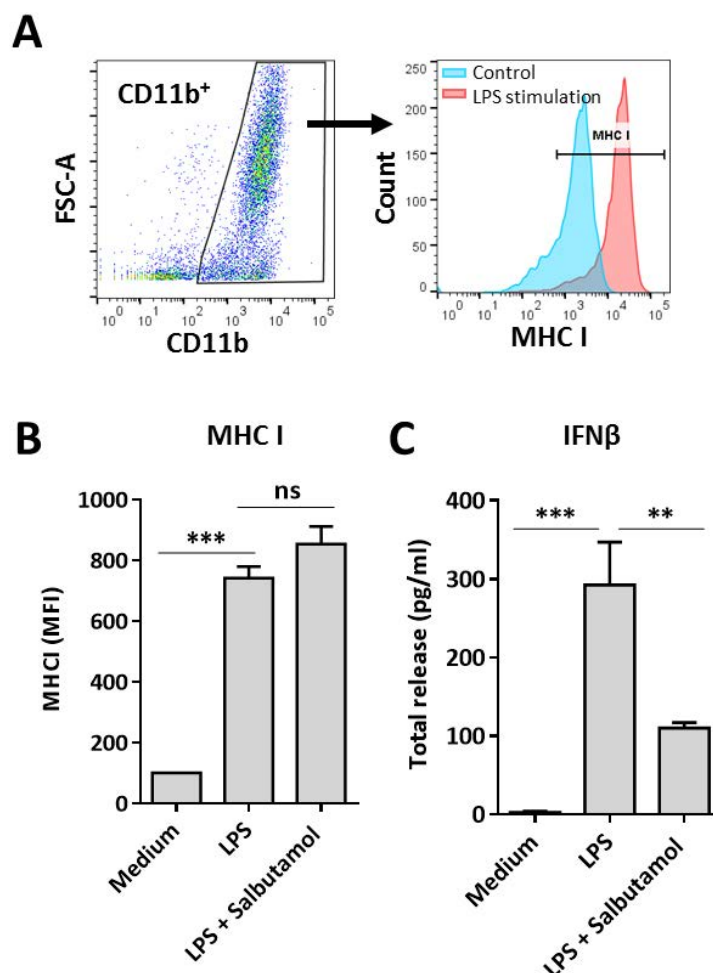


Figure 27: MHC I and IFN β expression analysis after TLR4 and β 2AR stimulation.

Microglia from neonatal WT mice (2×10^5 cells/well for MHC I or 1.5×10^4 cells/well for IFN β measurements) were stimulated with LPS (rough type; 10 ng/ml) alone or combined with salbutamol (1 μ M). MHC I expression was analysed after 24 hours and IFN β secretion after 18 hours. Control groups received complete DMEM without a stimulus. (A) Gating strategy of MHC I expression from flow cytometry data. 10,000 CD11b⁺ cells were recorded and investigated for the positive MHC I signal. (B) Mean fluorescent intensity (MFI) of the signal was calculated from the data. Data are normalized to 100% medium control. (C) Expression of IFN β upon TLR4 and β 2AR activation. The amount of IFN β was measured in the supernatant by using ELISA. Data are mean \pm SEM. N=6 for MHC I and 8 for IFN β from 3 independent experiments. (One-way ANOVA followed by Tukey's post-hoc test; *: p<0.05, **: p<0.01, ***: p<0.001)

3.3.3 Activation of β 2AR in the CNS inhibits infiltration of immune cells from the periphery

One of the consequences of an inflammatory response by immune cells is the production of cyto-/ chemokines which results in recruiting additional immune cells to the site of challenge such as infection (reviewed by Iwasaki & Medzhitov, 2004). Macrophages, including microglia are able to sense the immune challenges using their TLRs (reviewed by Akira et al., 2006). Contribution of the noradrenergic system in suppressing the immune response from immune cells has been shown previously (reviewed by Scanzano & Cosentino, 2015). In the healthy brain noradrenaline is constantly produced and delivered from the locus coeruleus (reviewed by Aston-Jones & Cohen, 2005).

To determine the effect of microglial β 2AR activation on recruitment of immune cells from the periphery, we stimulated microglia with LPS (strong infectious stimulus) alone or combined with salbutamol as a specific β 2AR agonist or ICI as a specific β 2AR antagonist intracerebrally using osmotic pumps. In addition two control groups of salbutamol and ICI only were used. Previous experiments in the lab showed no immune cell infiltrates into the brains upon PBS infusion (data not shown) thus, in the study PBS infusion was not applied. An installation of osmotic pumps in the tissue ensured a constant infusion of the solutions. Here, we used the speed of 0.5 μ l per hour and installed the cannula's of the pumps for 24 hours in the striatum of the brain. Afterwards, mice were perfused with PBS and by using flow cytometry brains were analysed for infiltrating neutrophils, monocytes and T cells as shown in Figure 28A. Infusion of salbutamol or ICI *per se* does not lead to infiltration of peripheral immune cells (Figure 28B-D). Clearly, LPS delivery leads to a massive increase of the infiltrated immune cells (Figure 28B-D; p value for neutrophils, 0.008; for monocytes 0.0004; for T cells, 0.03). A combination of salbutamol with LPS significantly inhibits this strong effect of LPS on neutrophils and monocytes. The reduced T cell infiltration is not statistically significant, probably due to the low number of mice used for this experiment (p value for neutrophils, 0.03; for monocytes, 0.0005; for T cells, 0.06). The data from Figure 28B-D also show that addition of ICI to LPS has no effect on LPS-induced infiltration (p value of LPS + salbutamol vs LPS + ICI for neutrophils, 0.001; for monocytes, 0.002; for T cells, 0.02).

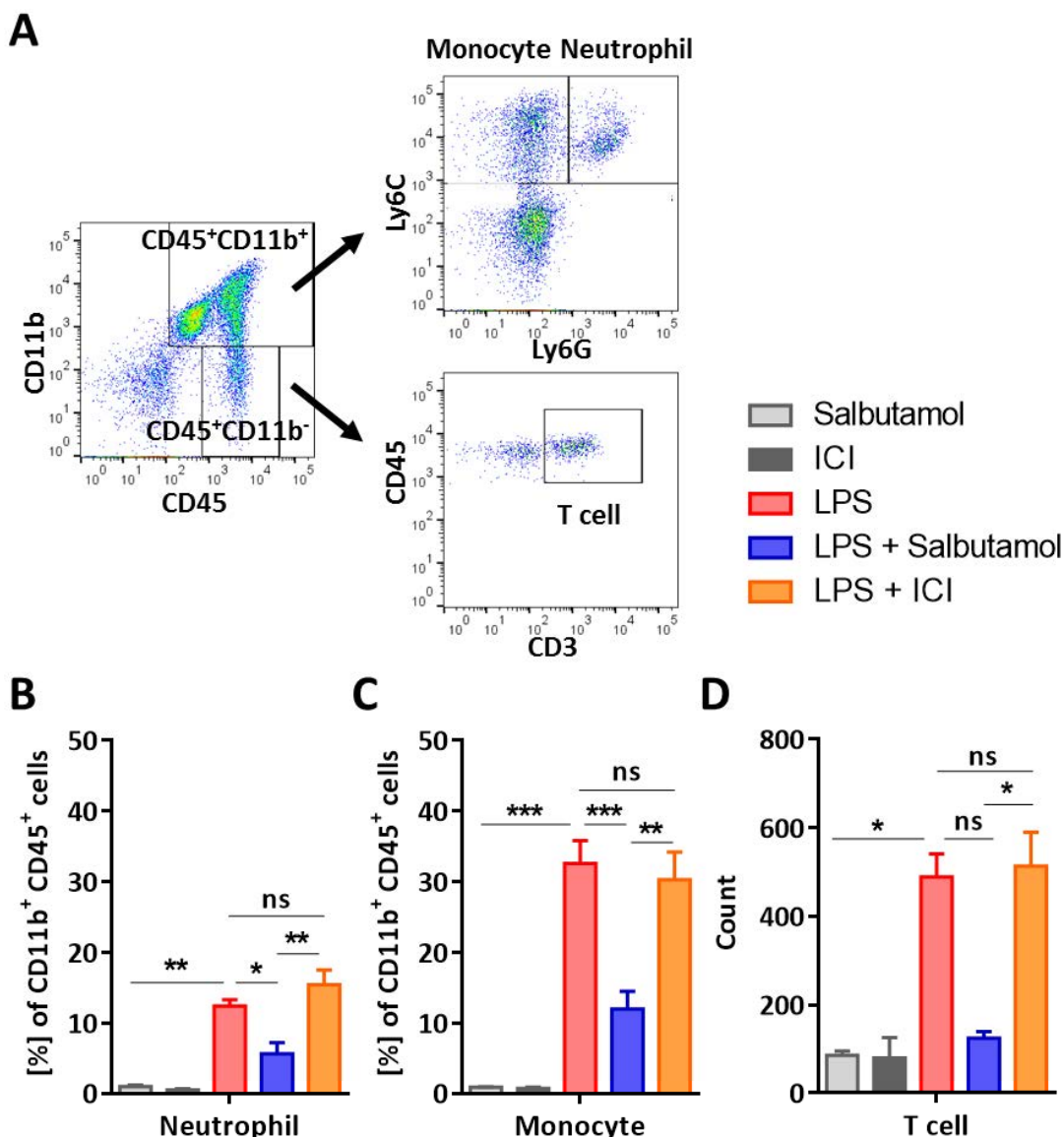


Figure 28: Effect of β 2AR activation in the CNS on immune cell infiltrates from the periphery.

8-12 weeks old female WT mice were intracerebrally infused with LPS (rough type; 1 mg/ml) or a combination of LPS with salbutamol or ICI (both 100 μ M) for 24 hours with a speed of 0.5 μ l/hour. Control groups were infused with salbutamol or ICI only. Cell suspensions isolated from the brains of individual mice were analysed by flow cytometry. (A) Example of brain analysis for monocytes (CD11b⁺, CD45⁺, Ly6C⁺, Ly6G⁻), neutrophils (CD11b⁺, CD45⁺, Ly6C⁻, Ly6G⁺) and T-cells (CD45⁺, CD11b⁻, CD3⁺). 10,000 CD11b⁺ cells were recorded via flow cytometry and the percentage of neutrophils (B) and monocytes (C) from CD11b⁺ and CD45⁺ population were evaluated. (D) Brain samples were analysed for the amount of T-cells infiltrating from the periphery. Absolute numbers of T-cells were counted from CD45⁺, CD11b⁻ cells. Data are mean \pm SEM. N for monocyte and neutrophil= 3-4 for control groups, 10-12 for LPS, LPS + salbutamol and LPS + ICI. N for T cells= 2 for control groups, 3-5 for treatment groups. (One-way ANNOVA followed by Tukey's post-hoc test; *: p<0.05, **: p<0.01, ***: p<0.001)

3.3.4 Activation of β 2AR in the CNS does not decrease gliosis

As described in the section 3.3.3 activation of β 2AR by salbutamol led to the reduction of the LPS effect on immune cell infiltrations (Figure 28B-D). We decided to further investigate this effect on activation of microglia/macrophages and astrocytes as well, since all these cell types express β 2AR (Scanzano & Cosentino, 2015; Aoki, 1992). To perform this experiment we used the same osmotic pumps and stimuli as mentioned in 3.3.3. The delivery of stimuli (LPS alone or combined with salbutamol or ICI) lasted 72 hours and the brains were processed and analysed by immunohistochemistry. Control groups received only salbutamol or ICI. The immunoreactivity for macrophage-1 antigen (Mac-3, macrophage/microglia marker), ionized calcium-binding adapter molecule 1 (Iba-1, microglia marker) and glial fibrillary acidic protein (GFAP, astrocyte marker) are shown in the Figure 29A-D, E-H and I-J, respectively. Quantification of Mac-3 signal reveals increased expression of this marker upon LPS infusion compared with the control condition with salbutamol (Figure 29K). Combination of salbutamol with LPS significantly reduces this outcome (p value 0.03). Combining ICI with LPS does not affect the LPS effect (p value LPS + salbutamol vs LPS + ICI, 0.02). Expression of Iba-1 and GFAP show a high induction of the markers after LPS infusion compared to salbutamol (Figure 29L and M). In contrast, LPS-induced Iba-1 and GFAP expressions are not affected by salbutamol. ICI has no effect either.

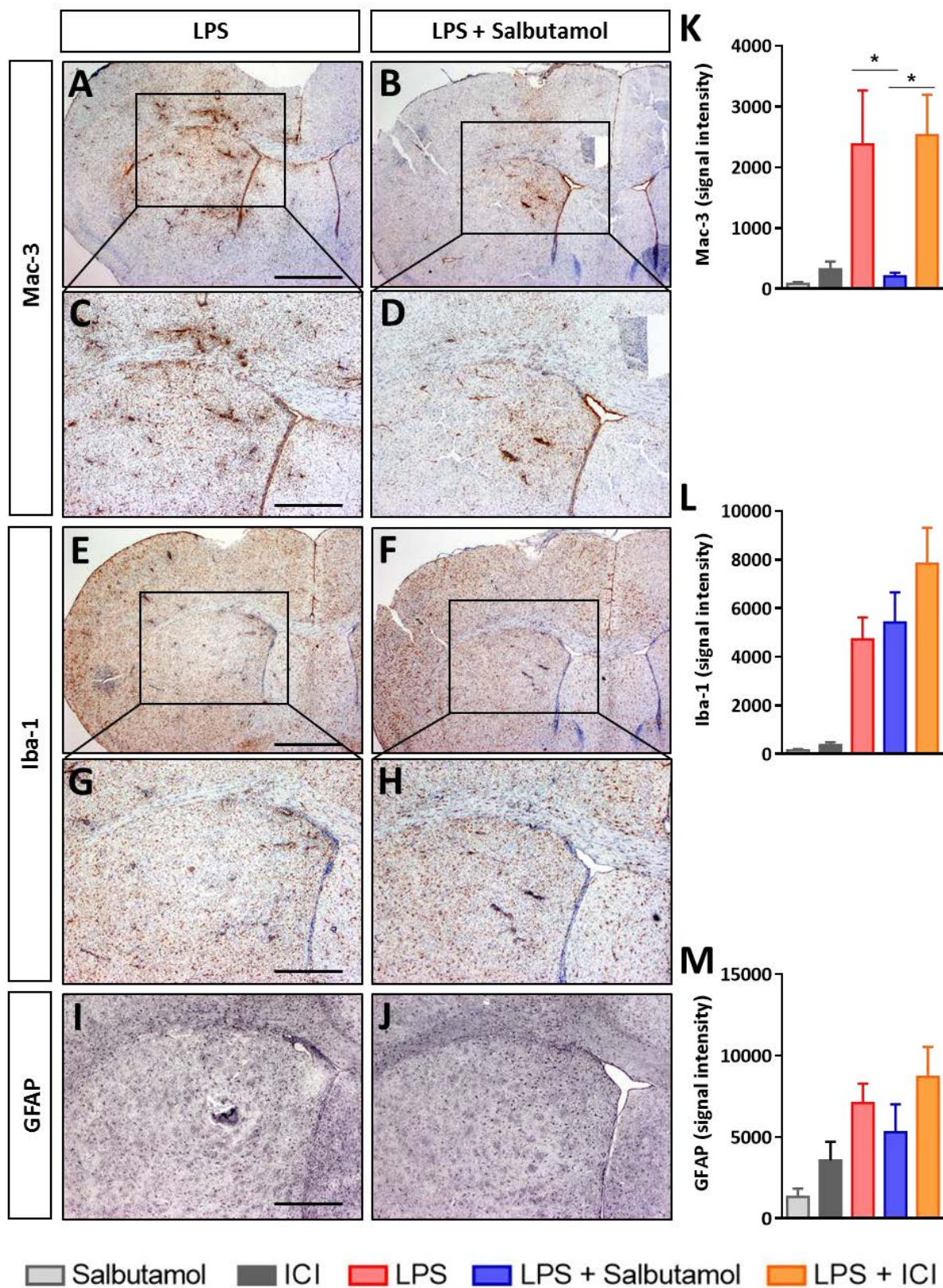


Figure 29: Immunohistochemistry analysis of β 2AR signalling effect on microglia and astrocyte activation.

8-12 weeks old WT female mice were intracerebrally infused with LPS (rough type; 1 mg/ml), combination of LPS and salbutamol or ICI (both 100 μ M) for 72 hours with speed of 0.5 μ l/hour.

Control groups received salbutamol or ICI alone. Mice were sacrificed and perfused with PBS followed by 4% PFA and, eventually, paraffin embedded. 3 μ m sections were stained by antibodies against Mac-3, Iba-1 and GFAP to indicate expression of these proteins in macrophages/ microglia and astrocytes, respectively. Mac-3 (**A-D**), Iba-1 (**E-H**) and GFAP (**I-J**) staining of two sections representing LPS (left) and LPS + Salbutamol (right) infused mice. Signal intensity of Mac-3, Iba-1 and GFAP staining, calculated after subtraction of background and gauss filtering using ImageJ, is depicted in graphs (**K-M**). Data are mean \pm SEM. N=4 for LPS, LPS + Salbutamol, LPS + ICI groups and 2 for control groups. From each brain 4 sections were evaluated. (One-way ANNOVA followed by Tukey's post-hoc test; *: $p < 0.05$, **: $p < 0.01$, ***: $p < 0.001$) Scale bars: A-B, E-F= 1 mm, C-D, G-H, I-J= 500 μ m.

3.3.5 The population size of microglia producing TNF α and CCL5 is altered by β 2AR activation

As mentioned earlier, the production of some cytokines such as TNF α by microglia is dramatically inhibited after β 2AR stimulation (Figure 25). These data were obtained by ELISA, which measures the concentration of the protein of interest and it cannot discriminate between producing and non-producing cells. To extend our study to the population size, which might be influenced by β 2AR activation, we performed flow cytometry analysis. Microglia were stimulated with LPS alone or in combination with salbutamol for 8 hours. To trap the produced proteins inside the cells and to inhibit their secretion we blocked the Golgi transport by monensin (an intracellular traffic inhibitor; Mollenhauer et al., 1990). Cells were in total stimulated for 8 hours with the respective stimuli while monensin was added 3 hours after the stimulation began. No major toxicity of monensin to the cells for this period of time was seen (data not shown). Illustrated in Figure 30B-C, the percentages of cells that produce TNF α and CCL5 under the medium conditions increase upon LPS stimulation to a much larger population sizes: almost 65% produced TNF α (p value < 0.0001) and about 30% produced CCL5 (p value 0.003). The TNF α -producing subpopulation was significantly reduced by addition of salbutamol to about 20% (p value < 0.0001 ; Figure 30B). The CCL5 producing subpopulation had a slight but insignificant increase to about 40% (Figure 30C). These data indicate that not only the amount of TNF α is reduced by β 2AR activation (data obtained from protein concentrations), but also the proportion of cells, which produce this cytokine is reduced. Similar to the unaffected amount of CCL5 by activation of β 2AR, the CCL5 producing population size does not alter either.

Some cells produce TNF α and CCL5 together. Therefore, to look closer, we divided the data to three groups of cells producing TNF α only, CCL5 only or both (Figure 30D). Here, we

observe that salbutamol dramatically decreases the number of cells which produce only TNF α upon LPS stimulation (p value < 0.0001), while increasing only-CCL5 positive population (p value < 0.001). The population size of the cells, which produce TNF α and CCL5 simultaneously is not altered upon salbutamol treatment.

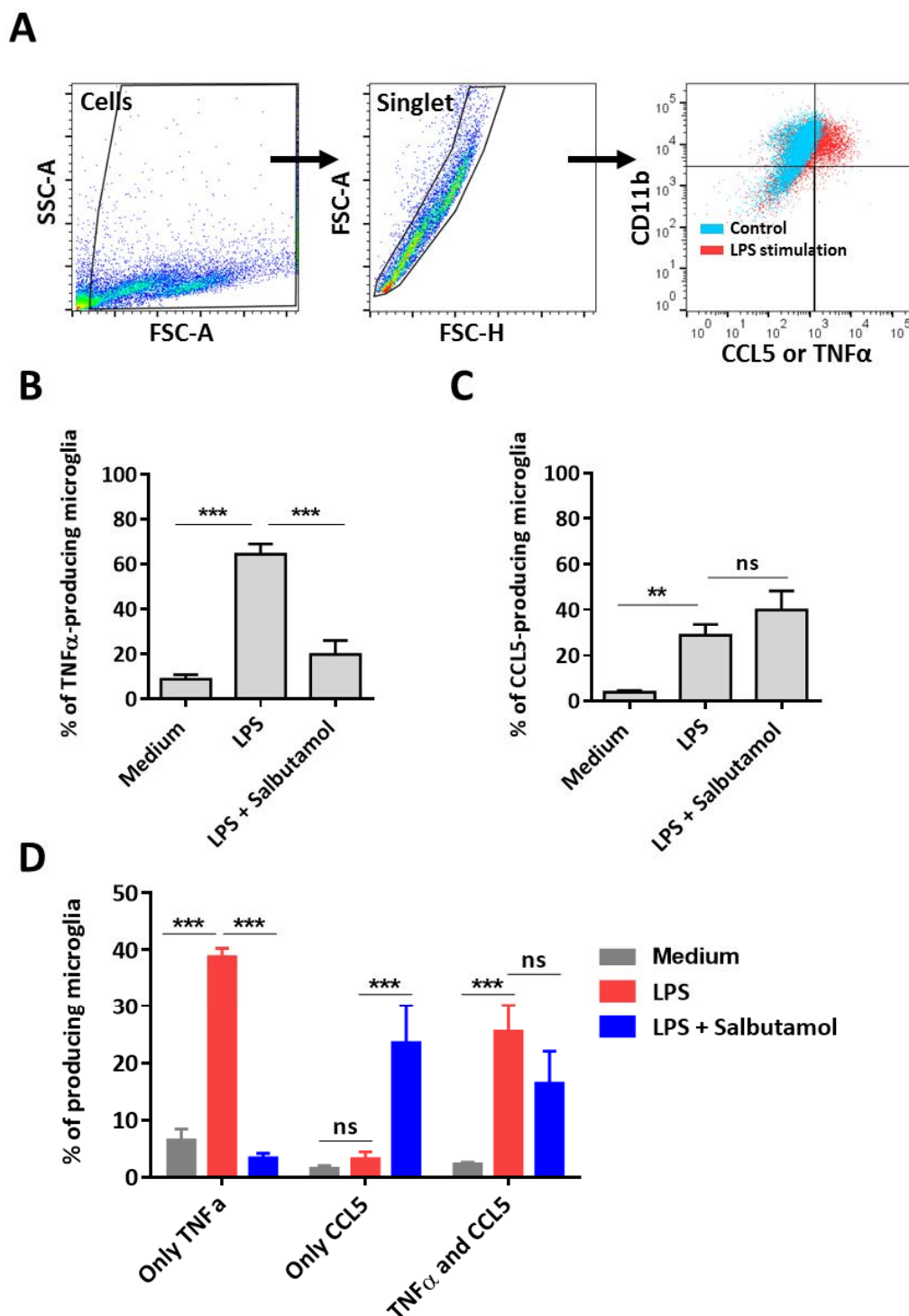


Figure 30: Evaluation of intracellular CCL5⁺ and TNFα⁺ production upon simultaneous TLR4 and β2AR stimulations.

Microglia from neonatal WT mice (3×10^5 cells/well) were stimulated with LPS (rough type; 1 ng/ml) or combination of LPS and salbutamol (10 ng/ml, 1 μM) for 8 hours. After 3 hours cells additionally received monensin to block cyto/ chemokine release and were subsequently analysed by flow cytometry. 10,000 CD11b⁺ cells were recorded and the percentage of microglia producing CCL5 or TNFα was calculated. (A) A schematic picture of intracellular CCL5 or TNFα evaluation by flow cytometry. TNFα positive (B) and CCL5 positive (C) microglia under LPS and combination of LPS with salbutamol. (D) Compares the population size of the cells which produce only TNFα, only CCL5 and both upon stimulation. Data are mean ± SEM. N=6-8 from 3 experiments. (One-way ANNOVA followed by Tukey's post-hoc test; *: p<0.05, **: p<0.01, ***: p<0.001)

3.3.6 The amount of CCL5 released from each cell but not the percentage of CCL5 producing cells is decreasing by β2AR activation

The previous data, shown in Figure 25 and Figure 30, revealed that β2AR activation by salbutamol has neither a considerable effect on the amount of produced CCL5, nor on the percentage of cells producing it. However, our data in Figure 30C showed that when stimulated with salbutamol a new cell population starts to produce CCL5. Hence, we aimed at a more detailed study on the cell functions regarding the CCL5 production. For this purpose, we used the ELISpot method in which the released CCL5 molecules from the cells are trapped by their specific capture antibodies on the surface of the wells (Figure 31). The bound CCL5 molecules can be detected by their specific detection antibodies. To have sufficient space between cells and to avoid overlapping of the spots, only 1,000 cells/well were plated. Figure 31A is a representing picture of an ELISpot well with CCL5 positive spots. The results demonstrate that some cells release CCL5 even without being stimulated (medium condition) and also β2AR activation by salbutamol does not decrease the percentage of cells that produce CCL5 upon LPS stimulation (Figure 31B). Since the developed spots varied in the size, we calculated the total area covered by the spots (Figure 31C). Comparing LPS-stimulated cells to cells which additionally received salbutamol, a significant smaller area after addition of salbutamol is observed (p value 0.01; Figure 31C).

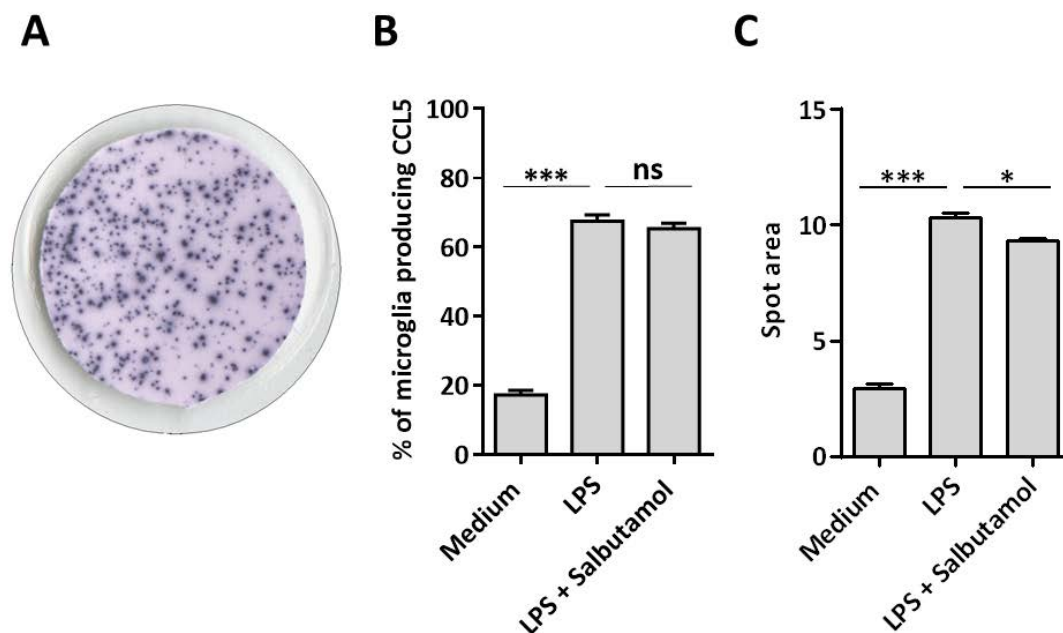


Figure 31: ELISpot analysis of the cells producing CCL5.

Microglia from neonatal WT mice were resuspended in complete medium containing LPS (rough type; 10 ng/ml) or a combination of LPS and salbutamol (1 μ M) and plated at the density of 1,000 cells/well on an ELISpot plate. The control group received medium only. Cells were incubated for 24 hours and subsequently analysed for the number of spots and the area covered by them. (A) An example of one well after the spots development. CCL5 released from cells is trapped by the bound capture antibody on the surface of the well, which after the development can be seen as dark spots. (B) Percentage of microglia produced CCL5. The data have been obtained by calculating the proportion of spot numbers from the plated cell number. (C) Sum of the area covered by all spots. Data are mean \pm SEM. N=16 for medium control and 8 for LPS and LPS+ Salbutamol, from 2 independent experiments. (One-way ANNOVA followed by Tukey's post-hoc test; *: $p < 0.05$, **: $p < 0.01$, ***: $p < 0.001$)

3.3.7 PKA mediates the downstream signalling from β 2AR to TLR4

Activated β 2AR activates the enzyme adenylyl cyclase, which leads to the production of cAMP. cAMP is a second messenger, which mainly activates the protein kinase A enzyme (PKA) through its classical pathway or exchange proteins activated by cAMP (Epac) through its non-classical pathway (reviewed by Gloerich & Bos, 2010). β 2AR might impose its effect on the expression of various genes through activation of PKA (via the classical pathway). To see if the activity of PKA influences the effect of salbutamol on the production of pro-inflammatory proteins, a cell-permeable PKA inhibitor (IIR-PKI) was applied to the cells to block its activity (Figure 32). Cells were stimulated with LPS alone or in combination with salbutamol and/or IIR-PKI. Released TNF α (Figure 32A), CCL5 (Figure 32B) and IFN β (Figure 32C) were measured in the supernatants of the microglia by ELISA. Figure 32A

shows that TNF α is inhibited by salbutamol (p value < 0.0001) which is partly rescued by IIR-PKI (p value < 0.0001). However, the produced amount of TNF α is significantly lower than the cells that received only LPS (p value 0.001). Besides, IIR-PKI itself has an additive effect on LPS-induced TNF α production (p value < 0.0001). CCL5 is not affected by salbutamol (Figure 32B, Figure 25) however, IIR-PKI significantly decreases the CCL5 production when added to the combination of LPS and salbutamol (p value < 0.0001). This reduced effect is also observed when IIR-PKI is combined with LPS only (p value 0.001). Figure 32C shows the effect of IIR-PKI on production of IFN β . Although production of IFN β is suppressed by salbutamol (p value 0.001; Figure 32C, Figure 27C; similar to TNF α and opposite to CCL5), IIR-PKI leads to a further reduction compared to the LPS stimulation (p value < 0.0001; opposite to TNF α , similar to CCL5). In addition, less IFN β is produced when IIR-PKI is added to LPS (p value < 0.0001).

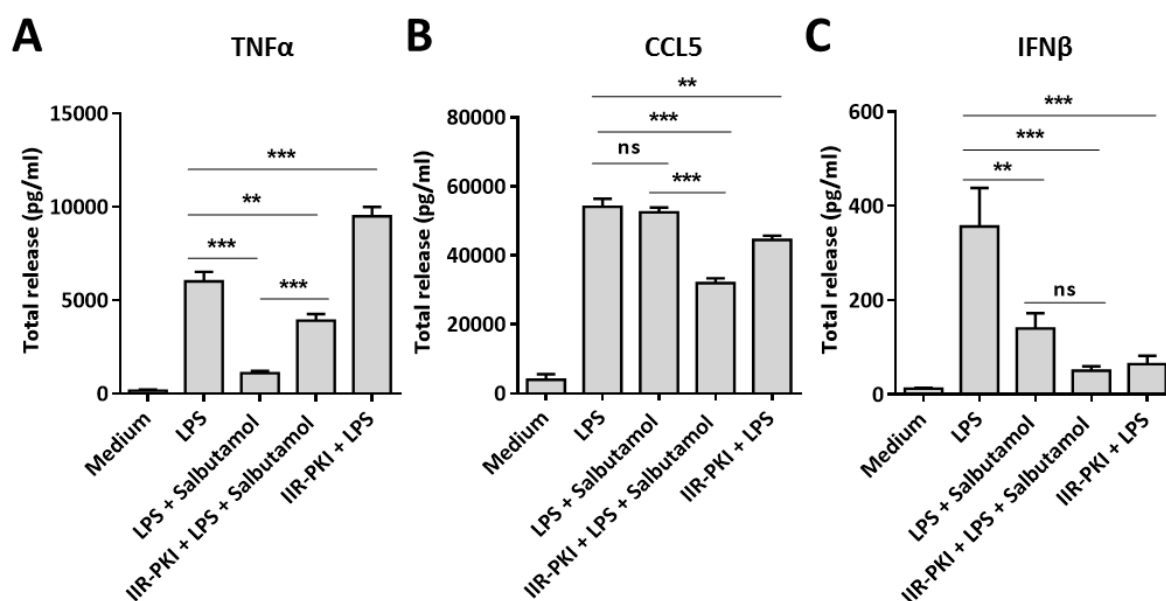


Figure 32: Evaluation of PKA inhibition on β 2AR activation.

Microglia from neonatal WT mice (1.5×10^4 cells/well) were stimulated with LPS (rough type; 10 ng/ml), combinations of LPS and salbutamol (1 μ M) or LPS, salbutamol and IIR-PKI (PKA inhibitor, 10 μ M) or LPS and PKA inhibitor for 18 hours. The inhibitor alone was added to the cells 30 min prior to the other stimuli and TNF α (A), CCL5 (B) and IFN β (C) were measured in the supernatants of the cells via ELISA. Data are mean \pm SEM. N=12 from 3 independent experiments. (One-way ANNOVA followed by Tukey's post-hoc test; *: p<0.05, **: p<0.01, ***: p<0.001)

3.3.8 Epac has no influence on β 2AR-induced inhibition of TNF α production

Through its non-classical pathway, cAMP activates Epac proteins (reviewed by Gloerich & Bos, 2010). Epac affects the activity of MAPKs (Gerits et al., 2008) which are also essential for TLR4 signalling (O'Neill et al., 2013). Thus, to determine the contribution of Epac activity in β 2AR signalling towards TLR4, we blocked the activity of Epac proteins, using three different available Epac inhibitors: HJC0197 and ESI-09 inhibiting Epac 1&2 simultaneously and ESI-05 inhibiting only Epac 2. The inhibitors were added in addition to LPS and salbutamol. The inhibition of TNF α production by salbutamol cannot be rescued by any of the Epac inhibitors (Figure 33A). Furthermore, Epac inhibitors do not show any influence on the production of CCL5 (Figure 33B). Epac inhibitors added to LPS without salbutamol showed no effect on the gene production either (data are not shown).

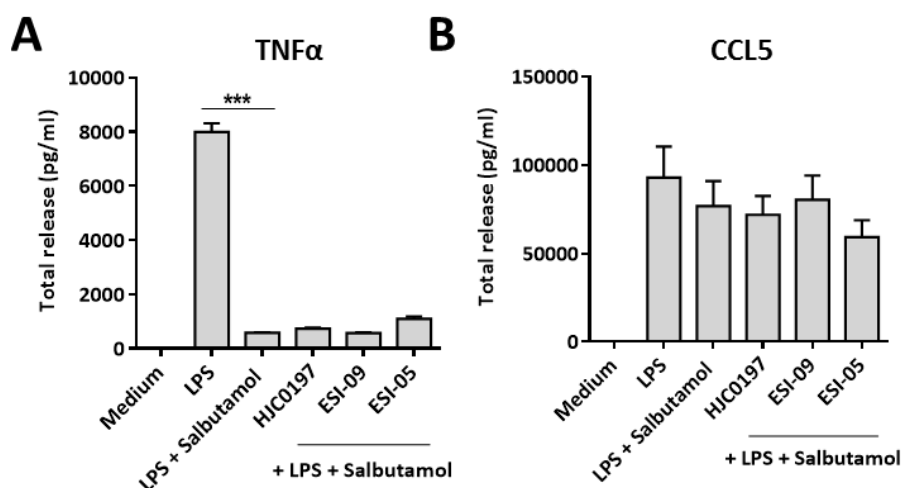


Figure 33: Effect of Epac inhibitors on β 2AR activation.

Microglia isolated from neonatal WT (1.5×10^4 cells/well) were stimulated simultaneously with LPS (rough type; 10 ng/ml), salbutamol (1 μ M) and Epac inhibitors (HJC0197, inhibitor of Epac 1&2; ESI-09, inhibitor for Epac 1&2; ESI-05, inhibiting Epac 2; all 25 μ M) or combinations of them. Inhibitors were added to the cells 30 min prior to the stimuli. Secreted TNF α and CCL5 in the supernatants were assessed 18 hours later by ELISA. TNF α (A) and CCL5 (B) secretion upon LPS (TLR4) stimulation, β 2AR activation and Epac inhibition. Data are mean \pm SEM. N=16 from 4 independent experiments. (One-way ANOVA followed by Tukey's post-hoc test; *: $p < 0.05$, **: $p < 0.01$, ***: $p < 0.001$)

3.3.9 Activation of PKA after β 2AR activation is increased by LPS

To address the question of how salbutamol, LPS or their combination affect the PKA activity in microglia and also whether the PKA inhibitor, IIR-PKI, is truly inhibiting the PKA activity

or not, we stimulated microglia with LPS, salbutamol or their combination with/without IIR-PKI for 15 min and determined the PKA activity in the cell lysates (Figure 34). LPS *per se* does not lead to PKA activity. Salbutamol significantly increases the PKA activity (p value 0.04). This activation by salbutamol can be further increased when it is combined with LPS (p value < 0.0001). The inhibitor slightly decreased the activity of PKA (Figure 34).

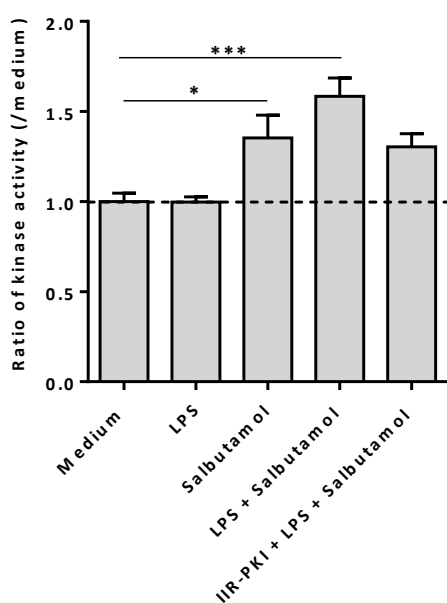


Figure 34: PKA activity assessment upon β 2AR activation.

Microglia from neonatal WT mice (8×10^5 cells/well) were stimulated with LPS (rough type; 10 ng/ml), salbutamol (1 μ M), a combination of LPS and salbutamol or a combination of LPS, salbutamol and IIR-PKA (PKA inhibitor, 10 μ M) for 15 min. IIR-PKI was added to the cells 20 min prior the stimulation. The PKA activity was assessed in the cell lysates. Data are presented as a ratio to the medium condition. Dotted line indicates the medium condition. Data are mean \pm SEM. N= 8-9 from 3 independent experiments. (One-way ANNOVA followed by Tukey's post-hoc test; *: p<0.05, **: p<0.01, ***: p<0.001)

3.3.10 Inhibition of TLR4-induced genes by β 2AR is not microglia specific

To investigate whether β 2AR has the same effect- that is seen on microglia- on other macrophages such as bone marrow derived macrophages (BMDM's), we stimulated BMDM's with LPS, salbutamol or their combination. Subsequently, release of TNF α and CCL5 were measured in the supernatants of the cells. The results show a significant reduction in TNF α production by a combination of LPS and salbutamol compared to LPS treatment (p value < 0.0001; Figure 35A) whereas CCL5 production is not affected (Figure 35B).

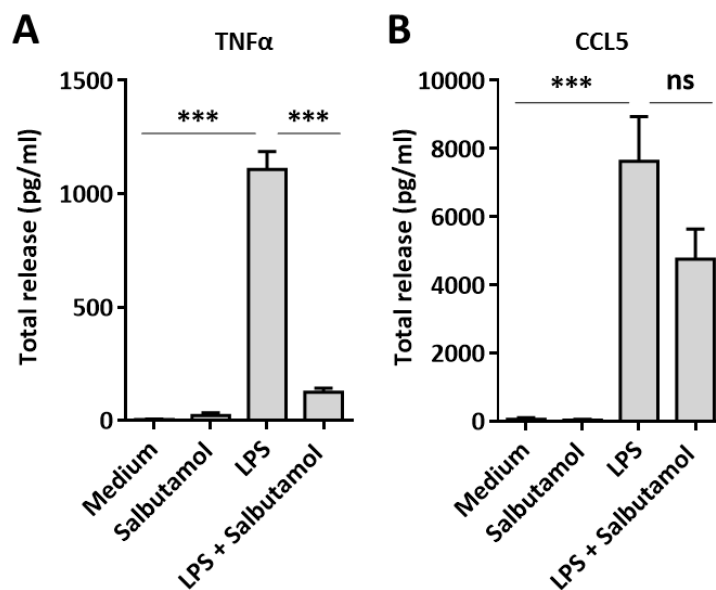


Figure 35: Evaluation of BMDM's response to the β 2AR activation.

BMDM's isolated from 8-12 weeks old WT mice were plated with a density of 1.5×10^4 cells/well and were stimulated with LPS (rough type; 10 ng/ml), salbutamol (1 μ M), or a combination of both for 18 hours. TNF α (A) and CCL5 (B) were measured in the supernatant of the cells using ELISA. Data are mean \pm SEM. N=12 from 3 independent experiments. (One-way ANNOVA followed by Tukey's post-hoc test; *: $p < 0.05$, **: $p < 0.01$, ***: $p < 0.001$)

3.3.11 β 2AR activation alters activation of STAT and IRF proteins

β 2AR activation by salbutamol stimulation specifically inhibits production of some pro-inflammatory proteins such as TNF α (Figure 25). To be able to study a larger number of genes, which are differentially transcribed upon β 2AR signalling, RNA sequencing analysis was performed. Microglia received LPS or a combination of LPS and salbutamol for 3 hours prior to the total mRNA sequencing. Control groups received medium alone. Apart from the known regulated genes (Figure 25) we focus on regulation of some transcription factors such as signal transducer and activator of transcription (STATs) and interferon regulatory factor (IRFs) genes (Figure 36). Comparing the data from control (medium) and LPS groups shows activation of most of STAT genes upon LPS stimulation (p value STAT1, 2 and 5a, < 0.0001 ; STAT5b, 0.02). Transcription of STAT4 is not altered by LPS and STAT6 is downregulated (p value 0.03; Figure 36A). Combination of salbutamol with LPS leads to a significant upregulation of STAT4 (p value < 0.0001) while having no effect on other STAT genes. Investigating regulation of IRF genes (Figure 36B) reveals that most of the IRF genes are upregulated by LPS stimulation (p value IRF1, 5, 7 and 9 < 0.0001 ; IRF2, 0.005, IRF8, 0.0008). In addition, IRF2 binding proteins (IRF2bp1 and 2) are significantly downregulated

(p value IRFbp1, 0.002; IRF2bp2 < 0.0001). LPS has no effect on regulation of IRF4. In contrast, addition of salbutamol to LPS results in upregulation of IRF4 and IRF2bp2 and downregulation of IRF8 (p value IRF4, 0.009; IRF8, < 0.0001; IRFbp2, 0.003).

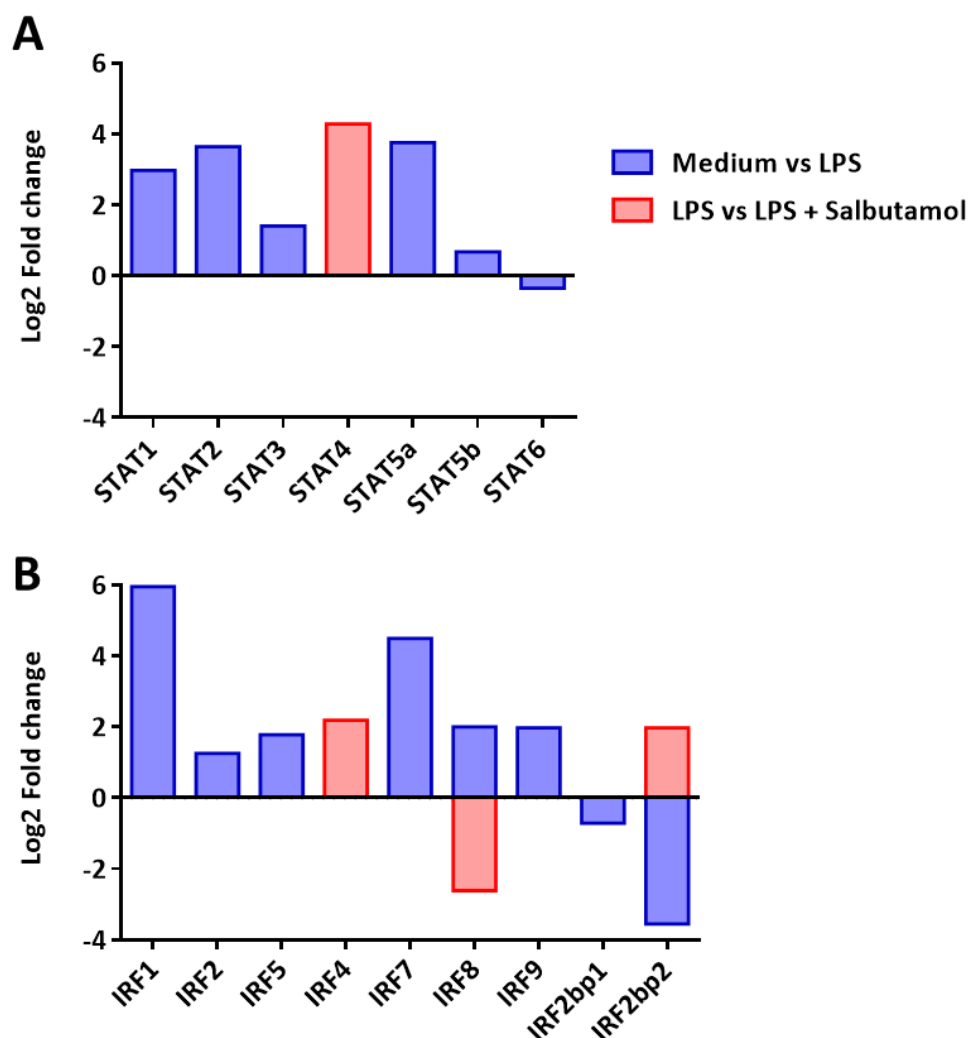


Figure 36: Regulation of STATs and IRFs genes upon β 2AR signalling.

Neonatal microglia (8×10^5 cells/well) were stimulated with LPS (rough type; 10 ng/ml) or combination of LPS and salbutamol (1 μ M) for 3 hours. Control groups (medium) received no stimuli. Subsequently, cells were washed and lysed. Total mRNA was sequenced in collaboration with Microarray and Deep-Sequencing Facility (Transkriptomeanalyselabor, TAL, Göttingen; Dr. Gabriela Salinas-Riester). Regulation of STAT (A) and IRF (B) genes for two groups of medium vs LPS and LPS vs combination of LPS and salbutamol is shown. Candidate genes were filtered to a minimum of 2-fold change and FDR-corrected p-value < 0.05. N=3 from 3 independent experiments. STAT: signal transducer and activator of transcription; IRF: interferon regulatory factor; IRFbp: IRF binding protein.

4 Discussion

4.1 Functional properties of microglia in 5XFAD mouse model

Alzheimer's disease (AD) is a neurodegenerative disorder and the most frequent form of dementia in the elderly population, with prevalence of about 10% of elderly people (Duthey, 2013). AD is characterized by a massive neuronal loss. Two hallmarks of the disease are extracellular A β plaque depositions and intracellular NFTs (Zhao et al., 2014). Although a role of the immune system in the AD pathology has been suggested since the 1900s, the most extensive studies which have proven this contribution were mainly published in the last decade, targeting microglia as the main innate immune cells in the CNS (reviewed by Heneka et al., 2015).

These studies showed microgliosis in the vicinity of A β plaque depositions in the brains of AD patients as well as various AD mouse models. Microgliosis is a sign of microglial activation, therefore, it has been proposed that the environment in an AD brain alters microglia to adapt to an increased reactive phenotype (reviewed by Perry et al., 2010). This increased reactive phenotype is characterized by a higher production of pro-inflammatory cyto-/ chemokines, NO and ROS, by deficits in A β phagocytosis and by overreaction to secondary stimuli. These results are supported by another publication where it was shown that the AD pathology can be improved by reducing this enhanced microglial reactivity (Heneka et al., 2013).

In the present study we aimed to investigate how the AD environment affects microglia and their TLRs systems *in vitro*. To do so, we compared the properties of microglia from various ages of 5XFAD mice to aged matched WT littermates from both genders.

4.1.1 Unaltered phagocytic activity of 5XFAD vs. WT microglia

One crucial function of microglia is phagocytosis. This activity involves clearing of dead cells, myelin debris, pathogens or misfolded proteins such as A β assemblies in the CNS. Increasing evidence suggests that microglial phagocytic activity is impaired in AD (e.g. Krabbe et al., 2013). Using cerebral slices, Krabbe and colleagues showed microglial impairment to phagocytose microspheres in 9 months old APP/PS1 and 20 months old APP23 mice compared to the age-matched WT littermates. Although phagocytosis of microbeads by microglia can be used to evaluate phagocytic activity, we consider physiological or

pathogenic materials such as A β and myelin as better tools for this investigation. To our knowledge, there have been no *ex vivo* studies to evaluate the phagocytic activity of AD-derived microglia of myelin, A β or E. coli. We therefore investigated the phagocytic activity of cultured microglia isolated from 3, 6 and 9 months old 5XFAD and WT mice for myelin, E. coli, A β_{1-40} and A β_{1-42} .

The experiments addressing myelin and E. coli phagocytosis showed no genotype specific differences of age or gender. However, in both genotypes the percentage of phagocytosing microglia dropped significantly at 9 months of age compared to microglia isolated from younger mice. This indicates an age-dependent microglial alteration. Investigation of phagocytosis of A β (A β_{1-40} and A β_{1-42}) by 3 and 6 months old female 5XFAD and WT microglia revealed also no differences between genotypes or ages. Unfortunately, due to the limited numbers of 9 months old mice, we could not study this group but we would expect to observe a reduction in the phagocytic rate as we saw for myelin and E. coli.

Recent data from other groups have shown an age-dependent reduction in A β phagocytosis by microglia in AD transgenic mice (Hickman et al., 2009; Floden & Combs, 2006). Hickman and colleagues showed that microglia from 14 months old APP/PS1 mice have reduced expression of A β -binding receptors and A β -degrading enzymes. Floden and Combs demonstrated a reduction of fibrillar A β phagocytosis by acutely isolated microglia from 5-8 months old WT mice compared to P1-P3 mice (Floden & Combs, 2006). They also reported that although opsonization by anti-A β antibodies increased A β phagocytosis by neonatal microglia, it failed to improve the phagocytic activity in adult microglia. The authors also argued that prolonged microglia culturing leads to phenotypic changes and is therefore not the optimal method to study microglial phenotypes.

In the present study we did not observe any phagocytic deficits of microglia in 5XFAD mice *ex vivo*. This suggests that the impairment of microglia *in vivo* might be derived from the continuous stimulation in the AD brains (by A β) and seems to be reversible once the environment is changed. This finding is in line with a previous publication (Krabbe et al., 2013). In this study, Krabbe and colleagues could show that impairment of microglial phagocytic capacity correlates with A β plaque deposition and this activity can be restored by decreasing amyloid burden.

We observed an age dependent phagocytic impairment in microglia isolated from WT and 5XFAD mice. Ageing is a physiological process and occurs regardless of AD transgenes. Earlier studies have shown that some microglial functions diminish with ageing (Streit et al., 2004; Streit & Xue, 2012). Also, microglia isolated from aged brains show lower phagocytic activity for A β fibrils compared to young mice (Floden, 2012).

These findings indicate that, firstly, ageing has a strong effect on microglial performance and, secondly, this senescence is independent of the AD environment. As we showed earlier, our data suggests that age-dependent alterations in microglia are much more persistent than AD-dependent changes, which seem to be reversible after isolation and time for possible recovery.

We next aimed to investigate whether the environmental conditions of AD pathology in the 5XFAD mouse model affect microglial TLR signalling. Due to the importance of TLR4 and its co-receptor CD14 in AD pathology (Reed-Geaghan et al., 2009) and phagocytosis (Rajbhandari et al., 2014), we investigated a possible effect of AD environment on TLR4 functionality in terms of phagocytosis. We applied LPS (a TLR4 agonist) to the microglia and assessed their phagocytic activity for myelin and *E. coli* upon the LPS pre-stimulation. We observed that there were no significant differences between 5XFAD and WT microglia at all ages and both genders. Although statistically not significant, 9 months old mice seemed to be more sensitive to LPS which led to higher *E. coli* phagocytosis than in younger groups.

Different sensitivity to LPS could be caused by different levels of its receptor on the cells. Overexpression of TLRs (including TLR4) on microglia has been shown in normal ageing (Letiembre et al., 2007), AD mouse models (Fassbender et al., 2004; Letiembre et al., 2007; Walter et al., 2007) and AD patients (Liu et al., 2005; Letiembre et al., 2007; Walter et al., 2007). Thus, further investigation of TLR4 expression level on microglia isolated from 5XFAD mice compared with WTs at various ages is essential.

4.1.2 Release activity of microglia isolated from 5XFAD and WT mice

Activated microglia and in addition, enhanced expression of their antigens related to the immunity (such as CD45, MHC, CD68 and complement receptors) and their increased production of pro-inflammatory cyto-/ chemokines has been shown to be present in human AD brains (reviewed by Boche et al., 2013; Ransohoff & Perry, 2009; Dickson et al., 1993). *In vitro* studies have shown that binding of A β to CD36 or TLR4 leads to production of pro-

inflammatory cyto-/ chemokines (Stewart et al., 2010; El Khoury et al., 2003). Moreover, *in vivo* investigations have revealed increased amounts of IL-1, IL-6, IL-12, IL-23 (Patel et al., 2005; vom Berg et al., 2012), TNF (Fillit et al., 1991; Janelins et al., 2005) and CCL2 (Janelins et al., 2005; Hillmann et al., 2012) in AD transgenic mice or in the brains and cerebrospinal fluid of patients with AD (reviewed by Prokop et al., 2013; Heppner et al., 2015). Recent studies based on gene expression analyses from mouse models of AD also revealed a higher production of cyto-/ chemokines (Orre et al., 2014; Landel et al., 2014).

TLRs such as TLR2, TLR4 and TLR9 have been so far introduced to be the most important TLRs contributing to the AD pathology (Suh et al., 2013; Reed-Geaghan et al., 2009; Fassbender et al., 2004; Scholtzova et al., 2009). For instance, Sly and colleagues reported an enhanced production of pro-inflammatory cyto-/ cytokines in Tg2576 mice compared to WT mice upon intravenous LPS injection (Sly et al., 2001). Therefore, in our study we investigated the activity of most of TLRs in microglia in terms of secretion of various cyto-/chemokines. We stimulated the cultured microglia from 5XFAD and WT brains of 3, 6 and 9 months old mice from both genders with a number of TLR agonists as well as anti-inflammatory cytokines such as IL-4 and IL-10.

In contrast to previous findings, the data from the present study showed no differences in cyto-/ chemokine production by WT and 5XFAD microglia. The previous publications were mainly based on *in vivo* studies where continuous stimulation of microglia leads to a higher pro-inflammatory activity of these cells (reviewed by Lull & Block, 2010). This indicates that once the environment is changed to healthy conditions, even if only for some days, microglia may have the capacity to return to a resting state. This may explain why microglia from 5XFAD mice in the culture even after being stimulated showed a similar reaction to WT mice/microglia.

The studies on age-dependent microglia alterations in terms of production of cyto-/ chemokines also represented a higher production of these inflammatory factors (Sierra et al., 2007; Sheng et al., 1998; Ye & Johnson, 1999). An *ex vivo* investigation of microglia cultures from young and adult mice revealed a higher production of pro-inflammatory cytokines (IL-6 and TNF α) in aged mice under basal conditions as well as upon stimulation with TLR2 and TLR4 agonists (Njie et al., 2012). Our data are in contrast with this finding as we observed a reduced production of pro-inflammatory factors IL-6, CCL2 and CCL3 in older mice upon

stimulation. Njie and colleagues isolated microglia using a percoll gradient and incubated the cells only overnight prior to be stimulated. In our study the cells were incubated in the culture for 2-4 weeks prior to the experiments. Our data suggest that the effect of the inflammatory environment of an aged brain which -as mentioned above- leads to a higher inflammatory activity of microglia, is also reversible. And interestingly it reveals the decreased activity of aged microglia *per se*.

4.1.3 Proliferation

One of the common features of AD is extensive gliosis. Previous studies showed proliferation of microglia around A β plaques in brains of AD patients (Marlatt et al., 2014) and in mouse models of AD (Bolmont et al., 2008; Kamphuis et al., 2012; Gomez-Nicola et al., 2013). Higher microglia proliferation has also been observed in normal ageing (D. Gomez-Nicola et al., 2013). Studies on AD mouse models revealed that circulating progenitors do not contribute to the microglial population (Mildner et al., 2011) thus, the increase in their number is the result of their own proliferation.

To explore if these proliferative changes are AD dependent, we investigated the proliferation rate of cultivated microglia isolated from 6 and 9 months old WT and 5XFAD mice from both genders. We show that in all groups the proliferation of 5XFAD microglia drops significantly in contrast to the WT controls. Moreover, we observed that microglial proliferation reduces by age in the female WTs as well as 5XFAD mice. Here, our data are in contrast with previous published results according to the increasing proliferation of microglia in AD environments (Marlatt et al., 2014; Bolmont et al., 2008; Kamphuis et al., 2012; Gomez-Nicola et al., 2013). In these studies, the data were obtained either from *in vivo* experiments or immunohistochemistry analysis, which allow study of the direct effect of A β on microglial proliferation. In contrast, our work was based on *ex vivo* conditions in which microglia were kept in cultures for at least 2-4 weeks prior to the experiments without A β in the culture medium. This could explain the contradictory outcomes. However, our results confirm our hypothesis according to the reversibility of microglial changes upon AD environment. The decreased proliferative activity of microglia by age in female groups is, in line with previous studies (D. Gomez-Nicola et al., 2013), indicating that microglial alterations upon age is independent of AD environments. To obtain a better insight into the proliferation rate of microglia in 5XFAD mice at difference ages, performing *in vivo* studies is crucial.

The proliferation rate of microglia is also affected by external stimuli such as LPS. The inhibitory effect of LPS on macrophage proliferation is well known (Vairo et al., 1992; Vadiveloo et al., 1996). In view of the importance of TLR4 functionality in AD pathology (Walter et al., 2007), we studied a possible effect of AD environment on TLR4 activity in terms of proliferation. The isolated microglia from 5XFAD and WT mice, as mentioned above, were stimulated with two concentrations of LPS. We detected a decrease of the proliferation rate caused by LPS in all examined groups (about 50% reduction), indicating that the functionality of TLR4 in microglia derived from 5XFAD mice is not altered.

4.1.4 Infiltration of immune cells to the brains of 5XFAD mice

Infiltration of immune cells such as monocytes and neutrophils from the periphery to the brains of AD mouse models has already been shown (Simard et al., 2006; Lebson et al., 2010; Stalder et al., 2005; Baik et al., 2014). A recent gene profiling study on various ages of 5XFAD mice has shown a major increase of expression of genes related to inflammation such as chemokines which may result in immune cells infiltrations (Landel et al., 2014). Another report has shown a significant increase in chemokine expression, blood brain barrier permeability and monocyte and neutrophil infiltrates in the brain of APP/PS1 mice compared to WT mice (Minogue et al., 2014). Gonzalez-Velasquez and Moss also reported that soluble A β oligomers trigger recruitment of circulating monocytes to the brain parenchyma by stimulating the endothelium and enhancing their adhesion molecules (Gonzalez-Velasquez & Moss, 2007).

In the current study, we investigated putative infiltration of peripheral immune cells in the brains of 5XFAD mice compared to controls by flow cytometry analysis. We observed that in both genotypes only 2-3% of the CD11b and CD45 positive cell populations were monocytes and neutrophils. This is in contrast to the studies mentioned above, which could be explained by differences in the sensitivity of the methods.

Previous studies have shown microglial activation upon intracerebral LPS (TLR4 agonist) applications (Mouihate, 2014; Houdek et al., 2014; Dickens et al., 2014). Pro-inflammatory cytokines released from LPS-activated microglia can increase the permeability of the blood brain barrier, which facilitates the infiltration of macrophages from the periphery (Wispelwey et al., 1988; Gaillard et al., 2003). According to the importance of the functionality of TLR4's in the AD pathology (reviewed by Downer, 2013), we studied a potential effect of AD

environment on TLR4 activity in terms of immune cells recruitment. Thus, we studied the infiltration of neutrophils and monocytes from the periphery to the brains of WT and 5XFAD mice upon LPS injection.

We focused on 6 and 9 months old mice since earlier data did not show any differences between microglia isolated from 3 and 6 month old mice. Our results showed that the application of a low LPS concentration (10 µg/ml) led to similar numbers of infiltrated neutrophils and monocytes in all groups. After injection of a higher LPS concentration (1 mg/ml) all groups had similar immune cells infiltrates in the brain except 9 months old males which had reduced neutrophil infiltrates.

Since we have previously shown that there is no considerable number of neutrophils and monocytes in intact 5XFAD and WT brains, all the monocytes and neutrophils are assumed to be infiltrated upon the LPS injections which seems to be independent of an AD environment.

The data indicate that -at least in the 5XFAD transgenic AD mouse model- the excessive amount of A β peptides in the brain is not altering the response of the TLR4 stimulation by LPS in terms of neutrophil and monocyte recruitment. As a driving force of immune cell infiltration, it would be essential to analyse the level of chemokines in such brains.

To sum up, our data bring evidence that microglial alteration in an AD environment is reversible once the environment is changed. Even in WT controls, microglia isolated from older mice show reduced activities compared to younger mice *ex vivo*. Exposure to A β depositions in 5XFAD mice seems not to change the activity of TLR4 in microglia till 9 months of age.

4.2 Amyloid beta (A β) plaque-associated microglia priming in transgenic mouse models of Alzheimer's disease

Activation of microglia around A β plaques has been demonstrated both in human post-mortem AD brain tissues as well as in transgenic mouse models (Benzing et al., 1999; Bornemann et al., 2001). These plaque-associated microglia show impaired phagocytosis (Griciuc et al., 2013) and enhanced immune activity (Apelt & Schliebs, 2001; Benzing et al., 1999; Bornemann et al., 2001; Jimenez et al., 2008). A wide range of surface molecules has been shown to be expressed by these plaque-associated microglia including MHC II (McGeer, Itagaki, & McGeer, 1988; Rogers, Lubert-Narod, Styren, & Civin, 1988), CD68 (Bornemann et al., 2001; Sasaki et al., 2002) and Fc γ receptor (Bornemann et al., 2001). Ageing, similar to neurodegeneration, shifts the microglia from homeostatic balance to a pro-inflammatory state which is also marked by higher levels of inflammatory cytokines and signs of an activated or dysfunctional microglia (reviewed by Streit et al., 2008 and Norden & Godbout, 2013).

As a result of low-grade inflammation -as seen in brain ageing and chronic neurodegenerative diseases such as AD- an enhanced type of microglia activation, known as microglia priming, has been described (reviewed by Norden & Godbout, 2013 and Perry & Holmes, 2014; Sierra et al., 2007; Raj et al., 2014). Perry and Holmes defined microglial priming as their exaggerated response to a second inflammatory stimulus compared with stimulus-naïve microglia (Perry & Holmes, 2014). Albeit no clear characteristics of primed microglia have been described yet, alterations in morphology towards loss of ramification, a higher proliferation rate and overexpression of cell surface antigens such as MHC II, scavenger receptor CD68 and complement receptors have been associated with microglia priming (Perry & Holmes, 2014).

As mentioned earlier, primed microglia show magnified responses to secondary stimuli. It has been reported that in animals with age-related or neurodegenerative pathology, LPS leads to a higher pro-inflammatory response in the brain, most likely due to microglial priming (Gatti & Bartfai, 1993; Cunningham et al., 2005; Sierra et al., 2007; Ramaglia et al., 2012). For instance, increased transcription of pro-inflammatory cytokines in the cortex and hippocampus of Tg2576 APP-transgenic mice and the provoked CNS inflammation in 3XTg-AD upon LPS challenges have been reported (Sly et al., 2001; Kitazawa et al., 2005). On the other hand, multiple peripheral infections may also increase the susceptibility to AD (Bu et al., 2014).

Although it has been hypothesized that microglia in the vicinity of A β depositions are primed, to this date it has not been proven. Therefore, in the current study, we investigated the phenotype of microglia in A β -plaque areas as well as non-plaque regions in three different AD mouse models. Besides, we studied how a second systemic stimulus affect the microglia of these two regions.

4.2.1 Microglia surrounding A β plaques reveal signs of priming

To investigate the primed phenotype of microglia in AD mouse models, we chose APP23, 5XFAD and APPswePS1dE9 transgenic mice. In these animals, overexpression of human APP protein leads to production of abundant A β depositions. The early formation of amyloid deposits in these mice separate the AD pathology from ageing and allow for distinguishing the effect of ageing and amyloid beta on microglia. We quantified the extent of microglia priming in these mouse AD models and investigated whether the priming effects of ageing and amyloid burden are related.

In the present study we show expression of these markers exclusively in the vicinity of A β plaques in APPswePS1dE9 (18 months old), 5XFAD (7.5 and 12 months old) and APP23 (20 months old) mice which became more pronounced in older mice. 5XFAD mice generate A β plaques earlier and faster than APPswePS1dE9 (Oakley et al., 2006; Jankowsky et al., 2004) and presence of the activation markers around the plaques at early ages indicates that presence of the A β plaques rather than the age is the main factor to activate microglia.

Furthermore, we observed a higher expression of genes related to phagocytosis and immune recognition such as CD11c, Dectin1, Lamp2 and Trem2 in APP23 and 5XFAD mice compared with WT controls. Activated microglia upregulate CD11c (Zilka et al., 2012), besides, CD11c and Dectin1 belong to the gene profile of microglia priming (Holtman et al., 2015), Lamp2 plays a role in maturation of phagosomes (Huynh et al., 2007) and Trem2 is essential for phagocytic activity of immune cells (Thrash et al., 2009). Our data confirm previous publications: upregulation of Trem2 in the microglia from plaque-loaded regions of 20-23 months old APP23 mice (Frank et al., 2008), upregulaed CD11c and Dectin-1 in 5XFAD mice using a gene profiling study (Landel et al., 2014), upregulation of Lamp2 in 5XFAD mice as found by deep sequencing analysis (Bouter et al., 2014). Our data as well as most of these studies were based on immunohistochemistry and mRNA expression, respectively and, therefore, lacked the information whether the cells expressing these genes

are located at the areas of A β depositions. Thus, for a better understanding of the phenotype of the microglia surrounding the A β plaques we sorted MHC II positive microglia from 5XFAD and WT mice and the expression of 842 microglia-specific genes was compared to MHC II negative cells from 5XFAD and WT mice.

A previous study defined two conserved gene expression networks in “general activated” and “primed” microglia in mouse models of accelerated ageing and neurodegenerative diseases (Holtman et al., 2015). The primed microglia gene network contained pro-inflammatory genes and specific markers including *Axl*, *Apoe*, *Clec7a* (*Dectin1*), *Itgax* (*Mac-1*, *CD11c*), *Lgals3* (*Mac-2*) (Holtman et al., 2015) which were also upregulated in MHC II⁺ microglia in the present study. Other upregulated genes such as *Spp1*, *Cst7*, *CD63* belong to the “general activated” module (Holtman et al., 2015). Apart from upregulated genes, few genes were downregulated such as *CD33*, which is a negative regulator of phagocytosis (Griciuc et al., 2013). In addition to a significant differences between MHC II positive and negative microglia from 5XFAD mice, MHC II negative microglia from 5XFAD mice compared to the WT controls revealed a remarkable contrast. This indicates that also non-plaque associated microglia from AD mouse brains undergo immunological activation even if not that robust to express MHC II. Immunological activation of microglia in an AD environment has already been shown (Kim et al., 2012; Orre et al., 2014). Among the upregulated genes, *TyroBp*, the key regulator in phagocytosis and LOAD networks (Zhang et al., 2013) was significantly upregulated in 5XFAD/MHC II⁺ microglia compared with WT/MHC II⁻ but not in comparison with 5XFAD/MHC II⁻ cells. This suggests that the change of *TyroBp* is likely due to the effect of genotype than A β deposition.

Ageing is the most important risk factor of AD and is shown to promote microglia priming as well (reviewed by Perry & Holmes, 2014). In this study we could also show that the expression of priming markers is present in 24 months old WT mice. Priming in plaque-associated microglia is already observed in younger AD transgenic mice. This observation indicates that microglia priming due to ageing and A β plaque depositions are two independent processes.

4.2.2 Systemic inflammation increases the inflammatory response of primed microglia

Higher sensitivity of AD patients to infectious diseases has often been reported: worsening of cognitive impairments upon systemic inflammation (Cunningham, 2011; Moon et al., 2011; Perry et al., 2007; Holmes et al., 2009) and a deleterious effect of increased serum inflammatory cytokines on the onset of dementia has been shown (Ravaglia et al., 2007; Schmidt et al., 2002). The cause of the severe cognitive deficits in AD patients upon peripheral inflammatory signals might be due to a higher response of primed microglia. Cunningham and colleagues showed that the secretory profile of primed microglia by prior neurodegeneration can be altered upon both systemic and central LPS challenges (Cunningham et al., 2005). Moreover, other studies suggested that clearance of A β can be boosted by an additional inflammatory stimulation (Akiyama & McGeer, 2004; DiCarlo et al., 2001; Herber et al., 2004). For a better understanding of the direct effect of systemic LPS injection on the microglia surrounding the A β plaques compared to the microglia in plaque-free regions, we injected PBS or LPS i.p. in APP23, 5XFAD and age matched WT mice. It has been shown that upon systemic LPS injection LPS can enter the brain through blood brain barrier which can directly stimulate the microglia (Banks & Robinson, 2010) and can lead to their morphological changes (Jeong et al., 2010).

Morphological analysis of the microglia in the current study showed signs of activation upon LPS injection (loss of ramifications, shortening and thickening of the processes) which was more pronounced in the microglia in the close vicinity of plaques. This effect was stronger in 24 months old APP23 mice and led to amoeboid shapes of microglia. A higher sensitivity of microglia around the plaques to a secondary stimulus (peripheral LPS injection) suggests that microglia around the plaques are primed. PBS-injected 24 months old WT mice as well as plaque-free areas of 24 months old APP23 mice also showed intermediate loss of ramification of the microglia which is another evidence of ageing effect on microglial activation.

We also investigated the expression of Mac-2, CD68 and MHC II proteins (priming markers) on microglia after i.p. PBS or LPS injection using immunohistochemistry analysis. Since a strong effect of LPS on the morphology of microglia from 20 months old APP23 mice was seen, for this study, this age was chosen. We did not observe expression of Mac-2, CD68 or MHC II on the microglia from WT mice even after LPS injection. However, transgenic mice showed a slight expression of Mac-2, CD68 and MHC II in the microglia surrounding the plaques which was strongly enhanced by LPS injection. We observed clear differences

between the microglia in contact with and remote from plaques. Thus, the expression level of these priming markers was additionally quantified and compared between WT and APP23 mice or plaque-associated microglia and microglia from non-plaque regions in APP23 mice. The quantification revealed that LPS did not have significant effects on microglia from WT mice or plaque-free areas of APP23 mice. Nevertheless, LPS had a considerable impact on the activation of plaque-associated microglia. This observation indicates the higher sensitivity and therefore stronger responses of plaque-associated microglia to a secondary stimulus (LPS).

It has been reported that LPS has an additive effect on production of cyto-/ chemokines in AD transgenic mice compared to WT mice (Sly et al., 2001; reviewed by Prokop et al., 2013). IL-1 β is one the pro-inflammatory cytokines which is produced by microglia in AD brains (Griffin et al., 1989; Benzing et al., 1999; Hickman et al., 2008b; Hickman et al., 2009) and also upon LPS stimulation (Nakamura et al., 1999). Since we showed the activation of microglia by i.p. LPS injections more prominently in the vicinity of plaques, we determined the expression of IL-1 β by the microglia surrounding the A β plaques or distant from them. LPS treatment led to the expression of IL-1 β in 20 months old APP23 mice on the cells surrounding the plaques and not in plaque-free areas. 24 months old mice revealed strong expression of IL-1 β on both cells adjacent to the plaques and far from them. This outcome once more indicates a higher sensitivity of plaque-associated microglia to a secondary stimulus (such as LPS). We already showed that microglia of 24 months old WT mice demonstrate signs of activation, likely due to the ageing. This explains why in these mice microglia in the plaque-free regions show a strong expression of IL-1 β (probably due to their priming).

Recruitment of the inflammasomes adaptor protein ASC and its interaction with pro-caspase 1 is necessary for the maturation of IL-1 β (reviewed by Singhal et al., 2014). Here, we could also show that indeed upon LPS treatment ASC was strongly present on the plaque-associated microglia in APP23 and 5XFAD mice, providing another evidence for priming of plaque-associated microglia.

Taken together, our data strongly propose that microglial priming in transgenic Alzheimer's disease mouse models is caused by the close vicinity of the A β plaque. Understanding the pathophysiological processes which lead to A β plaque-associated microglia priming and the following enhanced response to a secondary stimuli (such as systemic inflammation) suggests new therapeutic opportunities to improve the AD pathology.

4.3 Noradrenergic control on the activity of innate immune cells in the CNS

The adrenergic system is a part of the autonomic nervous system's fight-or-flight response and consists of the two neurotransmitters adrenaline and noradrenaline (NA) (Swanson & Hartman, 1975). Apart from its physiological role as neurotransmitters of the sympathetic nervous system, (nor-) adrenaline plays a crucial anti-inflammatory role both in the periphery and the CNS. In particular, neurodegenerative diseases such as AD show improvement by activation of the adrenergic system indicating a direct suppressive effect on inflammation and immune cell activity. Several studies have investigated the interactions between adrenergic and immune systems, focusing on various types of immune cells, which are affected by adrenaline and noradrenaline. For instance, it was shown that activation of β 2AR on neutrophils by adrenaline inhibits the respiratory burst (Nielson, 1987; Brunskole Hummel et al., 2013) and suppresses expression of adhesion molecules (Wahle et al., 2005). Anti-inflammatory and immunosuppressive effects of β AR activation on monocyte/macrophages have also been described. Inhibition of oxygen radical production (Schopf & Lemmel, 1983), inhibitory effects on production of $\text{TNF}\alpha$, MIP-1 α , IL-12 and IL-18 (Mizuno et al., 2005) are examples of such anti-inflammatory effects. LPS stimulated microglia also show decreased production of $\text{TNF}\alpha$, IL-6 and MCP-1 upon exposure to both β 1- and β 2AR agonists (Markus et al., 2010). It has been also found that upon activation of microglial β 2AR, migration of microglia to A β deposits and also uptake of A β peptides by these cells is increased (Kong et al., 2010; Heneka et al., 2010).

Extensive studies from our group also revealed similar anti-inflammatory effects of the adrenergic system on microglia. These studies showed that LPS-stimulated microglia were inhibited to produce some of the pro-inflammatory cytokines (master's thesis of Stefanie Riesenber; doctoral thesis of Tommy Regen).

4.3.1 Effect of β 2AR signalling on TLR4 signalling

Studies from our group showed that inhibition of cytokine production by salbutamol is selective. For instance, expression of $\text{TNF}\alpha$, IL-6 and IL-12p40 genes was inhibited, whereas expression of other genes such as CCL2, CCL3 and CCL5 was not affected (master's thesis of Stefanie Riesenber; doctoral thesis of Tommy Regen).

Responses to adrenergic system activation by diverse cell types requires stimulation of their adrenergic receptors (AR). Various studies have detected expression of β 2AR on microglia at

the RNA level using techniques such as PCR (doctoral thesis of Tommy Regen) and RT-PCR (Ishii et al., 2015). However, these methods are based on bulk measurements and do not allow an insight on single cell level. In the current study we used immunohistochemistry to examine on a single cell level if β 2AR is really expressed on all microglia or if it is a 'sub-population feature'. Using immunocytochemistry, we showed that all microglia express β 2AR. These data indicate that all microglial cells are capable of responding to β 2AR agonists.

Gene induction by LPS (through TLR4) stimulation is accomplished through MyD88, TRIF or both adaptor proteins (Regen et al., 2011). For instance, TNF α is exclusively MyD88 dependent whereas expression of CCL5 is regulated by both MyD88 and TRIF pathways (doctoral thesis of Tommy Regen). Previous data from our group have shown that microglia lacking TRIF signalling had a reduced CCL5 expression after receiving salbutamol. To study if the TRIF signalling serves as an escaping route from inhibitory effects of salbutamol, we assessed the salbutamol effect on expression of two exclusively TRIF dependent genes; MHC I and IFN β . We found that MHC I expression upon LPS stimulation was not inhibited by salbutamol. To our surprise, production of IFN β was significantly inhibited. This behaviour was in contrast to MHC I induction and we concluded that the mediator protein TRIF is not the reason why genes such as CCL5 are able to escape from the inhibitory effect of β 2AR activation.

To study all the genes that were affected by salbutamol, we performed a deep sequencing analysis of microglia. Cells received LPS alone or combined with salbutamol. The sequencing data revealed that β 2AR activation by salbutamol specifically increases the expression of STAT4, IRF4 and IRF2 binding protein 2 (IRF2bp2) genes and decreases the expression of IRF8 gene. TLR4 uses STAT and IRF proteins for its downstream signalling and subsequent production of cyto-/ chemokine and type 1 interferons, respectively (reviewed by Hanisch, 2014 and Takeda & Akira, 2004). The effects of STATs and IRFs proteins in regulation of immunity have been extensively studied. Various studies have pointed at the role of IRFs in MyD88-dependent TLR signalling. Direct interactions of IRF4, 5, 7 and 8 with MyD88 leads to the regulation of pro-inflammatory cytokines and type I IFNs (IFN α and - β) production (Honda et al., 2004; Kawai et al., 2004; Takaoka et al., 2005; Honda et al., 2005; Negishi et al., 2005).

The expression of type 1 IFN genes is not dependent on MyD88 (doctoral thesis of Tommy Regen). However, it was described that IRF8 binds directly to the promoters of type 1 IFNs, leading to the sustained RNA polymerase II recruitment to this region and therefore, higher expression of type 1 IFNs (Tailor et al., 2007). Since IRF8 is produced upon activation of TLR4, this indicates the indirect effect of TLRs on type 1 IFNs production. Although the expression of IRF8 is increased by TLR4 activation (Mancino et al., 2015), its production is strongly downregulated by β 2AR activation.

In opposition to IRF5, 7 and 8, IRF4 has anti-inflammatory effects through the MyD88 pathway (Rosenbauer et al., 1999; Mudter et al., 2009). Negishi and colleagues showed that IRF4 negatively regulates MyD88 signalling by competing with IRF5 to bind to it (Negishi et al., 2005).

Our data show that salbutamol leads to, specifically, STAT4 and IRF4 upregulation in spite of downregulation of IRF8. These data explain why the expression of MyD88-dependent genes is inhibited by salbutamol and also why IFN β (which is TRIF dependent) is inhibited as well (Salbutamol \rightarrow \uparrow cAMP \rightarrow \downarrow IRF8; \uparrow IRF4 \rightarrow \uparrow STAT4, \downarrow pro-inflammatory proteins and \downarrow IFN β). These data do not provide any evidence of interaction of β 2AR signalling with the TRIF pathway, thus suggesting that the TRIF pathway is the route to escape from the inhibition upon β 2AR activation.

4.3.2 *In vivo* studies of β 2AR activation

One of the consequences of an inflammatory response from immune cells is to recruit other immune cells to the site of challenge such as infection (Iwasaki & Medzhitov, 2004). To investigate how salbutamol alters the response of microglia to LPS stimulation *in vivo*, we focused on its effect on infiltration of peripheral immune cells and also on LPS-induced astrogliosis. LPS alone or combined with salbutamol was infused in the brains of mice and infiltration of neutrophils, monocytes and T cells from the periphery was investigated. Combination of salbutamol and LPS decreased infiltration of these cells, which could be caused by the anti-inflammatory effect of salbutamol (β 2AR activation) on microglia.

Infiltration of immune cells from the blood stream to tissues requires activation of their β 2 integrins upon exposure to cytokines and pro-inflammatory mediators (such as TNF α), which is followed by binding of activated β 2 integrins to the vascular endothelial adhesion

molecules (d'Alessio et al., 1998; reviewed by Radi et al., 2001). Anti-inflammatory effects of noradrenaline on the expression of adhesion molecules such as cell adhesion molecule (CAM), vascular cell adhesion molecule-1 (VCAM-1) and intercellular adhesion molecule (ICAM-1) *in vivo* was described (O'Sullivan et al., 2010). Therefore, decreased production of pro-inflammatory cytokines and, possibly, reduced numbers of adhesion molecules by salbutamol explain the decreased infiltration of immune cells into the brain upon salbutamol application.

It was shown that noradrenaline has anti-inflammatory effects on immune cells (reviewed by Ishii et al., 2015). In the healthy brain there is a constant production and delivery of noradrenaline from the locus coeruleus (Aston-Jones & Cohen, 2005) which results in a constant anti-inflammatory signal on microglia. Thus, we hypothesized that an elimination of this anti-inflammatory effect might lead to higher numbers of immune cell infiltrates upon LPS infusion. To exclude this possibility we used a β 2AR antagonist, ICI, in combination with LPS to block β 2ARs. We observed that ICI had no effect on the immune cell infiltration. The dose of ICI may not have been sufficient to completely block all β 2ARs. Probably, even a residual level of β 2AR activity may have been efficient to produce a chemokine level that was sufficient to attract immune cells from the periphery. Studying the dose response relationship of ICI would be necessary to exclude this possibility.

We also observed that salbutamol or ICI without LPS did not cause infiltration of peripheral immune cells, revealing that both substances are not sufficient for immune cell recruitment.

To study the effect of salbutamol on astrogliosis, immunohistochemistry analyses were performed. Brains of mice were infused with LPS alone or combined with salbutamol. We showed that salbutamol did not influence the activation of microglia and astrocytes. However, salbutamol significantly reduced the Mac-3 immunoreactivity. Since Mac-3 is expressed on microglia and other macrophages (monocytes) and also activation of microglia is not affected by salbutamol, this finding indicates decreased numbers of infiltrated monocytes by salbutamol.

4.3.3 Population size of TNF α and CCL5 producing cells

The effect of β 2AR activation on gene expression or protein production was shown by us and other groups mainly by the mRNA level or the amount of released proteins (reviewed by

Scanzano & Cosentino, 2015). Since these samples are collected from different cells, the information from specific cell types is lacking. To find out how the productions of TNF α and CCL5 in single cells are affected by salbutamol, we used flow cytometry and ELISpot analysis.

The flow cytometry data revealed a decreased number of TNF α producing cells by addition of salbutamol. Looking at the cells that produce only TNF α , only CCL5 or both (double positive), we recognised that this reduction was conducted by the TNF α producing population and not from the double positive one. Surprisingly, addition of salbutamol to LPS led to an increase in the percentage of the cells that produce only CCL5.

We have already shown that the concentration of TNF α protein is strongly reduced by salbutamol, thus, the cells that produce only TNF α might be able to produce much more TNF α than the group of cells which produce both TNF α and CCL5. On the other hands, CCL5 concentration is not changed by salbutamol and in the flow cytometry data we observed that the population size of only CCL5 producing cells is highly increased, therefore, we conclude that the cells which produce only CCL5 do not produce much of this protein while the double positive cells are the main source of CCL5.

In the ELISpot approach we observed a reduced spot area, which indicates a reduced CCL5 release from single cells. These data suggest that although the protein concentration and percentage of producing cells are not affected by β 2AR activation, CCL5 released from each cell is slightly decreased.

4.3.4 PKA mediates the downstream signalling from β 2AR to TLR4

Binding of agonists to the β 2AR, leads to its activation which in return activates the transmembrane adenylyl cyclase. The activated transmembrane adenylyl cyclase generates the second messenger, cAMP (reviewed by Sassone-Corsi, 2012).

In addition to the transmembrane adenylyl cyclase, cells express soluble adenylyl cyclase, which is distributed through the cytoplasm and in cellular organelles (Braun & Dods, 1975; reviewed by Tresguerres et al., 2011). Activity of soluble adenylyl cyclase to generate cAMP is independent of GPCRs (Braun et al., 1977) instead, it is shown to be regulated by both extra- and intracellular bicarbonate and calcium anions (Okamura et al., 1985; Garty & Salomon, 1987; Jaiswal & Conti, 2003).

Generated cAMP transduces its signal through two main mediators: PKA as the classical pathway and Epac as the non-classical pathway (reviewed by Sassone-Corsi, 2012). Elevated cAMP in immune cells is associated with a reduced cytokine production which represents its anti-inflammatory properties (Bourne et al., 1974; Elenkov, 1995; Nijhuis et al., 2014). The anti-inflammatory effects of cAMP has been often shown to be mainly PKA-dependent (Kammer, 1988; Ishii et al., 2015). Previous studies of our group, also showed production of cAMP in microglia upon salbutamol stimulation. However, these studies failed to confirm the involvement of PKA in the inhibition of cytokine production (doctoral thesis of Tommy Regen and master's thesis of Stefanie Riesenberg). Therefore, in the present study a new cell-permeable PKA inhibitor (IIR-PKI) was used to examine the effect of PKA activity on TNF α , CCL5 and IFN β protein secretion.

Microglia were stimulated with LPS alone or combined with salbutamol and/or the PKA inhibitor and these cytokines were measured in the supernatants of the cells. The results demonstrated that the PKA inhibitor can rescue the inhibited TNF α production, indicating the role of PKA in TNF α inhibition by salbutamol which is in line with previous studies (Gebhardt et al., 2005; Avni et al., 2010; reviewed by Scanzano & Cosentino, 2015). In contrast, IIR-PKI had a negative effect on expression of CCL5 and IFN β and led to their suppression.

The reason to add only PKA inhibitor to LPS was to exclude endogenous PKA activity. Endogenous PKA activity is regulated by endogenous cAMP, which is generated by the soluble adenylyl cyclase, independent of β 2AR signalling. Addition of PKA inhibitor to LPS led to an increase of TNF α production compared to the LPS. This reveals that under normal conditions, immune responses of microglia are suppressed by endogenously activated PKA, most likely representing a negative regulation of TLRs signalling. However, the effect of PKA inhibitor on LPS-mediated CCL5 and IFN β production was inhibitory rather than stimulatory.

Previous publications pointed at activation of phosphatidylinositol-4,5-bisphosphate 3-kinase (PI3K) by TLRs through the MyD88 adaptor protein (Arbibe et al., 2000; Laird et al., 2009). Activated PI3K results in production of phosphatidylinositol (3,4,5)-trisphosphate (PIP₃). The generated PIP₃ facilitates recruitment of signalling proteins such as protein kinase B (PKB), also known as Akt (Laird et al., 2009). LPS was shown to induce phosphorylation of PI3K

and subsequently Akt (Monick et al., 2001). PI3K acting through Akt plays an anti-inflammatory role in innate immune cells by reducing the activity of NF- κ B (X. Li et al., 2003). NF- κ B is a major transcription factor which regulates expression of the genes which shape the immune responses (Hayden et al., 2006). Although both MyD88 and TRIF signalling pathways use NF- κ B (reviewed by Kawasaki & Kawai, 2014), PI3K reduces TRIF-dependent NF- κ B activation, leading to the reduction of TRIF-dependent genes such as IFN β (Aksoy et al., 2005).

In the present study, we showed that PKA inhibition decreases the expression of LPS-mediated CCL5 and IFN β . The data from the deep sequencing experiments revealed significant reduction of PI3K by salbutamol (data not shown), indicating the negative effect of salbutamol (through PKA) on PI3K activation. As described above, PI3K activity leads to the reduction of IFN β expression. Therefore, inhibition of PKA results in the higher expression of PI3K and consequently, stronger reduction of IFN β . We also observed that CCL5 expression is reduced by the PKA inhibitor. CCL5 expression is partly TRIF-dependent (doctoral thesis of Tommy Regen). Thus, the same reduction as IFN β could be observed for CCL5.

Taken together, these data show that PKA uses different ways to affect expression of various genes.

Using a PKA inhibitor, we showed the involvement of PKA in the regulation of TLR4 signalling. To confirm this finding with a second method, we used a PKA activator (N6-Benzoyl-cAMP) in addition to LPS. We hypothesized that activation of PKA should mimic the effect of salbutamol. However, we could not see this effect and this PKA activator failed to suppress TNF α production (data not shown). This could be due to the inefficiency of the activator to enter the cells or not being 100% PKA specific.

Since the PKA activator could not confirm the PKA-dependent TNF α suppression, a PKA activity assay was performed to directly assess its activity in the cell lysates. Cells received salbutamol, LPS, combination of LPS and salbutamol or combination of LPS, salbutamol and the PKA inhibitor (IIR-PKI). We observed that LPS does not activate PKA. Salbutamol significantly activated PKA activity and combination of LPS and salbutamol yielded a stronger activation of PKA. Conversely, the PKA inhibitor decreased the activity of PKA to the level similar to the effect of salbutamol alone. This confirms the activity of PKA induced by exposure to salbutamol *per se*.

PKA is not the only protein activated by cAMP. In the non-classical pathway Epac proteins mediate cAMP signalling in numerous cells including microglia (Morioka et al., 2009; reviewed by Sassone-Corsi, 2012). Although we could show the PKA-mediated cytokine suppression, to exclude the contribution of Epac proteins, their activity was inhibited by specific Epac1 and 2 inhibitors. Three different Epac inhibitors failed to rescue TNF α suppression by salbutamol. In addition, an Epac activator (8-pCPT-2'-O-Me-cAMP) could not mimic the salbutamol effect (data not shown), indicating that Epac proteins are not involved in the anti-inflammatory effects of β 2AR signalling.

The anti-inflammatory influence of PKA has been described in various types of innate immune cells of different tissues (reviewed by Scanzano & Cosentino, 2015). To confirm the inhibitory effect of salbutamol on other macrophages as well, we studied bone marrow derived macrophages (BMDMs). In our approach, BMDMs received LPS alone or combined with salbutamol and subsequently the secretion of TNF α and CCL5 was measured in the supernatants. We could show that TNF α production is inhibited by salbutamol whereas CCL5 was not altered. This finding is in line with the data obtained from microglia and also other studies (reviewed by Scanzano & Cosentino, 2015) and indicates that anti-inflammatory effects of β 2AR signalling is a general immunological phenomenon rather than being immune cell types specific. Although BMDMs are significantly less responsive to stimuli compared to microglia (Janova et al., 2015), their immune reactions seems to be still controlled by the blood circulating adrenergic neurotransmitters.

In conclusion, the current data indicate the strong anti-inflammatory effects of adrenergic system on immune cells which is selective for cyto-/ chemokines. Although β 2AR signalling inhibits mainly signal transduction of the mediator protein MyD88, some of TRIF dependent genes are indirectly inhibited. Our data shows that this system does not reduced activation of microglia and astrocytes *per se* while reducing infiltration of immune cells as well as production of pro-inflammatory cytokines.

5 Summary and conclusions

The present PhD thesis consisted of three main parts: (1) to characterize microglia either isolated from 5XFAD mouse model (*ex vivo*) or (2) in the context of an AD environment in APP23, APP^{swe}PS1^{dE9} and 5XFAD mouse models (*in vivo*); and (3) to investigate the signalling pathways of adrenergic receptors on microglia and its effects on microglial activation.

In the first project we show that microglia isolated from 5XFAD mice at 3, 6 and 9 months of age behave comparable to the aged matched WT littermates. In addition, we could show that dysfunctions of microglia in terms of phagocytic activity and production of cyto-/ chemokines at older ages. This indicates clear age-dependent microglial changes independent of the AD environment.

In conclusion, microglia in an AD environment may still have healthy capacities and just behave abnormal as to the abnormal environment. This could offer therapeutic options. It might be still preferred to modulate the endogenous brain microglia accordingly rather than to build on bone marrow cell transfer.

In the second project which studied priming characteristics of microglia in AD environments, we could show a number of differences (all related to the priming markers) between microglia of WT *vs* AD transgenic mice or microglia in the vicinity of the A β plaques *vs* the microglia in plaque free regions. MHC II positive microglia in 5XFAD mice revealed overexpression of many genes related in neuroinflammation compared to MHC II negative microglia. Also, microglia challenged by a secondary stimulation (with LPS) showed an increased activation status in close vicinity to A β plaques compared to the microglia far from the plaques.

Taken together, our data clearly show that microglial priming in transgenic AD mouse models is driven by the close vicinity of the A β plaques which occurs before the age-associated priming. Understanding the pathophysiological processes of A β -plaque associated microglial priming and the subsequent hypersensitivity of these microglia to secondary systemic inflammation, suggests therapeutic opportunities to decrease neuroinflammation in AD.

The third project of the thesis involved the β 2AR signalling in microglia. We show that β 2AR signalling interferes with the signal induction of TLR4, leading to the inhibition of some pro-

inflammatory cyto-/ chemokines. This inhibition, however, did not include all proteins. We showed that β 2AR signalling, through activation of PKA, inhibits the genes which are induced via the adaptor protein MyD88. For instance, CCL5 could escape from this inhibition due to having the advantage of using the adaptor protein TRIF. Our data also show that INF β gene expression (exclusively TRIF dependent) is inhibited which is the result of a direct effect of β 2AR signalling on the IRFs and not of the TRIF. LPS-stimulated microglia were inhibited to recruit immune cells from the periphery when treated with the β 2AR agonist salbutamol.

In conclusion, β 2AR activation has anti-inflammatory effects on macrophages. β 2AR induces these anti-inflammatory effects on TLR4 signalling through different mechanisms which involve mainly the signal transduction through MyD88.

6 References

- Akira, S., Uematsu, S., & Takeuchi, O. (2006). Pathogen Recognition and Innate Immunity. *Cell*, 124(4), 783–801. <http://doi.org/10.1016/j.cell.2006.02.015>
- Akiyama, H., Barger, S., Barnum, S., Bradt, B., Bauer, J., Cole, G. M., ... Wyss-Coray, T. (2000). *Inflammation and Alzheimer's disease. Neurobiology of Aging* (Vol. 21). [http://doi.org/10.1016/S0197-4580\(00\)00124-X](http://doi.org/10.1016/S0197-4580(00)00124-X)
- Akiyama, H., & McGeer, P. L. (2004). Specificity of mechanisms for plaque removal after A beta immunotherapy for Alzheimer disease. *Nature Medicine*, 10(2), 117–8; author reply 118–9. <http://doi.org/10.1038/nm0204-117>
- Aksoy, E., Vanden Berghe, W., Detienne, S., Amraoui, Z., Fitzgerald, K. a, Haegeman, G., ... Willems, F. (2005). Inhibition of phosphoinositide 3-kinase enhances TRIF-dependent NF-kappa B activation and IFN-beta synthesis downstream of Toll-like receptor 3 and 4. *European Journal of Immunology*, 35(7), 2200–9. <http://doi.org/10.1002/eji.200425801>
- Anders, S., & Huber, W. (2010). Differential expression analysis for sequence count data. *Genome Biol*, 11(10), R106. <http://doi.org/10.1186/gb-2010-11-10-r106>
- Anders, S., Pyl, P. T., & Huber, W. (2014). HTSeq A Python framework to work with high-throughput sequencing data. *Bioinformatics*, 31(2), 166–169. <http://doi.org/10.1101/002824>
- Aoki, C. (1992). Beta-adrenergic receptors: astrocytic localization in the adult visual cortex and their relation to catecholamine axon terminals as revealed by electron microscopic immunocytochemistry. *The Journal of Neuroscience : The Official Journal of the Society for Neuroscience*, 12(3), 781–792.
- Apelt, J., & Schliebs, R. (2001). β -amyloid-induced glial expression of both pro- and anti-inflammatory cytokines in cerebral cortex of aged transgenic Tg2576 mice with Alzheimer plaque pathology. *Brain Research*, 894(1), 21–30. [http://doi.org/10.1016/S0006-8993\(00\)03176-0](http://doi.org/10.1016/S0006-8993(00)03176-0)
- Arbibe, L., Mira, J. P., Teusch, N., Kline, L., Guha, M., Mackman, N., ... Knaus, U. G. (2000). Toll-like receptor 2-mediated NF-kappa B activation requires a Rac1-dependent pathway. *Nature Immunology*, 1(6), 533–40. <http://doi.org/10.1038/82797>
- Aston-Jones, G., & Cohen, J. D. (2005). AN INTEGRATIVE THEORY OF LOCUS COERULEUS-NOREPINEPHRINE FUNCTION: Adaptive Gain and Optimal Performance. *Annual Review of Neuroscience*, 28(1), 403–450. <http://doi.org/10.1146/annurev.neuro.28.061604.135709>
- Avila, J., Lucas, J. J., Perez, M., & Hernandez, F. (2004). Role of tau protein in both physiological and pathological conditions. *Physiological Reviews*, 84(2), 361–384. <http://doi.org/10.1152/physrev.00024.2003>

- Avni, D., Ernst, O., Philosoph, A., & Zor, T. (2010). Role of CREB in modulation of TNFalpha and IL-10 expression in LPS-stimulated RAW264.7 macrophages. *Molecular Immunology*, 47(7-8), 1396–403. <http://doi.org/10.1016/j.molimm.2010.02.015>
- Baik, S. H., Cha, M.-Y., Hyun, Y.-M., Cho, H., Hamza, B., Kim, D. K., ... Mook-Jung, I. (2014). Migration of neutrophils targeting amyloid plaques in Alzheimer's disease mouse model. *Neurobiology of Aging*, 35(6), 1286–92. <http://doi.org/10.1016/j.neurobiolaging.2014.01.003>
- Banati, R. B. (2003). Neuropathological imaging: in vivo detection of glial activation as a measure of disease and adaptive change in the brain. *British Medical Bulletin*, 65, 121–131. <http://doi.org/10.1093/bmb/65.1.121>
- Banks, W. a, & Robinson, S. M. (2010). Minimal penetration of lipopolysaccharide across the murine blood–brain barrier. *Brain, Behavior, and Immunity*, 24(1), 102–109. <http://doi.org/10.1016/j.bbi.2009.09.001>
- Bayer, T. a, & Wirths, O. (2011). Intraneuronal A β as a trigger for neuron loss: can this be translated into human pathology? *Biochemical Society Transactions*, 39(4), 857–61. <http://doi.org/10.1042/BST0390857>
- Benarroch, E. E. (2009, November 17). The locus ceruleus norepinephrine system: Functional organization and potential clinical significance. *Neurology*. <http://doi.org/10.1212/WNL.0b013e3181c2937c>
- Benzing, W. C., Wujek, J. R., Ward, E. K., Shaffer, D., Ashe, K. H., Younkin, S. G., & Brunden, K. R. (1999). Evidence for glial-mediated inflammation in aged APPSW transgenic mice. *Neurobiology of Aging*, 20(6), 581–589. [http://doi.org/10.1016/S0197-4580\(99\)00065-2](http://doi.org/10.1016/S0197-4580(99)00065-2)
- Bias, W. B., Marsh, D. G., Mendell, N. R., Yunis, E. J., Levine, B. B., York, N., & Foss, J. A. (1975). Locus Coeruleus Lesions and Learning Chlorine Compounds and Stratospheric Ozone CF₂Cl₂ break brought stratospheric the. *Science*, 188(4186), 377–378.
- Boche, D., Perry, V. H., & Nicoll, J. A. R. (2013). Review: Activation patterns of microglia and their identification in the human brain. *Neuropathology and Applied Neurobiology*, 39(1), 3–18. <http://doi.org/10.1111/nan.12011>
- Bolmont, T., Haiss, F., Eicke, D., Radde, R., Mathis, C. A., Klunk, W. E., ... Calhoun, M. E. (2008). Dynamics of the Microglial/Amyloid Interaction Indicate a Role in Plaque Maintenance. *Journal of Neuroscience*, 28(16), 4283–4292. <http://doi.org/10.1523/JNEUROSCI.4814-07.2008>
- Bondareff, W., Mountjoy, C. Q., Roth, M., Rossor, M. N., Iversen, L. L., Reynolds, G. P., & Hauser, D. L. (1987). Neuronal degeneration in locus ceruleus and cortical correlates of Alzheimer disease. *Alzheimer Disease and Associated Disorders*, 1(4), 256–262.
- Bornemann, K. D., Wiederhold, K. H., Pauli, C., Ermini, F., Stalder, M., Schnell, L., ...

- Staufenbiel, M. (2001). Abeta-induced inflammatory processes in microglia cells of APP23 transgenic mice. *The American Journal of Pathology*, *158*(1), 63–73. [http://doi.org/10.1016/S0002-9440\(10\)63945-4](http://doi.org/10.1016/S0002-9440(10)63945-4)
- Botos, I., Segal, D. M., & Davies, D. R. (2011). The structural biology of Toll-like receptors. *Structure*, *19*(4), 447–459. <http://doi.org/10.1016/j.str.2011.02.004>
- Bourne, H. R., Lichtenstein, L. M., Melmon, K. L., Henney, C. S., Weinstein, Y., & Shearer, G. M. (1974). Modulation of inflammation and immunity by cyclic AMP. *Science (New York, N.Y.)*, *184*(4132), 19–28. Retrieved from <http://www.ncbi.nlm.nih.gov/pubmed/4131281>
- Bouter, Y., Kacprowski, T., Weissmann, R., Dietrich, K., Borgers, H., Brauß, A., ... Bayer, T. a. (2014). Deciphering the molecular profile of plaques, memory decline and neuron loss in two mouse models for Alzheimer’s disease by deep sequencing. *Frontiers in Aging Neuroscience*, *6*(APR), 1–28. <http://doi.org/10.3389/fnagi.2014.00075>
- Bowie, a, & O’Neill, L. a. (2000). The interleukin-1 receptor/Toll-like receptor superfamily: signal generators for pro-inflammatory interleukins and microbial products. *Journal of Leukocyte Biology*, *67*(4), 508–514.
- Braak H, B. E. (1991). Neuropathological staging of Alzheimer-related changes. *Acta Neuropathologica*, *82*(4), 239–259.
- Braun, T., & Dods, R. F. (1975). Development of a Mn²⁺-sensitive, “soluble” adenylate cyclase in rat testis. *Proceedings of the National Academy of Sciences of the United States of America*, *72*(3), 1097–101. <http://doi.org/10.1073/pnas.72.3.1097>
- Braun, T., Frank, H., Dods, R., & Sepsenwol, S. (1977). Mn²⁺-sensitive, soluble adenylate cyclase in rat testis. Differentiation from other testicular nucleotide cyclases. *Biochimica et Biophysica Acta*, *481*(1), 227–35. Retrieved from <http://www.ncbi.nlm.nih.gov/pubmed/14691>
- Brunskole Hummel, I., Reinartz, M. T., Kälble, S., Burhenne, H., Schwede, F., Buschauer, A., & Seifert, R. (2013). Dissociations in the effects of β 2-adrenergic receptor agonists on cAMP formation and superoxide production in human neutrophils: support for the concept of functional selectivity. *PloS One*, *8*(5), e64556. <http://doi.org/10.1371/journal.pone.0064556>
- Bruttger, J., Karram, K., Wörtge, S., Regen, T., Marini, F., Hoppmann, N., ... Waisman, A. (2015). Genetic Cell Ablation Reveals Clusters of Local Self-Renewing Microglia in the Mammalian Central Nervous System. *Immunity*, 92–106. <http://doi.org/10.1016/j.immuni.2015.06.012>
- Bu, X.-L., Yao, X.-Q., Jiao, S.-S., Zeng, F., Liu, Y.-H., Xiang, Y., ... Wang, Y. (2014). A study on the association between infectious burden and Alzheimer’s disease. *European Journal of Neurology*, 1–7. <http://doi.org/10.1111/ene.12477>

- Butovsky, O., Landa, G., Kunis, G., Ziv, Y., Avidan, H., Greenberg, N., ... Schwartz, M. (2006). Induction and blockage of oligodendrogenesis by differently activated microglia in an animal model of multiple sclerosis. *Journal of Clinical Investigation*, *116*(4), 905–915. <http://doi.org/10.1172/JCI26836>
- Chen CS, Ouyang P, Yeh YC, Lai CL, Liu CK, Yen CF, Ko CH, Yen JY, Liu GC, J. S. (2011). Apolipoprotein E Polymorphism and Behavioral and Psychological Symptoms of Dementia in Patients With Alzheimer Disease. *Alzheimer Disease and Associated Disorders*, 1–5. <http://doi.org/10.1097/WAD.0b013e31821f5787>
- Chen, S. K., Tvrđik, P., Peden, E., Cho, S., Wu, S., Spangrude, G., & Capecchi, M. R. (2010). Hematopoietic origin of pathological grooming in Hoxb8 mutant mice. *Cell*, *141*(5), 775–785.
- Cunningham, C. (2011). Systemic inflammation and delirium: important co-factors in the progression of dementia. *Biochemical Society Transactions*, *39*(4), 945–53. <http://doi.org/10.1042/BST0390945>
- Cunningham, C., Wilcockson, D. C., Champion, S., Lunnon, K., & Perry, V. H. (2005). Central and systemic endotoxin challenges exacerbate the local inflammatory response and increase neuronal death during chronic neurodegeneration. *The Journal of Neuroscience : The Official Journal of the Society for Neuroscience*, *25*(40), 9275–9284. <http://doi.org/10.1523/JNEUROSCI.2614-05.2005>
- d'Alessio, P., Moutet, M., Coudrier, E., Darquenne, S., & Chaudiere, J. (1998). ICAM-1 and VCAM-1 expression induced by TNF-alpha are inhibited by a glutathione peroxidase mimic. *Free Radical Biology & Medicine*, *24*(6), 979–87. Retrieved from <http://www.ncbi.nlm.nih.gov/pubmed/9607608>
- Davalos, D., Grutzendler, J., Yang, G., Kim, J. V, Zuo, Y., Jung, S., ... Gan, W.-B. (2005). ATP mediates rapid microglial response to local brain injury in vivo. *Nature Neuroscience*, *8*(6), 752–758. <http://doi.org/10.1038/nn1472>
- Dello Russo, C., Boullerne, A. I., Gavrilyuk, V., & Feinstein, D. L. (2004). Inhibition of microglial inflammatory responses by norepinephrine: effects on nitric oxide and interleukin-1beta production. *Journal of Neuroinflammation*, *1*(1), 9. <http://doi.org/10.1186/1742-2094-1-9>
- Diagnostic and statistical manual of mental disorders (DSM-IV)*. (1994) (Vol. 4th). Washington, DC: American Psychiatry Association.
- DiCarlo, G. (2001). Intrahippocampal LPS injections reduce A β load load in APP+PS1 transgenic mice. *Neurobiology of Aging*, *22*(6), 1007–1012. [http://doi.org/10.1016/S0197-4580\(01\)00292-5](http://doi.org/10.1016/S0197-4580(01)00292-5)
- Dickens, A. M., Vainio, S., Marjamäki, P., Johansson, J., Lehtiniemi, P., Rokka, J., ... Airas, L. (2014). Detection of microglial activation in an acute model of neuroinflammation

- using PET and radiotracers 11C-(R)-PK11195 and 18F-GE-180. *Journal of Nuclear Medicine: Official Publication, Society of Nuclear Medicine*, 55(3), 466–72. <http://doi.org/10.2967/jnumed.113.125625>
- Dickson, D. W., Lee, S. C., Mattiace, L. a, Yen, S.-H. C., & Brosnan, C. (1993). Microglia and cytokines in neurological disease, with special reference to AIDS and Alzheimer's disease. *Glia*, 7(1), 75–83. <http://doi.org/10.1002/glia.440070113>
- Dobin, A., Davis, C. a, Schlesinger, F., Drenkow, J., Zaleski, C., Jha, S., ... Gingeras, T. R. (2013). STAR: ultrafast universal RNA-seq aligner. *Bioinformatics (Oxford, England)*, 29(1), 15–21. <http://doi.org/10.1093/bioinformatics/bts635>
- Downer, E. (2013). Toll-Like Receptor Signaling in Alzheimer's Disease Progression. *J Alzheimers Dis Parkinsonism*. <http://doi.org/10.4172/2161-0460.S10-006>
- Durinck, S., Moreau, Y., Kasprzyk, a., Davis, S., De Moor, B., Brazma, a., & Huber, W. (2005). BioMart and Bioconductor: a powerful link between biological databases and microarray data analysis. *Bioinformatics*, 21(16), 3439–3440. <http://doi.org/10.1093/bioinformatics/bti525>
- Duthey, B. (2013). Background Paper 6.11 Alzheimer Disease and other Dementias, Update on 2004. *A Public Health Approach to Innovation*, (February), 1 – 77.
- El Khoury, J. B., Moore, K. J., Means, T. K., Leung, J., Terada, K., Toft, M., ... Luster, A. D. (2003). CD36 mediates the innate host response to beta-amyloid. *The Journal of Experimental Medicine*, 197(12), 1657–66. <http://doi.org/10.1084/jem.20021546>
- Elenkov, I. (1995). Modulation of lipopolysaccharide-induced tumor necrosis factor- α production by selective α - and β -adrenergic drugs in mice. *Journal of Neuroimmunology*, 61(2), 123–131. [http://doi.org/10.1016/0165-5728\(95\)00080-L](http://doi.org/10.1016/0165-5728(95)00080-L)
- Fassbender, K., Walter, S., Kühl, S., Landmann, R., Ishii, K., Bertsch, T., ... Beyreuther, K. (2004). The LPS receptor (CD14) links innate immunity with Alzheimer's disease. *FASEB Journal: Official Publication of the Federation of American Societies for Experimental Biology*, 18(1), 203–5. <http://doi.org/10.1096/fj.03-0364fje>
- Fillit, H., Ding, W., Buee, L., Kalman, J., Altstiel, L., Lawlor, B., & Wolf-Klein, G. (1991). Elevated circulating tumor necrosis factor levels in Alzheimer's disease. *Neuroscience Letters*, 129(2), 318–320. [http://doi.org/10.1016/0304-3940\(91\)90490-K](http://doi.org/10.1016/0304-3940(91)90490-K)
- Floden, A. M. (2012). NIH Public Access, 25(2), 279–293. <http://doi.org/10.3233/JAD-2011-101014>.Microglia
- Floden, A. M., & Combs, C. K. (2006). Beta-amyloid stimulates murine postnatal and adult microglia cultures in a unique manner. *The Journal of Neuroscience: The Official Journal of the Society for Neuroscience*, 26(17), 4644–8. <http://doi.org/10.1523/JNEUROSCI.4822-05.2006>
- Forstl, H., Burns, A., Levy, R., & Cairns, N. (1994). Neuropathological correlates of

- psychotic phenomena in confirmed Alzheimer's disease. *British Journal of Psychiatry*, 164(JULY), 53–59.
- Frank, S., Burbach, G. J., Bonin, M., Walter, M., Streit, W., Bechmann, I., & Deller, T. (2008). TREM2 is upregulated in amyloid plaque-associated microglia in aged APP23 transgenic mice. *Glia*, 56(13), 1438–47. <http://doi.org/10.1002/glia.20710>
- Fujita, H., Tanaka, J., Maeda, N., & Sakanaka, M. (1998). Adrenergic agonists suppress the proliferation of microglia through beta 2-adrenergic receptor. *Neuroscience Letters*, 242(1), 37–40. [http://doi.org/S0304-3940\(98\)00003-2](http://doi.org/S0304-3940(98)00003-2) [pii]
- Gaillard, P. J., De Boer, a. G., & Breimer, D. D. (2003). Pharmacological investigations on lipopolysaccharide-induced permeability changes in the blood-brain barrier in vitro. *Microvascular Research*, 65(1), 24–31. [http://doi.org/10.1016/S0026-2862\(02\)00009-2](http://doi.org/10.1016/S0026-2862(02)00009-2)
- Gatti, S., & Bartfai, T. (1993). Induction of tumor necrosis factor- α mRNA in the brain after peripheral endotoxin treatment: comparison with interleukin-1 family and interleukin-6. *Brain Research*, 624(1-2), 291–294. [http://doi.org/10.1016/0006-8993\(93\)90090-A](http://doi.org/10.1016/0006-8993(93)90090-A)
- Gebhardt, T., Gerhard, R., Bedoui, S., Erpenbeck, V. J., Hoffmann, M. W., Manns, M. P., & Bischoff, S. C. (2005). beta2-Adrenoceptor-mediated suppression of human intestinal mast cell functions is caused by disruption of filamentous actin dynamics. *European Journal of Immunology*, 35(4), 1124–32. <http://doi.org/10.1002/eji.200425869>
- Gerits, N., Kostenko, S., Shiryayev, A., Johannessen, M., & Moens, U. (2008). Relations between the mitogen-activated protein kinase and the cAMP-dependent protein kinase pathways: Comradeship and hostility. *Cellular Signalling*, 20(9), 1592–1607. <http://doi.org/10.1016/j.cellsig.2008.02.022>
- Ginhoux, F., Greter, M., Leboeuf, M., Nandi, S., See, P., Gokhan, S., ... Merad, M. (2010). Fate mapping analysis reveals that adult microglia derive from primitive macrophages. *Science (New York, N.Y.)*, 330(6005), 841–845.
- Glass, C. K., Saijo, K., Winner, B., Marchetto, M. C., & Gage, F. H. (2010). Mechanisms underlying inflammation in neurodegeneration. *Cell*, 140(6), 918–34. <http://doi.org/10.1016/j.cell.2010.02.016>
- Gloerich, M., & Bos, J. L. (2010). Epac: defining a new mechanism for cAMP action. *Annual Review of Pharmacology and Toxicology*, 50, 355–75. <http://doi.org/10.1146/annurev.pharmtox.010909.105714>
- Goedert M, S. M. (2006). A century of Alzheimer's disease. *Science*, 314(5800), 777–81. <http://doi.org/10.1126/science.1132814>
- Goings, G. E., Kozlowski, D. A., & Szele, F. G. (2006). Differential activation of microglia in neurogenic versus non-neurogenic regions of the forebrain. *GLIA*, 54(4), 329–342.
- Gomez-Nicola, D., & Boche, D. (2015). Post-mortem analysis of neuroinflammatory changes in human Alzheimer's disease. *Alzheimer's Research & Therapy*, 7(1), 42.

- <http://doi.org/10.1186/s13195-015-0126-1>
- Gomez-Nicola, D., Fransen, N. L., Suzzi, S., & Perry, V. H. (2013). Regulation of Microglial Proliferation during Chronic Neurodegeneration. *Journal of Neuroscience*, *33*(6), 2481–2493. <http://doi.org/10.1523/JNEUROSCI.4440-12.2013>
- Gonzalez-Velasquez, F. J., & Moss, M. a. (2007). Soluble aggregates of the amyloid- β protein activate endothelial monolayers for adhesion and subsequent transmigration of monocyte cells. *Journal of Neurochemistry*, *104*(2), 071024001518004–???. <http://doi.org/10.1111/j.1471-4159.2007.04988.x>
- Griciuc, A., Serrano-pozo, A., Parrado, A. R., Lesinski, A. N., Asselin, C. N., Mullin, K., ... Tanzi, R. E. (2013). Alzheimer's disease risk gene CD33 inhibits microglial uptake of amyloid beta. *Neuron*, *78*(4), 631–643.
- Griffin, W. S., Stanley, L. C., Ling, C., White, L., MacLeod, V., Perrot, L. J., ... Araoz, C. (1989). Brain interleukin 1 and S-100 immunoreactivity are elevated in Down syndrome and Alzheimer disease. *Proceedings of the National Academy of Sciences of the United States of America*, *86*(19), 7611–5. <http://doi.org/10.1073/pnas.86.19.7611>
- Guerreiro, R., Wojtas, A., Bras, J., Carrasquillo, M., Rogaeva, E., Majounie, E., ... Hardy, J. (2013). TREM2 variants in Alzheimer's disease. *The New England Journal of Medicine*, *368*(2), 117–27. <http://doi.org/10.1056/NEJMoa1211851>
- Gyoneva, S., & Traynelis, S. F. (2013). Norepinephrine modulates the motility of resting and activated microglia via different adrenergic receptors. *The Journal of Biological Chemistry*, *288*(21), 15291–302. <http://doi.org/10.1074/jbc.M113.458901>
- Hempel H, Frank R, Broich K, Teipel SJ, Katz RG, Hardy J, Herholz K, Bokde AL, Jessen F, Hoessler YC, Sanhai WR, Zetterberg H, Woodcock J, B. K. (2010). Biomarkers for Alzheimer's disease: academic, industry and regulatory perspectives. *Nature Reviews. Drug Discovery*, *9*(7), 560–74. <http://doi.org/10.1038/nrd3115>
- Hanisch, U. K. (2014). Linking STAT and TLR signaling in microglia: a new role for the histone demethylase Jmjd3. *Journal of Molecular Medicine*, 1–4. <http://doi.org/10.1007/s00109-014-1122-9>
- Hanisch, U.-K., & Kettenmann, H. (2007). Microglia: active sensor and versatile effector cells in the normal and pathologic brain. *Nature Neuroscience*, *10*(11), 1387–94. <http://doi.org/10.1038/nn1997>
- Harry, G. J. (2013). Microglia during development and aging. *Pharmacology & Therapeutics*, *139*(3), 313–26. <http://doi.org/10.1016/j.pharmthera.2013.04.013>
- Hayden, M. S., West, A. P., & Ghosh, S. (2006). NF- κ B and the immune response. *Oncogene*, *25*(51), 6758–6780. <http://doi.org/10.1038/sj.onc.1209943>
- Heneka, M. T., Carson, M. J., Khoury, J. El, Landreth, G. E., Brosseron, F., Feinstein, D. L., ... Kummer, M. P. (2015). Neuroinflammation in Alzheimer's disease. *The Lancet*

- Neurology*, 14(4), 388–405. [http://doi.org/10.1016/S1474-4422\(15\)70016-5](http://doi.org/10.1016/S1474-4422(15)70016-5)
- Heneka, M. T., Kummer, M. P., Stutz, A., Delekate, A., Schwartz, S., Vieira-Saecker, A., ... Golenbock, D. T. (2013). NLRP3 is activated in Alzheimer's disease and contributes to pathology in APP/PS1 mice. *Nature*, 493(7434), 674–8. <http://doi.org/10.1038/nature11729>
- Heneka, M. T., Nadrigny, F., Regen, T., Martinez-Hernandez, A., Dumitrescu-Ozimek, L., Terwel, D., ... Kummer, M. P. (2010). Locus ceruleus controls Alzheimer's disease pathology by modulating microglial functions through norepinephrine. *Proceedings of the National Academy of Sciences of the United States of America*, 107(13), 6058–63. <http://doi.org/10.1073/pnas.0909586107>
- Heppner, F. L., Ransohoff, R. M., & Becher, B. (2015). Immune attack: the role of inflammation in Alzheimer disease. *Nature Reviews Neuroscience*, 16(6), 358–372. <http://doi.org/10.1038/nrn3880>
- Herber, D. L., Roth, L. M., Wilson, D., Wilson, N., Mason, J. E., Morgan, D., & Gordon, M. N. (2004). Time-dependent reduction in A β levels after intracranial LPS administration in APP transgenic mice. *Experimental Neurology*, 190(1), 245–253. <http://doi.org/10.1016/j.expneurol.2004.07.007>
- Hickman, S. E., Allison, E. K., & El Khoury, J. (2008a). Microglial Dysfunction and Defective β -Amyloid Clearance Pathways in Aging Alzheimer's Disease Mice. *Journal of Neuroscience*, 28(33), 8354–8360. <http://doi.org/10.1523/JNEUROSCI.0616-08.2008>
- Hickman, S. E., Allison, E. K., & El Khoury, J. (2008b). Microglial dysfunction and defective beta-amyloid clearance pathways in aging Alzheimer's disease mice. *The Journal of Neuroscience: The Official Journal of the Society for Neuroscience*, 28(33), 8354–60. <http://doi.org/10.1523/JNEUROSCI.0616-08.2008>
- Hillmann, A., Hahn, S., Schilling, S., Hoffmann, T., Demuth, H. U., Bulic, B., ... Wirths, O. (2012). No improvement after chronic ibuprofen treatment in the 5XFAD mouse model of Alzheimer's disease. *Neurobiology of Aging*, 33(4), 833.e39–833.e50. <http://doi.org/10.1016/j.neurobiolaging.2011.08.006>
- Holmes, C., Cunningham, C., Zotova, E., Woolford, J., Dean, C., Kerr, S., ... Perry, V. H. (2009). Systemic inflammation and disease progression in Alzheimer disease. *Neurology*, 73(10), 768–774. <http://doi.org/10.1212/WNL.0b013e3181b6bb95>
- Holtman, I. R., Raj, D. D., Miller, J. A., Schaafsma, W., Yin, Z., Brouwer, N., ... Eggen, B. J. L. (2015). Induction of a common microglia gene expression signature by aging and neurodegenerative conditions: a co-expression meta-analysis. *Acta Neuropathologica Communications*, 3(1), 31. <http://doi.org/10.1186/s40478-015-0203-5>
- Honda, K., Yanai, H., Mizutani, T., Negishi, H., Shimada, N., Suzuki, N., ... Taniguchi, T. (2004). Role of a transductional-transcriptional processor complex involving MyD88 and

- IRF-7 in Toll-like receptor signaling. *Proceedings of the National Academy of Sciences of the United States of America*, 101(43), 15416–15421. <http://doi.org/10.1073/pnas.0406933101>
- Honda, K., Yanai, H., Negishi, H., Asagiri, M., Sato, M., Mizutani, T., ... Taniguchi, T. (2005). IRF-7 is the master regulator of type-I interferon-dependent immune responses. *Nature*, 434(7034), 772–777. <http://doi.org/10.1038/nature03464>
- Hoover, B. R., Reed, M. N., Su, J., Penrod, R. D., Kotilinek, L. a., Grant, M. K., ... Liao, D. (2010). Tau Mislocalization to Dendritic Spines Mediates Synaptic Dysfunction Independently of Neurodegeneration. *Neuron*. <http://doi.org/10.1016/j.neuron.2010.11.030>
- Houdek, H. M., Larson, J., Watt, J. A., & Rosenberger, T. A. (2014). Bacterial lipopolysaccharide induces a dose-dependent activation of neuroglia and loss of basal forebrain cholinergic cells in the rat brain. *Inflammation and Cell Signaling*, 1–9. <http://doi.org/10.14800/ics.47>
- Huynh, K. K., Eskelinen, E.-L., Scott, C. C., Malevanets, A., Saftig, P., & Grinstein, S. (2007). LAMP proteins are required for fusion of lysosomes with phagosomes. *The EMBO Journal*, 26(2), 313–324. <http://doi.org/10.1038/sj.emboj.7601511>
- Ishii, Y., Yamaizumi, A., Kawakami, A., Islam, A., Choudhury, M. E., Takahashi, H., ... Tanaka, J. (2015). Anti-inflammatory effects of noradrenaline on LPS-treated microglial cells: Suppression of NFκB nuclear translocation and subsequent STAT1 phosphorylation. *Neurochemistry International*, 90, 56–66. <http://doi.org/10.1016/j.neuint.2015.07.010>
- Iversen, L. L., Rossor, M. N., Reynolds, G. P., Hills, R., Roth, M., Mountjoy, C. Q., ... Bloom, F. E. (1983). Loss of pigmented dopamine-??-hydroxylase positive cells from locus coeruleus in senile dementia of Alzheimer's type. *Neuroscience Letters*, 39(1), 95–100. [http://doi.org/10.1016/0304-3940\(83\)90171-4](http://doi.org/10.1016/0304-3940(83)90171-4)
- Iwasaki, A., & Medzhitov, R. (2004). Toll-like receptor control of the adaptive immune responses. *Nature Immunology*, 5(10), 987–995. <http://doi.org/10.1038/ni1112>
- Jaiswal, B. S., & Conti, M. (2003). Calcium regulation of the soluble adenylyl cyclase expressed in mammalian spermatozoa. *Proceedings of the National Academy of Sciences of the United States of America*, 100(19), 10676–10681. <http://doi.org/10.1073/pnas.1831008100>
- Janelins, M. C., Mastrangelo, M. a, Oddo, S., LaFerla, F. M., Federoff, H. J., & Bowers, W. J. (2005). Early correlation of microglial activation with enhanced tumor necrosis factor- α and monocyte chemoattractant protein-1 expression specifically within the entorhinal cortex of triple transgenic Alzheimer's disease mice. *Journal of Neuroinflammation*, 2(1), 23. <http://doi.org/10.1186/1742-2094-2-23>

- Jankowsky, J. L., Slunt, H. H., Gonzales, V., Jenkins, N. A., Copeland, N. G., & Borchelt, D. R. (2004). APP processing and amyloid deposition in mice haplo-insufficient for presenilin 1. *Neurobiology of Aging*, 25(7), 885–92. <http://doi.org/10.1016/j.neurobiolaging.2003.09.008>
- Janova, H., Böttcher, C., Holtman, I. R., Regen, T., van Rossum, D., Götz, A., ... Hanisch, U.-K. (2015). CD14 is a key organizer of microglial responses to CNS infection and injury. *Glia*, n/a–n/a. <http://doi.org/10.1002/glia.22955>
- Janus, C., Flores, A. Y., Xu, G., & Borchelt, D. R. (2015). Behavioral abnormalities in APPSwe/PS1dE9 mouse model of AD-like pathology: comparative analysis across multiple behavioral domains. *Neurobiology of Aging*, 36(9), 2519–2532. <http://doi.org/10.1016/j.neurobiolaging.2015.05.010>
- Jawhar S, Trawicka A, Jenneckens C, Bayer TA, W. O. (2012). Motor deficits, neuron loss, and reduced anxiety coinciding with axonal degeneration and intraneuronal A β aggregation in the 5XFAD mouse model of Alzheimer’s disease. *Neurobiology of Aging*, 33(1), 196.e29–40.
- Jeong, H.-K., Jou, I., & Joe, E. (2010). Systemic LPS administration induces brain inflammation but not dopaminergic neuronal death in the substantia nigra. *Experimental and Molecular Medicine*, 42(12), 823. <http://doi.org/10.3858/emm.2010.42.12.085>
- Jimenez, S., Baglietto-Vargas, D., Caballero, C., Moreno-Gonzalez, I., Torres, M., Sanchez-Varo, R., ... Vitorica, J. (2008). Inflammatory response in the hippocampus of PS1M146L/APP751SL mouse model of Alzheimer’s disease: age-dependent switch in the microglial phenotype from alternative to classic. *The Journal of Neuroscience: The Official Journal of the Society for Neuroscience*, 28(45), 11650–11661. <http://doi.org/10.1523/JNEUROSCI.3024-08.2008>
- Johnson, J. D., Zimomra, Z. R., & Stewart, L. T. (2013). Beta-adrenergic receptor activation primes microglia cytokine production. *Journal of Neuroimmunology*, 254(1-2), 161–4. <http://doi.org/10.1016/j.jneuroim.2012.08.007>
- Kammer, G. M. (1988). The adenylate cyclase-cAMP-protein kinase A pathway and regulation of the immune response. *Immunology Today*, 9(7-8), 222–229. Retrieved from <http://www.sciencedirect.com/science/article/B6VHW-485Y1DR-47/2/8270ebf5457fa5bb21bde850b5fae625>
- Kamphuis, W., Orre, M., Kooijman, L., Dahmen, M., & Hol, E. M. (2012). Differential cell proliferation in the cortex of the APPSwePS1dE9 Alzheimer’s disease mouse model. *Glia*, 60(January), 615–629. <http://doi.org/10.1002/glia.22295>
- Karch, C. M., & Goate, A. M. (2014). Alzheimer’s Disease Risk Genes and Mechanisms of Disease Pathogenesis. *Biological Psychiatry*, 77(1), 43–51. <http://doi.org/10.1016/j.biopsych.2014.05.006>

- Kawai, T., Sato, S., Ishii, K. J., Coban, C., Hemmi, H., Yamamoto, M., ... Akira, S. (2004). Interferon- α induction through Toll-like receptors involves a direct interaction of IRF7 with MyD88 and TRAF6. *Nature Immunology*, 5(10), 1061–1068. <http://doi.org/10.1038/ni1118>
- Kawasaki, T., & Kawai, T. (2014). Toll-Like Receptor Signaling Pathways. *Frontiers in Immunology*, 5(September), 1–8. <http://doi.org/10.3389/fimmu.2014.00461>
- Kierdorf, K., Erny, D., Goldmann, T., Sander, V., Schulz, C., Perdiguero, E. G., ... Prinz, M. (2013). Microglia emerge from erythromyeloid precursors via Pu.1- and Irf8-dependent pathways. *Nature Neuroscience*, 16(3), 273–80. <http://doi.org/10.1038/nn.3318>
- Kilgore, M., Miller, C. a, Fass, D. M., Hennig, K. M., Haggarty, S. J., Sweatt, J. D., & Rumbaugh, G. (2010). Inhibitors of Class 1 Histone Deacetylases Reverse Contextual Memory Deficits in a Mouse Model of Alzheimer's Disease. *Neuropsychopharmacology*, 35(4), 870–880. <http://doi.org/10.1038/npp.2009.197>
- Kim, K. H., Moon, M., Yu, S.-B., Mook-Jung, I., & Kim, J.-I. (2012). RNA-Seq analysis of frontal cortex and cerebellum from 5XFAD mice at early stage of disease pathology. *Journal of Alzheimer's Disease: JAD*, 29(4), 793–808. <http://doi.org/10.3233/JAD-2012-111793>
- Kitazawa, M., Oddo, S., Yamasaki, T. R., Green, K. N., & LaFerla, F. M. (2005). Lipopolysaccharide-induced inflammation exacerbates tau pathology by a cyclin-dependent kinase 5-mediated pathway in a transgenic model of Alzheimer's disease. *The Journal of Neuroscience: The Official Journal of the Society for Neuroscience*, 25(39), 8843–53. <http://doi.org/10.1523/JNEUROSCI.2868-05.2005>
- Kojro, E., & Fahrenholz, F. (2005). The non-amyloidogenic pathway: structure and function of alpha-secretases. *Sub-Cellular Biochemistry*, 38, 105–127.
- Kong, Y., Ruan, L., Qian, L., Liu, X., & Le, Y. (2010). Norepinephrine promotes microglia to uptake and degrade amyloid beta peptide through upregulation of mouse formyl peptide receptor 2 and induction of insulin-degrading enzyme. *The Journal of Neuroscience: The Official Journal of the Society for Neuroscience*, 30(35), 11848–57. <http://doi.org/10.1523/JNEUROSCI.2985-10.2010>
- Kono, H., & Kenneth, K. L. (2008). How dying cells alert the immune system to danger. *Nature Reviews. Immunology*, 8(4), 279–289.
- Krabbe, G., Halle, A., Matyash, V., Rinnenthal, J. L., Eom, G. D., Bernhardt, U., ... Heppner, F. L. (2013). Functional Impairment of Microglia Coincides with Beta-Amyloid Deposition in Mice with Alzheimer-Like Pathology. *PLoS ONE*, 8(4), e60921. <http://doi.org/10.1371/journal.pone.0060921>
- Lai, A. Y., & McLaurin, J. (2012). Clearance of amyloid- β peptides by microglia and macrophages: the issue of what, when and where. *Future Neurology*, 7(2), 165–176.

- <http://doi.org/10.2217/fnl.12.6>
- Laird, M. H. W., Rhee, S. H., Perkins, D. J., Medvedev, A. E., Piao, W., Fenton, M. J., & Vogel, S. N. (2009). TLR4/MyD88/PI3K interactions regulate TLR4 signaling. *Journal of Leukocyte Biology*, *85*(6), 966–77. <http://doi.org/10.1189/jlb.1208763>
- Landel, V., Baranger, K., Virard, I., Loriod, B., Khrestchatisky, M., Rivera, S., ... Féron, F. (2014). Temporal gene profiling of the 5XFAD transgenic mouse model highlights the importance of microglial activation in Alzheimer's disease. *Molecular Neurodegeneration*, *9*(1), 33. <http://doi.org/10.1186/1750-1326-9-33>
- Larson ME, L. S. (2012). Soluble A β oligomer production and toxicity. *Journal of Neurochemistry*, *120*, 125–39. <http://doi.org/10.1111/j.1471-4159.2011.07478.x>
- Lebson, L., Nash, K., Kamath, S., Herber, D., Carty, N., Lee, D. C., ... Gordon, M. N. (2010). Trafficking CD11b-Positive Blood Cells Deliver Therapeutic Genes to the Brain of Amyloid-Depositing Transgenic Mice. *Journal of Neuroscience*, *30*(29), 9651–9658. <http://doi.org/10.1523/JNEUROSCI.0329-10.2010>
- Letiembre, M., Hao, W., Liu, Y., Walter, S., Mihaljevic, I., Rivest, S., ... Fassbender, K. (2007). Innate immune receptor expression in normal brain aging. *Neuroscience*, *146*(1), 248–254. <http://doi.org/10.1016/j.neuroscience.2007.01.004>
- Li, H., Handsaker, B., Wysoker, A., Fennell, T., Ruan, J., Homer, N., ... Subgroup, 1000 Genome Project Data Processing. (2009). The Sequence Alignment/Map format and SAMtools. *Bioinformatics*, *25*(16), 2078–2079. <http://doi.org/10.1093/bioinformatics/btp352>
- Li, X., Tupper, J. C., Bannerman, D. D., Winn, R. K., Rhodes, C. J., & Harlan, J. M. (2003). Phosphoinositide 3 kinase mediates Toll-like receptor 4-induced activation of NF- κ B in endothelial cells. *Infection and Immunity*, *71*(8), 4414–4420. <http://doi.org/10.1128/IAI.71.8.4414-4420.2003>
- Liu, Y., Walter, S., Stagi, M., Cherny, D., Letiembre, M., Schulz-Schaeffer, Holger Heine, W., ... Fassbender, K. (2005). LPS receptor (CD14): a receptor for phagocytosis of Alzheimer's amyloid peptide. *Brain*, *128*(8), 1778–1789. <http://doi.org/10.1093/brain/awh531>
- Lull, M. E., & Block, M. L. (2010). Microglial activation and chronic neurodegeneration. *Neurotherapeutics*, *7*(4), 354–365. <http://doi.org/10.1016/j.nurt.2010.05.014>
- Lyketsos, C. G., Carrillo, M. C., Ryan, J. M., Khachaturian, A. S., Trzepacz, P., Amatniek, J., ... Miller, D. S. (2011). Neuropsychiatric symptoms in Alzheimer's disease. *Alzheimer's & Dementia: The Journal of the Alzheimer's Association*, *7*(5), 532–9. <http://doi.org/10.1016/j.jalz.2011.05.2410>
- Mancino, A., Termanini, A., Barozzi, I., Ghisletti, S., Ostuni, R., Prosperini, E., ... Natoli, G. (2015). A dual cis-regulatory code links IRF8 to constitutive and inducible gene

- expression in macrophages. *Genes & Development*, 29(4), 394–408. <http://doi.org/10.1101/gad.257592.114>
- Markus, T., Hansson, S. R., Cronberg, T., Cilio, C., Wieloch, T., & Ley, D. (2010). β -Adrenoceptor activation depresses brain inflammation and is neuroprotective in lipopolysaccharide-induced sensitization to oxygen-glucose deprivation in organotypic hippocampal slices. *Journal of Neuroinflammation*, 7(1), 94. <http://doi.org/10.1186/1742-2094-7-94>
- Marlatt, M. W., Bauer, J., Aronica, E., van Haastert, E. S., Hoozemans, J. J. M., Joels, M., & Lucassen, P. J. (2014). Proliferation in the Alzheimer Hippocampus Is due to Microglia, Not Astroglia, and Occurs at Sites of Amyloid Deposition. *Neural Plasticity*, 2014, 1–12. <http://doi.org/10.1155/2014/693851>
- Marshall, G. P., Deleyrolle, L. P., Reynolds, B. a, Steindler, D. a, & Laywell, E. D. (2014). Microglia from neurogenic and non-neurogenic regions display differential proliferative potential and neuroblast support. *Frontiers in Cellular Neuroscience*, 8(July), 180. Retrieved from <http://www.pubmedcentral.nih.gov/articlerender.fcgi?artid=4100441&tool=pmcentrez&rendertype=abstract>
- Matthews, K. L., Chen, C. P. L. H., Esiri, M. M., Keene, J., Minger, S. L., & Francis, P. T. (2002). Noradrenergic changes, aggressive behavior, and cognition in patients with dementia. *Biological Psychiatry*, 51(5), 407–416. [http://doi.org/10.1016/S0006-3223\(01\)01235-5](http://doi.org/10.1016/S0006-3223(01)01235-5)
- McGeer, P. L., Itagaki, S., & McGeer, E. G. (1988). Expression of the histocompatibility glycoprotein HLA-DR in neurological disease. *Acta Neuropathologica*, 76(6), 550–7.
- Michell-Robinson, M. a., Touil, H., Healy, L. M., Owen, D. R., Durafourt, B. a., Bar-Or, A., ... Moore, C. S. (2015). Roles of microglia in brain development, tissue maintenance and repair. *Brain*, 138(5), 1138–1159. <http://doi.org/10.1093/brain/awv066>
- Mildner, A., Schlevogt, B., Kierdorf, K., Bottcher, C., Erny, D., Kummer, M. P., ... Prinz, M. (2011). Distinct and Non-Redundant Roles of Microglia and Myeloid Subsets in Mouse Models of Alzheimer's Disease. *Journal of Neuroscience*, 31(31), 11159–11171. <http://doi.org/10.1523/JNEUROSCI.6209-10.2011>
- Minogue, A. M., Jones, R. S., Kelly, R. J., McDonald, C. L., Connor, T. J., & Lynch, M. a. (2014). Age-associated dysregulation of microglial activation is coupled with enhanced blood-brain barrier permeability and pathology in APP/PS1 mice. *Neurobiology of Aging*, 35(6), 1442–1452. <http://doi.org/10.1016/j.neurobiolaging.2013.12.026>
- Mizuno, K., Takahashi, H. K., Iwagaki, H., Katsuno, G., Kamurul, H. a S. M., Ohtani, S., ... Tanaka, N. (2005). β 2-Adrenergic receptor stimulation inhibits LPS-induced IL-18 and IL-12 production in monocytes. *Immunology Letters*, 101, 168–172. <http://doi.org/10.1016/j.imlet.2005.05.008>

- Mollenhauer, H. H., Morré, D. J., & Rowe, L. D. (1990). Alteration of intracellular traffic by monensin; mechanism, specificity and relationship to toxicity. *Biochimica et Biophysica Acta*, *1031*(2), 225–46. [http://doi.org/10.1016/0304-4157\(90\)90008-Z](http://doi.org/10.1016/0304-4157(90)90008-Z)
- Monick, M. M., Carter, a B., Robeff, P. K., Flaherty, D. M., Peterson, M. W., & Hunninghake, G. W. (2001). Lipopolysaccharide activates Akt in human alveolar macrophages resulting in nuclear accumulation and transcriptional activity of beta-catenin. *Journal of Immunology (Baltimore, Md. : 1950)*, *166*(7), 4713–20. <http://doi.org/10.4049/jimmunol.166.7.4713>
- Moon, M. L., McNeil, L. K., & Freund, G. G. (2011). Macrophages make me sick: how macrophage activation states influence sickness behavior. *Psychoneuroendocrinology*, *36*(10), 1431–40. <http://doi.org/10.1016/j.psyneuen.2011.07.002>
- Morioka, N., Tanabe, H., Inoue, A., Dohi, T., & Nakata, Y. (2009). Noradrenaline reduces the ATP-stimulated phosphorylation of p38 MAP kinase via ??-adrenergic receptors-cAMP-protein kinase A-dependent mechanism in cultured rat spinal microglia. *Neurochemistry International*, *55*(4), 226–234. <http://doi.org/10.1016/j.neuint.2009.03.004>
- Mouihate, A. (2014). TLR4-mediated brain inflammation halts neurogenesis: impact of hormonal replacement therapy. *Frontiers in Cellular Neuroscience*, *8*(May), 146. <http://doi.org/10.3389/fncel.2014.00146>
- Mudter, J., Yu, J., Amoussina, L., Weigmann, B., Hoffman, A., Rücknagel, K., ... Neurath, M. F. (2009). IRF4 selectively controls cytokine gene expression in chronic intestinal inflammation. *Archivum Immunologiae et Therapiae Experimentalis*, *57*(5), 369–76. <http://doi.org/10.1007/s00005-009-0046-5>
- Nakamura, Y., Si, Q. S., & Kataoka, K. (1999). Lipopolysaccharide-induced microglial activation in culture: Temporal profiles of morphological change and release of cytokines and nitric oxide. *Neuroscience Research*, *35*(2), 95–100. [http://doi.org/10.1016/S0168-0102\(99\)00071-1](http://doi.org/10.1016/S0168-0102(99)00071-1)
- Negishi, H., Ohba, Y., Yanai, H., Takaoka, A., Honma, K., Yui, K., ... Honda, K. (2005). Negative regulation of Toll-like-receptor signaling by IRF-4. *Proceedings of the National Academy of Sciences of the United States of America*, *102*(44), 15989–94. <http://doi.org/10.1073/pnas.0508327102>
- Newton, K., & Dixit, V. M. (2012). Signaling in innate immunity and inflammation. *Cold Spring Harbor Perspectives in Biology*, *4*(3). <http://doi.org/10.1101/cshperspect.a006049>
- Nielson, C. P. (1987). Beta-adrenergic modulation of the polymorphonuclear leukocyte respiratory burst is dependent upon the mechanism of cell activation. *Journal of Immunology (Baltimore, Md. : 1950)*, *139*(7), 2392–2397.
- Nijhuis, L. E., Olivier, B. J., Dhawan, S., Hilbers, F. W., Boon, L., Wolkers, M. C., ... De Jonge, W. J. (2014). Adrenergic β 2 receptor activation stimulates anti-inflammatory

- properties of dendritic cells in vitro. *PLoS ONE*, 9(1), 2–3. <http://doi.org/10.1371/journal.pone.0085086>
- Nimmerjahn, A., Kirchhoff, F., & Helmchen, F. (2005). Resting microglial cells are highly dynamic surveillants of brain parenchyma in vivo. *Neuroforum*, 11(3), 95–96.
- Njie, eMalick G., Boelen, E., Stassen, F. R., Steinbusch, H. W. M., Borchelt, D. R., & Streit, W. J. (2012). Ex vivo cultures of microglia from young and aged rodent brain reveal age-related changes in microglial function. *Neurobiology of Aging*, 33(1), 195.e1–12. <http://doi.org/10.1016/j.neurobiolaging.2010.05.008>
- Norden, D. M., & Godbout, J. P. (2013). Review: microglia of the aged brain: primed to be activated and resistant to regulation. *Neuropathology and Applied Neurobiology*, 39(1), 19–34. <http://doi.org/10.1111/j.1365-2990.2012.01306.x>
- Norton, W. T., & Poduslo, S. E. (1973). Myelination in rat brain: method of myelin isolation. *Journal of Neurochemistry*, 21(4), 749–757.
- O'Brien, R. J., & Wong, P. C. (2011). Amyloid Precursor Protein Processing and Alzheimer's Disease. *Annual Review of Neuroscience*, 34(1), 185–204. <http://doi.org/10.1146/annurev-neuro-061010-113613>
- O'Neill, L. a J., Golenbock, D., & Bowie, A. G. (2013). The history of Toll-like receptors - redefining innate immunity. *Nature Reviews. Immunology*, 13(6), 453–60. <http://doi.org/10.1038/nri3446>
- O'Sullivan, J. B., Ryan, K. M., Harkin, A., & Connor, T. J. (2010). Noradrenaline reuptake inhibitors inhibit expression of chemokines IP-10 and RANTES and cell adhesion molecules VCAM-1 and ICAM-1 in the CNS following a systemic inflammatory challenge. *Journal of Neuroimmunology*, 220(1-2), 34–42. <http://doi.org/10.1016/j.jneuroim.2009.12.007>
- Oakley H1, Cole SL, Logan S, Maus E, Shao P, Craft J, Guillozet-Bongaarts A, Ohno M, Disterhoft J, Van Eldik L, Berry R, V. R. (2006). Intraneuronal beta-amyloid aggregates, neurodegeneration, and neuron loss in transgenic mice with five familial Alzheimer's disease mutations: potential factors in amyloid plaque formation. *The Journal of Neuroscience*, 26(40), 10129–40. <http://doi.org/10.1523/JNEUROSCI.1202-06.2006>
- Okamura, N., Tajima, Y., Soejima, a, Masuda, H., & Sugita, Y. (1985). Sodium bicarbonate in seminal plasma stimulates the motility of mammalian spermatozoa through direct activation of adenylate cyclase. *The Journal of Biological Chemistry*, 260(17), 9699–705. Retrieved from <http://www.ncbi.nlm.nih.gov/pubmed/2991260>
- Orre, M., Kamphuis, W., Osborn, L. M., Jansen, A. H. P., Kooijman, L., Bossers, K., & Hol, E. M. (2014). Isolation of glia from Alzheimer's mice reveals inflammation and dysfunction. *Neurobiology of Aging*, 35(12), 2746–60. <http://doi.org/10.1016/j.neurobiolaging.2014.06.004>

- Palop, J., & Mucke, L. (2010). Amyloid-beta Induced Neuronal Disease: From Synapses toward Neural Networks. *Nature Neuroscience*, *13*(7), 812–818. <http://doi.org/10.1038/nn.2583>. Amyloid-
- Paolicelli, R. C., Bolasco, G., Pagani, F., Maggi, L., Scianni, M., Panzanelli, P., ... Gross, C. T. (2011). Synaptic Pruning by Microglia Is Necessary for Normal Brain Development. *Science*, *333*(6048), 1456–8.
- Patel, N. S., Paris, D., Mathura, V., Quadros, A. N., Crawford, F. C., & Mullan, M. J. (2005). Inflammatory cytokine levels correlate with amyloid load in transgenic mouse models of Alzheimer's disease. *Journal of Neuroinflammation*, *2*(1), 9. <http://doi.org/10.1186/1742-2094-2-9>
- Perry, V. H., Cunningham, C., Holmes, C., 'Perry, V. H., 'Cunningham, C., & 'Holmes, C. (2007). Systemic infections and inflammation affect chronic neurodegeneration. *Nature Review Immunology*, *7*(2), 161–167. <http://doi.org/10.1038/nri2015>
- Perry, V. H., & Holmes, C. (2014). Microglial priming in neurodegenerative disease. *Nature Reviews. Neurology*, *10*(4), 217–24. Retrieved from <http://www.ncbi.nlm.nih.gov/pubmed/24638131>
- Perry, V. H., Nicoll, J. a R., & Holmes, C. (2010). Microglia in neurodegenerative disease. *Nature Reviews. Neurology*, *6*(4), 193–201. <http://doi.org/10.1038/nrneurol.2010.17>
- Prinz, M., Häusler, K. G., Kettenmann, H., & Hanisch, U. K. (2001). β -adrenergic receptor stimulation selectively inhibits IL-12p40 release in microglia. *Brain Research*, *899*(1-2), 264–270. [http://doi.org/10.1016/S0006-8993\(01\)02174-6](http://doi.org/10.1016/S0006-8993(01)02174-6)
- Prokop, S., Miller, K. R., & Heppner, F. L. (2013). Microglia actions in Alzheimer's disease. *Acta Neuropathologica*, *126*(4), 461–477. <http://doi.org/10.1007/s00401-013-1182-x>
- Puchtler, H., Sweat, F., & Levine, M. (1967). on the binding of congo red by amyloid. *Nuclear Physics B*, *1*(5), 269–276. [http://doi.org/10.1016/0550-3213\(67\)90127-7](http://doi.org/10.1016/0550-3213(67)90127-7)
- Qiu, C., Kivipelto, M., & Von Strauss, E. (2009). Epidemiology of Alzheimer's disease: Occurrence, determinants, and strategies toward intervention. *Dialogues in Clinical Neuroscience*, *11*(2), 111–128. <http://doi.org/10.1097/ALN.0b013e318212ba87>
- Querfurth HW, L. F. (2010). Alzheimer's Disease. *The New England Journal of Medicine*, *362*(4), 329–344.
- Radi, Z. a, Kehrl, M. E., & Ackermann, M. R. (2001). Cell adhesion molecules, leukocyte trafficking, and strategies to reduce leukocyte infiltration. *Journal of Veterinary Internal Medicine / American College of Veterinary Internal Medicine*, *15*(6), 516–29. [http://doi.org/10.1892/0891-6640\(2001\)015<0516:CAMLTA>2.3.CO;2](http://doi.org/10.1892/0891-6640(2001)015<0516:CAMLTA>2.3.CO;2)
- Raj, D. D. a, Jaarsma, D., Holtman, I. R., Olah, M., Ferreira, F. M., Schaafsma, W., ... Boddeke, H. W. G. M. (2014). Priming of microglia in a DNA-repair deficient model of accelerated aging. *Neurobiology of Aging*, *35*(9), 2147–2160.

- <http://doi.org/10.1016/j.neurobiolaging.2014.03.025>
- Rajbhandari, L., Tegenge, M. A., Shrestha, S., Ganesh Kumar, N., Malik, A., Mithal, A., ... Venkatesan, A. (2014). Toll-like receptor 4 deficiency impairs microglial phagocytosis of degenerating axons. *Glia*, *62*(12), 1982–1991. <http://doi.org/10.1002/glia.22719>
- Ramaglia, V., Hughes, T. R., Donev, R. M., Ruseva, M. M., Wu, X., Huitinga, I., ... Morgan, B. P. (2012). C3-dependent mechanism of microglial priming relevant to multiple sclerosis. *Proceedings of the National Academy of Sciences of the United States of America*, *109*(3), 965–70. <http://doi.org/10.1073/pnas.1111924109>
- Ransohoff, R. M., & Perry, V. H. (2009). Microglial Physiology: Unique Stimuli, Specialized Responses. *Annual Review of Immunology*, *27*(1), 119–145. <http://doi.org/10.1146/annurev.immunol.021908.132528>
- Ravaglia, G., Forti, P., Maioli, F., Chiappelli, M., Montesi, F., Tumini, E., ... Patterson, C. (2007). Blood inflammatory markers and risk of dementia: The Conselice Study of Brain Aging. *Neurobiology of Aging*, *28*(12), 1810–20. <http://doi.org/10.1016/j.neurobiolaging.2006.08.012>
- Reed-Geaghan, E. G., Savage, J. C., Hise, A. G., & Landreth, G. E. (2009). CD14 and toll-like receptors 2 and 4 are required for fibrillar A β -stimulated microglial activation. *The Journal of Neuroscience: The Official Journal of the Society for Neuroscience*, *29*(38), 11982–92. <http://doi.org/10.1523/JNEUROSCI.3158-09.2009>
- Regen, T., van Rossum, D., Scheffel, J., Kastriti, M.-E., Revelo, N. H., Prinz, M., ... Hanisch, U.-K. (2011). CD14 and TRIF govern distinct responsiveness and responses in mouse microglial TLR4 challenges by structural variants of LPS. *Brain, Behavior, and Immunity*, *25*(5), 957–70. <http://doi.org/10.1016/j.bbi.2010.10.009>
- Reiserer, R. S., Harrison, F. E., Syverud, D. C., & McDonald, M. P. (2007). Impaired spatial learning in the APPSwe + PSEN1DeltaE9 bigenic mouse model of Alzheimer's disease. *Genes, Brain, and Behavior*, *6*(1), 54–65. <http://doi.org/10.1111/j.1601-183X.2006.00221.x>
- Ribes, S., Ebert, S., Czesnik, D., Regen, T., Zeug, A., Bukowski, S., ... Nau, R. (2009). Toll-Like Receptor Prestimulation Increases Phagocytosis of Escherichia coli DH5 and Escherichia coli K1 Strains by Murine Microglial Cells. *Infection and Immunity*, *77*(1), 557–564. <http://doi.org/10.1128/IAI.00903-08>
- Ritchie, K., Kildea, D., & Robine, J. M. (1992). The relationship between age and the prevalence of senile dementia: a meta-analysis of recent data. *International Journal of Epidemiology*, *21*(4), 763–769. <http://doi.org/10.1093/ije/21.4.763>
- Rogers, J., Lubner-Narod, J., Styren, S. D., & Civin, W. H. (1988). Expression of immune system-associated antigens by cells of the human central nervous system: relationship to the pathology of Alzheimer's disease. *Neurobiology of Aging*, *9*(4), 339–49.

- Rosenbauer, F., Waring, J. F., Foerster, J., Wietstruk, M., Philipp, D., & Horak, I. (1999). Interferon consensus sequence binding protein and interferon regulatory factor-4/Pip form a complex that represses the expression of the interferon-stimulated gene-15 in macrophages. *Blood*, *94*(12), 4274–81. Retrieved from <http://www.ncbi.nlm.nih.gov/pubmed/10590072>
- Sara, S. J. (2009). The locus coeruleus and noradrenergic modulation of cognition. *Nature Reviews. Neuroscience*, *10*(3), 211–223.
- Sasaki, A., Shoji, M., Harigaya, Y., Kawarabayashi, T., Ikeda, M., Naito, M., ... Nakazato, Y. (2002). Amyloid cored plaques in Tg2576 transgenic mice are characterized by giant plaques, slightly activated microglia, and the lack of paired helical filament-typed, dystrophic neurites. *Virchows Archiv: An International Journal of Pathology*, *441*(4), 358–67. <http://doi.org/10.1007/s00428-002-0643-8>
- Sassone-Corsi, P. (2012). The cyclic AMP pathway. *Cold Spring Harbor Perspectives in Biology*, *4*(12). <http://doi.org/10.1101/cshperspect.a011148>
- Scanzano, A., & Cosentino, M. (2015). Adrenergic regulation of innate immunity: a review. *Frontiers in Pharmacology*, *6*. <http://doi.org/10.3389/fphar.2015.00171>
- Scheffel, J., Regen, T., Van Rossum, D., Seifert, S., Ribes, S., Nau, R., ... Hanisch, U.-K. (2012). Toll-like receptor activation reveals developmental reorganization and unmasks responder subsets of microglia. *Glia*, *60*(12), 1930–43. <http://doi.org/10.1002/glia.22409>
- Schmidt, R., Schmidt, H., Curb, J. D., Masaki, K., White, L. R., & Launer, L. J. (2002). Early inflammation and dementia: a 25-year follow-up of the Honolulu-Asia Aging Study. *Annals of Neurology*, *52*(2), 168–74. <http://doi.org/10.1002/ana.10265>
- Scholtzova, H., Kascsak, R. J., Bates, K. A., Boutajangout, A., Kerr, D. J., Meeker, H. C., ... Wisniewski, T. (2009). Induction of Toll-Like Receptor 9 Signaling as a Method for Ameliorating Alzheimer's Disease-Related Pathology. *Journal of Neuroscience*, *29*(6), 1846–1854. <http://doi.org/10.1523/JNEUROSCI.5715-08.2009>
- Schopf, R. E., & Lemmel, E. M. (1983). Control of the Production of Oxygen Intermediates of Human Polymorphonuclear Leukocytes and Monocytes by B-Adrenergic Receptors. *Immunopharmacology and Immunotoxicology*, *5*(3), 203–216. <http://doi.org/10.3109/08923978309039106>
- Sheng, J. G., Mrak, R. E., & Griffin, W. S. T. (1998). Enlarged and phagocytic, but not primed, interleukin-1α-immunoreactive microglia increase with age in normal human brain. *Acta Neuropathologica*, *95*(3), 229–234. <http://doi.org/10.1007/s004010050792>
- Sierra, A., Gottfried-Blackmore, A. C., McEwen, B. S., Bulloch, K., 'Sierra, A., 'Gottfried-Blackmore, A. C. ', ... 'Bulloch, K. (2007). Microglia derived from aging mice exhibit an altered inflammatory profile. *Glia*, *55*(4), 412–424. <http://doi.org/10.1002/glia.20468>

- Sierra¹, A., Gottfried-Blackmore, A. C., McEwen, B. S., & Bulloch², K. (2007). Microglia derived from aging mice exhibit an altered inflammatory profile. *Glia*, *424*(August 2006), 412–424. <http://doi.org/10.1002/glia>
- Simard, A. R., Soulet, D., Gowing, G., Julien, J.-P., & Rivest, S. (2006). Bone Marrow-Derived Microglia Play a Critical Role in Restricting Senile Plaque Formation in Alzheimer's Disease. *Neuron*, *49*(4), 489–502. <http://doi.org/10.1016/j.neuron.2006.01.022>
- Singhal, G., Jaehne, E. J., Corrigan, F., Toben, C., & Baune, B. T. (2014). Inflammasomes in neuroinflammation and changes in brain function: a focused review. *Frontiers in Neuroscience*, *8*(October), 1–13. <http://doi.org/10.3389/fnins.2014.00315>
- Sly, L. ., Krzesicki, R. ., Brashler, J. ., Buhl, A. ., McKinley, D. ., Carter, D. ., & Chin, J. . (2001). Endogenous brain cytokine mRNA and inflammatory responses to lipopolysaccharide are elevated in the Tg2576 transgenic mouse model of Alzheimer's disease. *Brain Research Bulletin*, *56*(6), 581–588. [http://doi.org/10.1016/S0361-9230\(01\)00730-4](http://doi.org/10.1016/S0361-9230(01)00730-4)
- Sörensen, M., Lippuner, C., Kaiser, T., Mißlitz, A., Aebischer, T., & Bumann, D. (2003). Rapidly maturing red fluorescent protein variants with strongly enhanced brightness in bacteria. *FEBS Letters*, *552*(2-3), 110–114. [http://doi.org/10.1016/S0014-5793\(03\)00856-1](http://doi.org/10.1016/S0014-5793(03)00856-1)
- Stalder, A. K., Ermini, F., Bondolfi, L., Krenger, W., Burbach, G. J., Deller, T., ... Coomaraswamy, J. (2005). Invasion of Hematopoietic Cells into the Brain of Amyloid Precursor Protein Transgenic Mice. *Journal of Neuroscience*, *25*(48), 11125–11132. <http://doi.org/10.1523/JNEUROSCI.2545-05.2005>
- Stewart, C. R., Stuart, L. M., Wilkinson, K., van Gils, J. M., Deng, J., Halle, A., ... Moore, K. J. (2010). CD36 ligands promote sterile inflammation through assembly of a Toll-like receptor 4 and 6 heterodimer. *Nature Immunology*, *11*(2), 155–61. <http://doi.org/10.1038/ni.1836>
- Streit, W. J. (2002). Microglia as neuroprotective, immunocompetent cells of the CNS. *Glia*, *40*(2), 133–139. <http://doi.org/10.1002/glia.10154>
- Streit, W. J., Miller, K. R., Lopes, K. O., & Njie, E. (2008). Microglial degeneration in the aging brain--bad news for neurons? *Frontiers in Bioscience: A Journal and Virtual Library*, *13*(3), 3423–38. Retrieved from <http://www.ncbi.nlm.nih.gov/pubmed/18508444>
- Streit, W. J., Sammons, N. W., Kuhns, A. J., & Sparks, D. L. (2004). Dystrophic microglia in the aging human brain. *Glia*, *45*(2), 208–12. <http://doi.org/10.1002/glia.10319>
- Streit, W. J., & Xue, Q. S. (2012). Alzheimer's disease, neuroprotection, and CNS immunosenescence. *Frontiers in Pharmacology*, *3* JUL(July), 1–7.

- <http://doi.org/10.3389/fphar.2012.00138>
- Sturchler-Pierrat, C., Abramowski, D., Duke, M., Wiederhold, K. H., Mistl, C., Rothacher, S., ... Sommer, B. (1997). Two amyloid precursor protein transgenic mouse models with Alzheimer disease-like pathology. *Proceedings of the National Academy of Sciences of the United States of America*, *94*(24), 13287–92. <http://doi.org/10.1073/pnas.94.24.13287>
- Suh, E. C., Jung, Y. J., Kim, Y. a, Park, E.-M., Lee, S. J., & Lee, K. E. (2013). Knockout of Toll-like receptor 2 attenuates A β 25-35-induced neurotoxicity in organotypic hippocampal slice cultures. *Neurochemistry International*, (November), 1–8. <http://doi.org/10.1016/j.neuint.2013.10.007>
- Swanson, L. W., & Hartman, B. K. (1975). The central adrenergic system. An immunofluorescence study of the location of cell bodies and their efferent connections in the rat utilizing dopamine-beta-hydroxylase as a marker. *The Journal of Comparative Neurology*, *163*(4), 467–505. <http://doi.org/10.1002/cne.901630406>
- Taylor, P., Tamura, T., Kong, H. J., Kubota, T., Kubota, M., Borghi, P., ... Ozato, K. (2007). The feedback phase of type I interferon induction in dendritic cells requires interferon regulatory factor 8. *Immunity*, *27*(2), 228–39. <http://doi.org/10.1016/j.immuni.2007.06.009>
- Takahashi, K., Naito, M., & Takeya, M. (1996). Development and heterogeneity of macrophages and their related cells through their differentiation pathways. *Pathology International*, *46*(7), 473–485.
- Takaoka, A., Yanai, H., Kondo, S., Duncan, G., Negishi, H., Mizutani, T., ... Taniguchi, T. (2005). Integral role of IRF-5 in the gene induction programme activated by Toll-like receptors. *Nature*, *434*(7030), 243–249. <http://doi.org/10.1038/nature03308>
- Takeda, K., & Akira, S. (2004). TLR signaling pathways. *Seminars in Immunology*, *16*(1), 3–9. <http://doi.org/10.1016/j.smim.2003.10.003>
- Takeda, K., & Akira, S. (2015). Toll-Like Receptors. In *Current Protocols in Immunology* (Vol. 16, pp. 14.12.1–14.12.10). Hoboken, NJ, USA: John Wiley & Sons, Inc. Retrieved from <http://linkinghub.elsevier.com/retrieve/pii/S1044532303000964>
- Tanaka, K. F., Kashima, H., Suzuki, H., Ono, K., & Sawada, M. (2002). Existence of functional beta1- and beta2-adrenergic receptors on microglia. *Journal of Neuroscience Research*, *70*(2), 232–7. <http://doi.org/10.1002/jnr.10399>
- Thrash, J. C., Torbett, B. E., & Carson, M. J. (2009). Developmental Regulation of TREM2 and DAP12 Expression in the Murine CNS: Implications for Nasu-Hakola Disease. *Neurochemical Research*, *34*(1), 38–45. <http://doi.org/10.1007/s11064-008-9657-1>
- Tresguerres, M., Levin, L. R., & Buck, J. (2011). Intracellular cAMP signaling by soluble adenylyl cyclase. *Kidney International*, *79*(12), 1277–88.

<http://doi.org/10.1038/ki.2011.95>

- Vadiveloo, P. K., Vairo, G., Novak, U., Royston, A. K., Whitty, G., Filonzi, E. L., ... Hamilton, J. A. (1996). Differential regulation of cell cycle machinery by various antiproliferative agents is linked to macrophage arrest at distinct G1 checkpoints. *Oncogene*, *13*(3), 599–608.
- Vairo, G., Royston, A. K., & Hamilton, J. A. (1992). Biochemical events accompanying macrophage activation and the inhibition of colony-stimulating factor-1-induced macrophage proliferation by tumor necrosis factor- α , interferon- γ , and lipopolysaccharide. *Journal of Cellular Physiology*, *151*(3), 630–641. <http://doi.org/10.1002/jcp.1041510324>
- Van Dam, D., D’Hooge, R., Staufenbiel, M., Van Ginneken, C., Van Meir, F., & De Deyn, P. P. (2003). Age-dependent cognitive decline in the APP23 model precedes amyloid deposition. *European Journal of Neuroscience*, *17*(2), 388–396. <http://doi.org/10.1046/j.1460-9568.2003.02444.x>
- Van Dam, D., & De Deyn, P. P. (2006). Drug discovery in dementia: the role of rodent models. *Nature Reviews Drug Discovery*, *5*(11), 956–970. <http://doi.org/10.1038/nrd2075>
- vom Berg, J., Prokop, S., Miller, K. R., Obst, J., Kälin, R. E., Lopategui-Cabezas, I., ... Heppner, F. L. (2012). Inhibition of IL-12/IL-23 signaling reduces Alzheimer’s disease–like pathology and cognitive decline. *Nature Medicine*, *18*(12), 1812–1819. <http://doi.org/10.1038/nm.2965>
- Wahle, M., Greulich, T., Baerwald, C. G. O., Häntzschel, H., & Kaufmann, A. (2005). Influence of catecholamines on cytokine production and expression of adhesion molecules of human neutrophils in vitro. *Immunobiology*, *210*(1), 43–52. <http://doi.org/10.1016/j.imbio.2005.02.004>
- Walter, S., Letiembre, M., Liu, Y., Heine, H., Penke, B., Hao, W., ... Fassbender, K. (2007). Role of the toll-like receptor 4 in neuroinflammation in Alzheimer’s disease. *Cellular Physiology and Biochemistry: International Journal of Experimental Cellular Physiology, Biochemistry, and Pharmacology*, *20*(6), 947–956. <http://doi.org/10.1159/000110455>
- Weinshenker, D. (2008). Functional consequences of locus coeruleus degeneration in Alzheimer’s disease. *Current Alzheimer Research*, *5*(3), 342–345.
- Wenk, G. L. (2003). Neuropathologic changes in Alzheimer’s disease. *Journal of Clinical Psychiatry*.
- Wirh O, Multhaupt G, TA., B. (2004). A modified beta-amyloid hypothesis: intraneuronal accumulation of the beta-amyloid peptide--the first step of a fatal cascade. *Journal of Neurochemistry*, *91*(3), 513–20. <http://doi.org/10.1111/j.1471-4159.2004.02737.x>

- Wispelwey, B., Lesse, a. J., Hansen, E. J., & Scheld, W. M. (1988). Haemophilus influenzae lipopolysaccharide-induced blood brain barrier permeability during experimental meningitis in the rat. *The Journal of Clinical Investigation*, 82(4), 1339–46. <http://doi.org/10.1172/JCI113736>
- Wojtera, M., Sobów, T., Kłoszewska, I., Liberski, P. P., Brown, D. R., & Sikorska, B. (2012). Expression of immunohistochemical markers on microglia in Creutzfeldt-Jakob disease and Alzheimer's disease: morphometric study and review of the literature. *Folia Neuropathologica / Association of Polish Neuropathologists and Medical Research Centre, Polish Academy of Sciences*, 50(1), 74–84. Retrieved from <http://www.ncbi.nlm.nih.gov/pubmed/22505366>
- Wolfe, M. S. (2007). When loss is gain: reduced presenilin proteolytic function leads to increased Abeta42/Abeta40. Talking Point on the role of presenilin mutations in Alzheimer disease. *EMBO Reports*, 8(2), 136–40. <http://doi.org/10.1038/sj.embor.7400896>
- Wyss-coray, T., & Mucke, L. (2002). Inflammation in Neurodegenerative Disease — A Double-Edged Sword. *Neuron*, 35(3), 419–432.
- Ye, S. M., & Johnson, R. W. (1999). Increased interleukin-6 expression by microglia from brain of aged mice. *Journal of Neuroimmunology*, 93(1-2), 139–148. [http://doi.org/10.1016/S0165-5728\(98\)00217-3](http://doi.org/10.1016/S0165-5728(98)00217-3)
- Young, M. D., Wakefield, M. J., Smyth, G. K., & Oshlack, A. (2010). Gene ontology analysis for RNA-seq: accounting for selection bias. *Genome Biology*, 11(2), R14. <http://doi.org/10.1186/gb-2010-11-2-r14>
- Zhang, B., Gaiteri, C., Bodea, L.-G., Wang, Z., McElwee, J., Podtelezchnikov, A. A., ... Emilsson, V. (2013). Integrated Systems Approach Identifies Genetic Nodes and Networks in Late-Onset Alzheimer's Disease. *Cell*, 153(3), 707–720. <http://doi.org/10.1016/j.cell.2013.03.030>
- Zhang YW, Thompson R, Zhang H, X. H. (2011). APP processing in Alzheimer's disease. *Molecular Brain*, 4(1), 3. <http://doi.org/10.1186/1756-6606-4-3>
- Zhao, L. N., Lu, L., Chew, L. Y., & Mu, Y. (2014). Alzheimer's disease-A panorama glimpse. *International Journal of Molecular Sciences*, 15(7), 12631–12650. <http://doi.org/10.3390/ijms150712631>
- Zilka, N., Kazmerova, Z., Jadhav, S., Neradil, P., Madari, A., Obetkova, D., ... Novak, M. (2012). Who fans the flames of Alzheimer's disease brains? Misfolded tau on the crossroad of neurodegenerative and inflammatory pathways. *Journal of Neuroinflammation*, 9(1), 47. <http://doi.org/10.1186/1742-2094-9-47>
- Ziv, Y., Ron, N., Butovsky, O., Landa, G., Sudai, E., Greenberg, N., ... Schwartz, M. (2006). Immune cells contribute to the maintenance of neurogenesis and spatial learning abilities

in adulthood. *Nature Neuroscience*, 9(2), 268–275. <http://doi.org/10.1038/nn1629>

List of Abbreviations

∞	Infinite
AD	Alzheimer's disease
Akt	Protein kinase B
ANOVA	Analysis of variance
ApoE	Apolipoprotein E
APP	Amyloid precursor protein
AR	Adrenergic receptor
ASC	Apoptosis-associated speck like protein
ATP	Adenosine triphosphate
A β	Amyloid β
BBB	Blood-brain barrier
BMDMs	Bone marrow derived macrophages
CD	Cluster of differentiation
Clec7a	C-type lectin domain family 7 member A
CNS	Central nervous system
Cox6a2	Cytochrome c oxidase subunit VIa polypeptide 2
CRE	Cyclic AMP response element
CREB	Cyclic AMP-responsive element-binding protein
Cst7	Cystatin-F
DAMP	Damage/danger associated molecular pattern
Dectin1	C-type lectin domain family 7 member A
DMEM	Dulbecco's modified Eagle's medium
DNA	Deoxyribonucleic acid
ELISA	Enzyme-linked immunosorbent assay
ELISpot	Enzyme-Linked ImmunoSpot
Epac	Exchange proteins activated by cAMP
FAD	Familial Alzheimer's disease
Fc	Fragment crystallisable
FCS	Fetal calf serum
g	Gram
GFAP	Glial fibrillary acidic protein
GPCR	G protein-coupled receptors
h	Hour(s)
hAPP	Human APP
HBSS	Hanks balanced salt solution
HRP	Horse radish peroxidase
i.p.	Intraperitoneally
Iba-1	Ionized calcium-binding adapter molecule 1
ICAM-1	Intercellular adhesion molecule
IFN	Interferon
IL	Interleukin
IRF	Interferon regulatory factor
IRF2bp	IRF2 binding proteins
Itgax	Integrin alpha
KC	Keratinocyte-derived chemokine,

Lamp2	Lysosomal-associated membrane protein 2
LC	Locus coeruleus
Ldlr	Low density lipoprotein receptor
Lgals3	Lectin galactoside binding soluble 3
LOAD	Late onset Alzheimer's disease
LPS	Lipopolysaccharide
M	Molar
Mac-1	Integrin alpha
Mac-2	Lectin galactoside binding soluble 3
Mac-3	Macrophage-1 antigen 3
Mamdc2	MAM domain containing 2
MAPK	Mitogen-activated protein kinases
MCP	Monocyte chemoattractant protein
MFI	Mean fluorescent intensity
mg	Milligram
MHC I & II	Major histocompatibility complex class I & II
min	Minute
MIP	Macrophage inflammatory protein
ml	Milliliter
mm	Millimeter
mRNA	Messenger Ribonucleic acid
MYD88	Myeloid differentiation primary-response protein 88
N	Number of independent samples
NA	Noradrenaline
NFT	Neurofibrillary tangles
NF- κ B	Nuclear factor-kappa B
ng	Nanogram
NGS	Normal goat serum
NLR	Nod-like receptor
NLRP	NLR family containing pyrin domain
NO	Nitric oxide
OD	Optical density
PAMP	Pathogen-associated molecular patterns
PBS	Phosphate buffered saline
PCR	Polymerase chain reaction
PFA	Paraformaldehyde
pg	Picogram
PI3K	Phosphatidylinositol-4,5-bisphosphate 3-kinase
PIP ₃	Phosphatidylinositol (3,4,5)-trisphosphate
PKA	Protein kinase A
PLL	Poly-L-Lysin
PRR	Pattern-recognition receptors
PSEN	Presenilin
RANTES	Regulated upon activation normal T-cell expressed and presumably secreted
Re-LPS	Rough chemotype LPS
ROS	Reactive oxygen species
RT	Room temperature
SAD	Sporadic type of AD
sAPP α	Soluble APP α

List of abbreviations

SB	Salbutamol
SEM	Standard error of the mean
S-LPS	Smooth chemotype LPS
Spp1	Secreted phosphoprotein 1
STAT	Signal transducer and activator of transcription
tg	Transgenic
Thy	Thymocyte differentiation antigen
TIR	Toll–interleukin 1 (IL-1) receptor
TLR	Toll-like receptor
TNF α	Tumor necrosis factor alpha
TREM	Triggering receptor expressed on myeloid cells
TRIF	TIR domain-containing adaptor protein inducing IFN β
TYROBP	TYRO protein tyrosine kinase-binding protein
WT	Wild-type
β 2AR	Beta 2 Adrenergic receptor
μ g	Microgram
μ l	Microliter
μ m	Micrometer

List of Figures

Figure 1: Drawing of mammalian TLR signalling pathways..... 5

Figure 2: Schematic picture of brain atrophy in AD..... 9

Figure 3: Schematic picture of amyloid precursor protein (APP)..... 10

Figure 4: Schematic representation of APP processing and A β oligomerization..... 11

Figure 5: *Ex vivo* myelin phagocytosis assessment by adult microglia..... 41

Figure 6: *E. coli* phagocytosis assessment by adult cultured microglia..... 42

Figure 7: A β phagocytosis assessment by adult cultured microglia..... 43

Figure 8: LPS pre-incubation effects on myelin and *E. coli* phagocytosis by adult microglia..... 45

Figure 9: Cyto-/ chemokine production by 5XFAD microglia compared with WTs..... 48

Figure 10: Proliferation rate of cultured adult microglia..... 50

Figure 11: Number of monocytes and neutrophils in the brains of WT and 5XFAD mice..... 51

Figure 12: LPS injection into the striatum leads to immune cell infiltration from the periphery to the brain in 5XFAD mice as in WT..... 53

Figure 13: Age-dependent increase of A β plaque depositions in APP23 mouse model..... 55

Figure 14: Expression of priming markers on plaque-associated microglia of APP^{swe}PS1dE9 mice..... 57

Figure 15: Expression of priming markers on A β associated microglia in 5XFAD mice..... 58

Figure 16: Expression of CD11c, Dectin1, Lamp2 and Trem2 in A β plaque-associated microglia of APP23 and 5XFAD mice..... 60

Figure 17: A β -associated microglia priming occurs prior to age-induced microglia priming..... 61

Figure 18: MHC II⁺ microglia from 5XFAD mice have an activated microglial phenotype..... 64

Figure 19: Morphological changes in plaque-associated microglia in APP23 and 5XFAD mice upon LPS injections..... 66

Figure 20: Increased expression of microglial activation markers after peripheral LPS injections..... 68

Figure 21: No expression of microglial activation markers on astrocytes..... 68

Figure 22: Production of IL-1 β in APP23 mice after i.p. LPS injection.....	70
Figure 23: Expression of LPS-induced IL-1 β by plaque-associated microglia in APP23 and 5XFAD transgenic mice.....	71
Figure 24: LPS-induced ASC activation by plaque-associated microglia in APP23 and 5XFAD transgenic mice.....	72
Figure 25: β 2ARs regulate LPS-induced gene expression.....	73
Figure 26: Immunocytochemistry analysis for β 2AR expression on microglia.....	74
Figure 27: MHC I and IFN β expression analysis after TLR4 and β 2AR stimulation.	75
Figure 28: Effect of β 2AR activation in the CNS on immune cell infiltrates from the periphery.....	77
Figure 29: Immunohistochemistry analysis of β 2AR signalling effect on microglia and astrocyte activation.....	79
Figure 30: Evaluation of intracellular CCL5 ⁺ and TNF α ⁺ production upon simultaneous TLR4 and β 2AR stimulations.	82
Figure 31: ELISpot analysis of the cells producing CCL5.	83
Figure 32: Evaluation of PKA inhibition on β 2AR activation.....	84
Figure 33: Effect of Epac inhibitors on β 2AR activation.....	85
Figure 34: PKA activity assessment upon β 2AR activation.	86
Figure 35: Evaluation of BMDM's response to the β 2AR activation.	87
Figure 36: Regulation of STATs and IRFs genes upon β 2AR signalling.....	88

List of Tables

Table 1: PCR conditions 21

Table 2: Constituents used for ex vivo stimulations 23

Table 3: Antibodies used for flow cytometry analysis of cultured microglia 27

Table 4: Antibodies used for Immunocytochemistry analysis 29

Table 5: Antibodies used for flow cytometry analysis of brain 33

Table 6: Antibodies used for immunohistochemistry analysis of intracerebral infused mice . 35

Table 7: List of antibodies used for immunohistochemistry analysis of intact or intraperitoneal injected mice 36

Table 8: List of secondary antibodies used for immunofluorescence staining 37

Table 9: Antibodies used for sorting brain cells 38

Acknowledgement

With thanks to my original dissertation supervisor and mentor, **Prof. Dr. Uwe K. Hanisch** who sadly passed away few months before completion of this work. It was privilege to have studied with him. I hope that he would have approved the end results of this work and that in some way this dissertation reflects his influence and scholarly spirit.

Prof. Dr. Wolfgang Brück kindly took over the supervision of the thesis after this tragic. Thanks a lot, Prof. Brück!

I would like to especially acknowledge **Prof. Dr. Hendrikus W.G.M. Boddeke** for his advice, support, involvement in my thesis and providing opportunities for a joint project.

Sincere thanks to the members of thesis committee, **Prof. Dr. Thomas A. Bayer** and **Prof. Dr. Mikael Simons** for their scientific input and discussions during the thesis committee meetings.

Special thanks to our technical assistances **Elke Pralle, Susanne Kiecke** for all their support and help and for all nice chats we had together. Dear Elke, thanks for being my strongest motivation to learn German! Furthermore, I would like to thank **Uta Scheidt** and **Katja Reimann** for their technical helps.

Many thanks to **Ulla Gertig, Martina Ott** and **Franziska Paap** who happily helped and supported me during my PhD. I will miss our chats, girls.

I would like to acknowledge **Zhuoran Yin** for performing experiments used in this study. Thanks to **Hana Janova, Sebastian Torke** and **Erik Schöffner** for contributing in the work. Acknowledgements to **Michael Gertig** and **Inge Holtman** for their support for the data analysis.

Also, thanks to **Mahboobeh, Erika** and **Erik** for making a great atmosphere in the office, though short time. I would like to thank other members in the department of Neuropathology including **Sara, Insa, Verena, Nielsen, Anne, Silke, Linda** and all the other colleagues for making a nice environment.

My deepest thankfulness to **my family** specially my parents. Although far from me, they endlessly supported me during my studying. Grateful to have you!

Acknowledgement

Last but not the least, I would like to thank **Nico Westphal** for all his understandings and supports towards me. Without you, maybe I could not overcome the difficulties during this journey.

Curriculum vitae (CV)

Personal information

Name: Nasrin Saiepour
Date of birth: 09.09.1983
Nationality: Iranian
E-mail: nasrin.saiepour@gmail.com

Education

July 2012 - present
PhD student, Biology faculty, Goerge-August University of Göttingen, Göttingen, Germany.

Oct 2010- May 2012
Master in Molecular Medicine, Goerge-August Medical University of Göttingen, Göttingen, Germany.

Feb 2007- Feb 2009
Bachelor in Medical Laboratory Science, Para clinical faculty, Ahwaz Jundishapour University of Medical Sciences, Ahwaz, Iran.

Feb 2003 - Feb 2005
Associates Degree Medical Laboratory Science, Para clinical faculty, Ahwaz Jundishapour University of Medical Sciences, Ahwaz, Iran.

Publications

Hana Janova, Chotima Böttcher, Inge R. Holtman, Tommy Regen, Denise van Rossum, Alexander Götz, Anne-Sophie Ernst, Christin Fritsche, Ulla Gertig, **Nasrin Saiepour**, Konrad Gronke, Claudia Wrzos, Sandra Ribes, Simone Rolfes, Jonathan Weinstein, Hannelore Ehrenreich, Tobias Pukrop, Jens Kopatz, Christine Stadelmann, Gabriela Salinas-Riester, Martin S. Weber, Marco Prinz, Wolfgang Brück, Bart J.L. Eggen, Hendrikus W.G.M. Boddeke, Josef Priller and Uwe-Karsten Hanisch (2015). CD14 is a key organizer of microglial responses to CNS infection and Injury. *GLIA* (Epub ahead of print).

Anne Albrecht , Sebastian Ivens, Ismini E Papageorgiou, Gürsel Çalışkan, **Nasrin Saiepour**, Wolfgang Brück, Gal Richter-Levin, Uwe Heinemann and Oliver Stork (2015). Shifts in excitatory/ inhibitory balance by juvenile stress: A role for neuron-astrocyte interaction in the dentate gyrus. *GLIA* (submitted).

Schaafsma W, Zhang X, van Zomeren KC, Jacobs S, Georgieva PB, Wolf SA, Kettenmann H, Janova H, **Saiepour N**, Hanisch UK, Meerlo P, van den Elsen PJ, Brouwer N, Boddeke HW, Eggen BJ (2015). Long-lasting pro-inflammatory suppression of microglia by LPS-preconditioning is mediated by RelB-dependent epigenetic silencing. *Brain Behav Immun*, 48, 205-21.

Gregory Antonios*, **Nasrin Saiepour***, Yvonne Bouter*, Bernhard C. Richard*, Anders Paetau, Auli Verkkoniemi-Ahola, Lars Lannfelt, Martin Ingelsson, Gabor G. Kovacs, Thierry Pillot, Oliver Wirths, Thomas A. Bayer (2013). N-truncated Abeta starting with position four: early intraneuronal accumulation and rescue of toxicity using NT4X-167, a novel monoclonal antibody. *Acta Neuropathol Commun*, 1, 56.

* Equal contribution